Supplementary Information

Copper(I) Complexes Bearing the Pyrrole-Bridged *S,N* and *N*-Donor Ligands as Catalysts for the Tandem Hydroamination-Alkynylation: Effect of Anions on Product Formation

Munmun Mondal, and Ganesan Mani*

Department of Chemistry, Indian Institute of Technology, Kharagpur, Kharagpur-721302, West Bengal, India.

1. X-ray structures and refinement data

The suitable single crystals of complexes **5-11a** were grown from the solvents mentioned in their respective experimental sections. Data collections were performed using a Bruker APEX-II or D8 Venture APEX3 CCD diffractometer with graphite monochromated Mo Kα radiation (λ = 0.71073 Å). The space group for every structure was obtained by XPREP program. The structures were solved by SHELXT[1] which successfully located most of the nonhydrogen atoms. Subsequently, least-squares refinements were carried out on F^2 using SHELXL version 2018/3[2] to locate the remaining nonhydrogen atoms. Nonhydrogen atoms were refined with anisotropic displacement parameters. Hydrogen atoms attached to carbon atoms were fixed in calculated positions. For complex **11a**·CH_2Cl_2, the lattice CH_2Cl_2 could not be modelled and hence it was squeezed using SQUEEZE/PLATON.[3] As a result, its cif file shows mismatch between the calculated and reported formulae. The PF_6^- anion, SO_2 and phenyl rings are also disordered and they were successfully resolved using SADI, EADP, DFIX, SIMU, RIGU restraints. The refinement data for all the structures are summarized in Table S1 and Table S2. Crystallographic data were deposited with the Cambridge Crystallographic Data Centre, CCDC, 12 Union Road, Cambridge CB21EZ, UK. These data can be obtained free of charge upon quoting the depository numbers CCDC 2331548-2331554 and 2349043 from web interface (at http://www.ccdc.cam.ac.uk).

Table S1. Crystallographic data for complexes **5-8**.

	Complex **5**	Complex **6**	Complex **7**	Complex **8**
Empirical formula	$C_{34}H_{38}Cl_2Cu_2N_6S_2$	$C_{34}H_{38}Br_2Cu_2N_6S_2$	$C_{34}H_{38}Cu_2I_2N_6S_2$	$C_{34}H_{38}Cu_2Cl_2N_6O_4S_2$
Formula weight	792.80	881.72	975.70	856.80
Wavelength (Å)	0.71073	0.71073	0.71073	0.71073
Temperature (K)	296(2)	150(2)	296(2)	296(2)
Crystal system	Triclinic	Triclinic	Triclinic	Triclinic
Space group	$P\bar{1}$	$P\bar{1}$	$P\bar{1}$	$P\bar{1}$
a/Å	7.819(5)	7.7907(9)	7.9902(3)	8.623(2)
b/Å	10.872(6)	10.8092(12)	10.9861(5)	9.240(2)
c/Å	11.705	11.6165(14)	11.7073(5)	12.560(3)
α/degree	70.240(18)	70.825(7)	70.051(2)	88.202(9)
β/degree	72.284(19)	72.813(8)	75.137(2)	71.740(8)
γ/degree	77.609(18)	80.038(8)	82.751(2)	75.243(9)
Volume (Å^3)	885.0(9)	879.58(18)	932.85(7)	917.8(4)
Z	1	1	1	1
D_{calcd}, mg m^{-3}	1.488	1.665	1.737	1.550
μ/mm^{-1}	1.504	3.633	2.939	1.465
F(000)	408	444	480	440
θ range (degree)	2.330 to 27.239	2.746 to 28.580	2.257 to 33.142	2.282 to 30.087
Data/restr/params.	3778 / 0 / 212	4449 / 0 / 212	7012 / 0 / 212	5316 / 0 / 230
GOF (F^2)	1.037	1.028	1.082	1.045
Limiting Indices	-10<=h<=10 -13<=k<=13 -12<=l<=14	-8<=h<=10 -14<=k<=13 -15<=l<=15	-12<=h<=12 -16<=k<=15 -18<=l<=17	-12<=h<=12 -13<=k<=13 -17<=l<=17
R1, *wR2*	0.0805, 0.2088	0.0535, 0.0825	0.0325, 0.0694	0.0533, 0.1292
R indices (all data) *R1*, *wR2*	0.1351, 0.2718	0.1086, 0.1048	0.0480, 0.0775	0.0925, 0.1518
Largest different peak and hole (e Å^{-3})	0.957 and –1.025	0.660, -0.703	0.729, -0.853	1.248, -0.866

Table S2. Crystallographic data for complexes **9-11a** and morpholinium copper(I) salt.

	Complex **9**	Complex **10**	Complex **11a**·CH_2Cl_2	$[C_4H_{10}NO]_4^+[Cu_2Cl_6]^{4-}$
Empirical formula	$C_{34}H_{38}CuBrN_6O_4S_2$	$C_{34}H_{38}CuIN_6O_4S_2$	$C_{35}H_{40}Cl_2CuF_6N_6O_4PS_2$	$C_{16}H_{40}Cl_6Cu_2N_4O_4$
Formula weight	802.27	849.26	952.26	692.30
Wavelength (Å)	0.71073	0.71073	0.71073	0.71073
Temperature (K)	296(2)	296(2)	150(2)	120(2)
Crystal system	Monoclinic	Monoclinic	Triclinic	Monoclinic
Space group	*C*2/*c*	*C*2/*c*	$P\bar{1}$	$P2_1/c$
a/Å	13.3242(11)	13.3756(11)	12.8983(7)	9.5628(3)
b/Å	11.9239(11)	12.0339(11)	18.2783(11)	17.6110(6)
c/Å	22.9313(17)	23.0349(18)	20.3179(11)	8.4952(2)
α/degree	90	90	74.971(2)	90
β/degree	100.561(4)	100.211(7)	71.551(2)	97.1890(10)
γ/degree	90	90	69.355(2)	90
Volume ($Å^3$)	3581.5(5)	3649.0(5)	4192.8(4)	1419.43(7)
Z	4	4	4	2
D_{calcd}, mg m^{-3}	1.488	1.546	1.509	1.620
μ/mm^{-1}	1.888	1.604	0.858	2.092
F(000)	1648	1720	1952	712
θ range (degree)	2.310 to 30.628	2.293 to 29.831	2.143 to 25.000	2.147 to 33.221
Data/restr/params.	5486 / 0 / 223	5227 / 0 / 222	14738 / 972 / 1129	5431 / 0 / 161
GOF (F^2)	1.077	1.001	1.034	1.037
Limiting Indices	-18<=h<=18 -16<=k<=17 -32<=l<=32	-17<=h<=18 -16<=k<=16 -32<=l<=32	-15<=h<=14 -21<=k<=21, -24<=l<=24	-14<=h<=14 -27<=k<=27 -13<=l<=12
R1, *wR2*	0.0498, 0.1365	0.0429, 0.0954	0.0595, 0.1307	0.0344, 0.0796
R indices (all data) *R1*, *wR2*	0.0677, 0.1469	0.1136, 0.1264	0.1010, 0.1492	0.0495, 0.0877
Largest different peak and hole (e $Å^{-3}$)	0.806, -0.694	0.817, -0.624	0.530, -0.713	0.501, -0.644

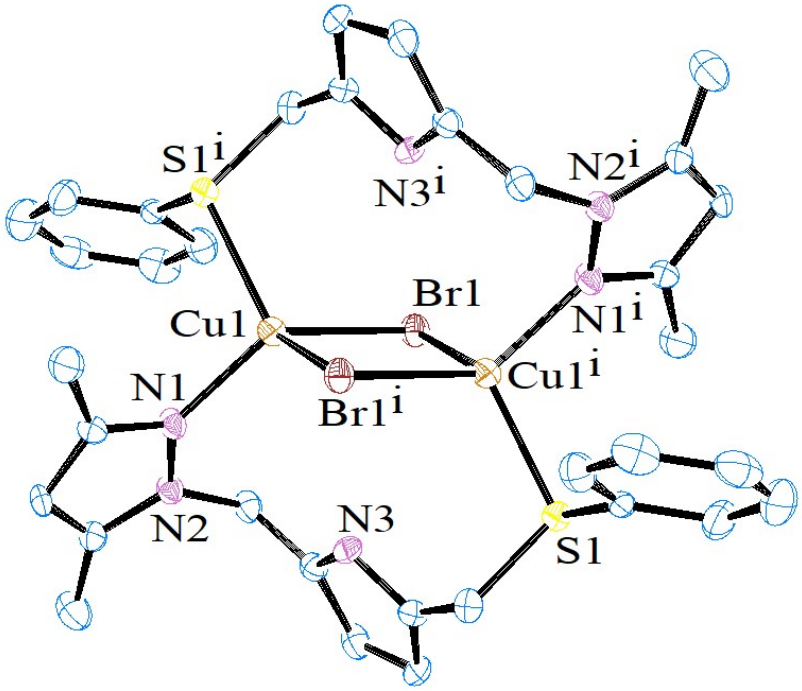

Figure S1. ORTEP diagram of Complex **6** with 50% probability ellipsoids. All hydrogen atoms are omitted for clarity. Selected bond lengths (Å) and angles (°): Cu1^{i}-S1 2.3021(14), Cu1-N1 2.028(4), Cu1-Br1^{i} 2.5389(9), Cu1-Br1 2.4973(8), N1-Cu1-S1^{i} 105.78(12), N1-Cu1-Br1 124.04(11), S1^{i}-Cu1-Br1 108.42(4), N1-Cu1-Br1^{i} 103.24(12), S1^{i}-Cu1-Br1^{i} 118.38(4), Br1-Cu1-Br1^{i} 97.74(3), Cu1-Br1-Cu1^{i} 82.26(3). Hydrogen bonding: N3···Br1^{i} 3.517(4), H··· Br1^{i} 2.82(4), N3-H···Br1^{i} 155(4). Symmetry transformations used to generate equivalent atoms: (i) –x+1, –y+1, –z.

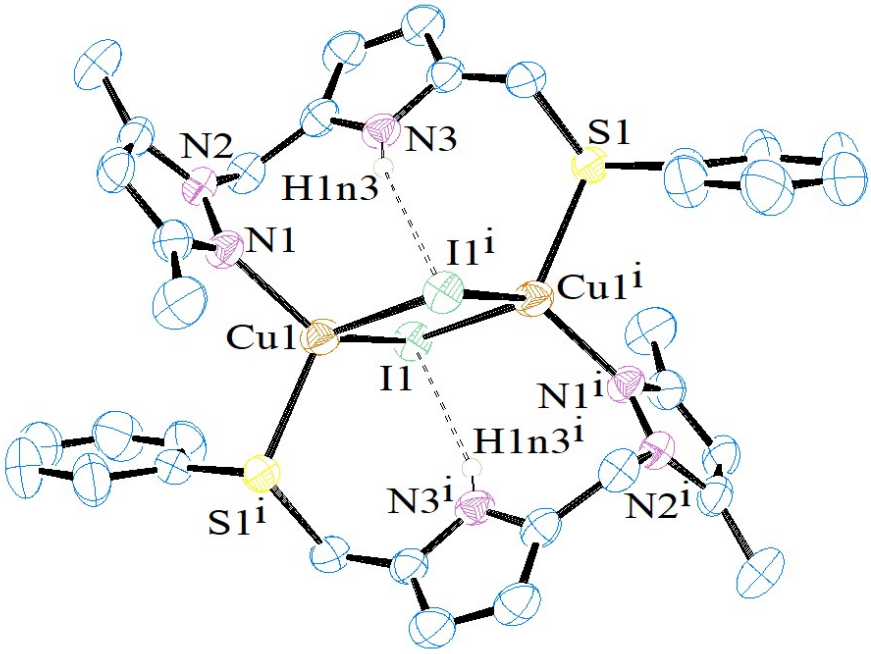

Figure S2. ORTEP diagram of **7** with 50% probability ellipsoids. Most hydrogen atoms are omitted for clarity. Selected bond lengths (Å) and angles (°): Cu1^{i}- S1 2.3350(7), Cu1-N1 2.0415(19), Cu1-I1^{i} 2.7128(4), Cu1-I1 2.6606(4), N1-Cu1-S1^{i} 107.04(6), N1-Cu1-I1 124.05(6), S1^{i}-Cu1-I1 108.039(19), N1-Cu1-I1^{i} 102.92(6), S1^{i}-Cu1-I1^{i} 113.71(2), I1-Cu1-I1^{i} 101.084(11), Cu1-I1-Cu1^{i} 78.916(12). Hydrogen bonding: N3···I1^{i} 3.715(2), H··· I1^{i} 2.99(3), N3-H···I1^{i} 163(3). Symmetry transformations used to generate equivalent atoms: (i) –x, –y, –z+2.

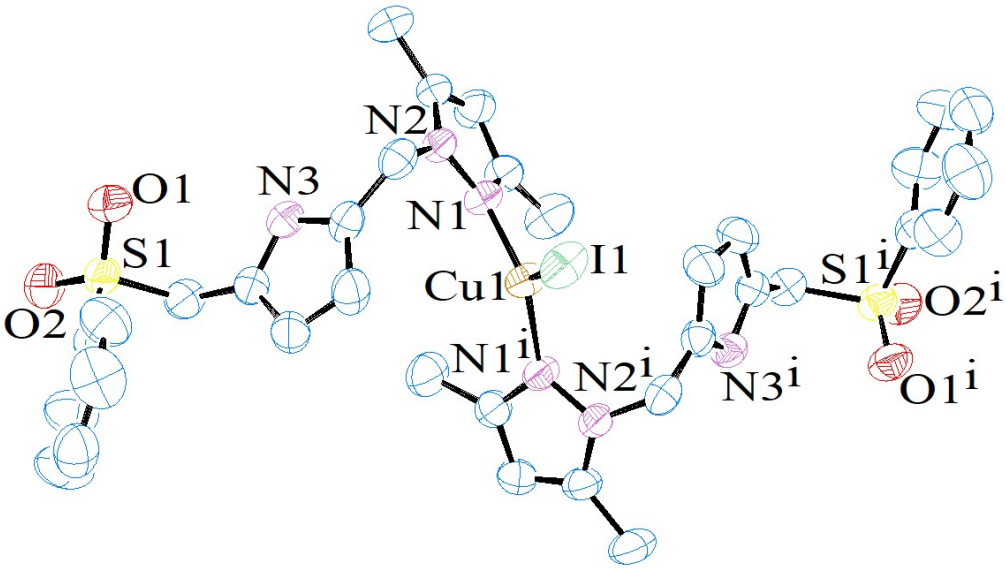

Figure S3. ORTEP diagram of **10** with 50% probability ellipsoids. All hydrogen atoms are omitted for clarity. Selected bond lengths (Å) and angles (°): Cu1-N1 1.983(3), Cu1-I1 2.5610(8), O2-S1 1.443(3), O1-S1 1.437(3), N1-Cu1-N1^{i} 121.59(18), N1-Cu1-I1 119.21(9). Hydrogen bonding: N3···O2^{ii} 3.103(5), H···O2^{ii} 2.31(4), N3-H···O2^{ii} 174(4). Symmetry transformations used to generate equivalent atoms: (i) –x+1, y, –z+1/2, (ii) –x+3/2, –y+1/2, –z.

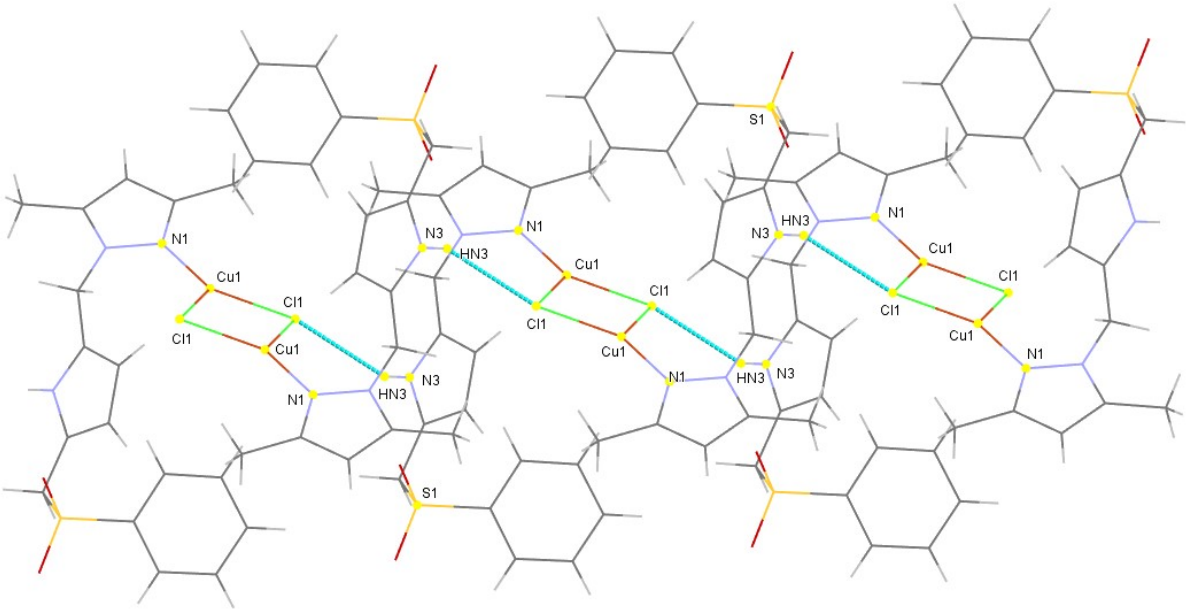

Figure S4. The intermolecular pyrrole NH…Cl hydrogen bonds in the crystal lattice of structure **8**.

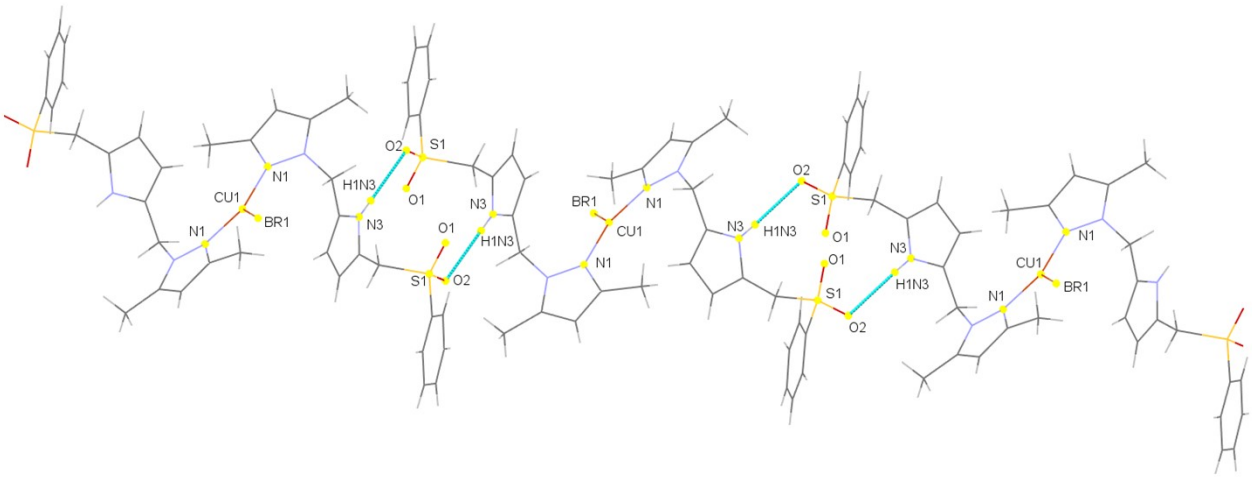

Figure S5. The intermolecular pyrrole NH…O(SO_2) hydrogen bonds in the crystal lattice of structure **9**.

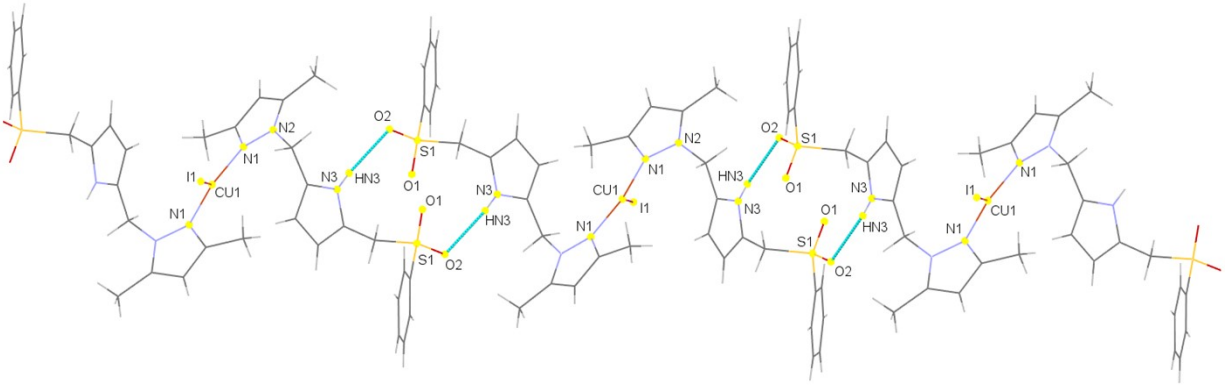

Figure S6. The intermolecular pyrrole NH…O(SO_2) hydrogen bonds in the crystal lattice of structure **10**.

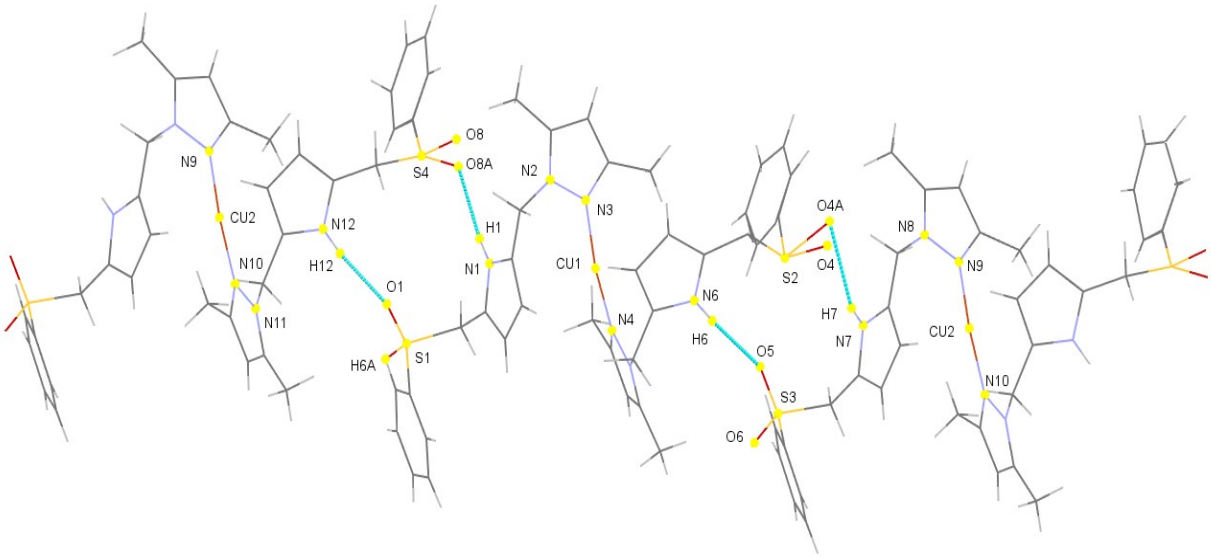

Figure S7. The intermolecular pyrrole NH…O(SO_2) hydrogen bonds in the crystal lattice of structure **11a**.

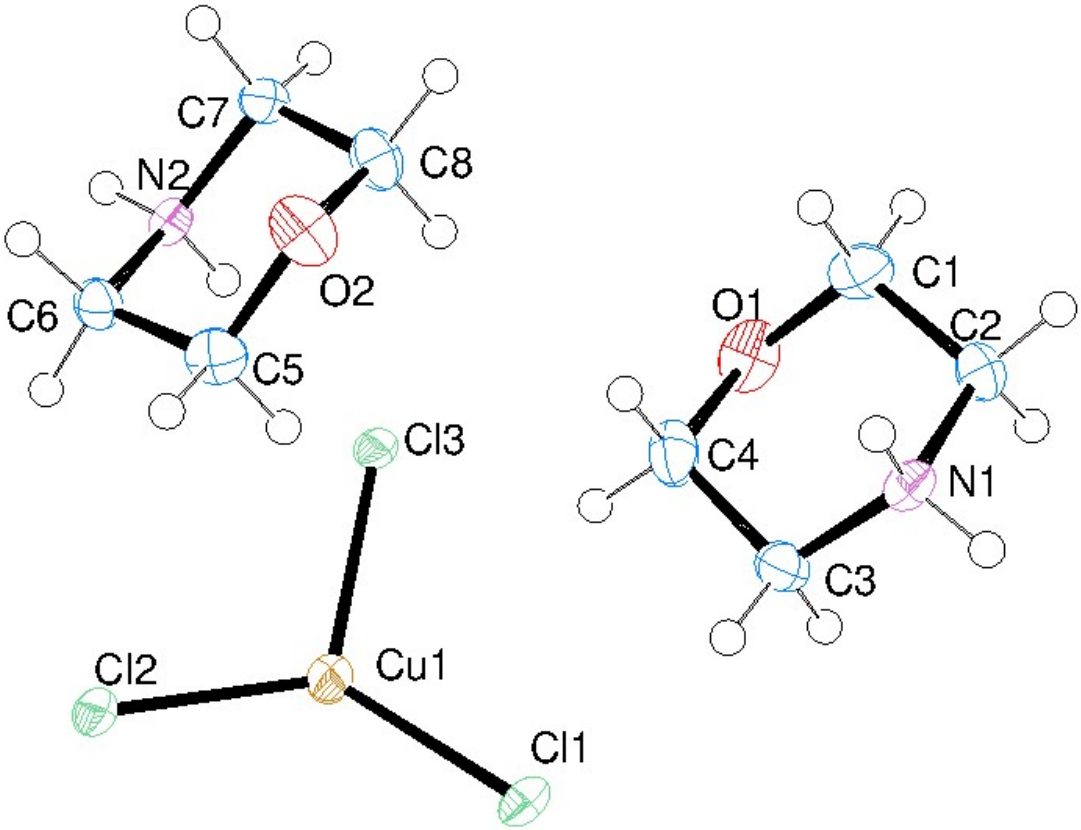

Figure S8. ORTEP diagram of asymmetric unit of the structure of morpholinium copper(I) salt with 50% probability ellipsoids. Selected bond lengths (Å) and angles (°): Cu1-Cl2 2.2660(4), Cu1-Cl1 2.2670(4), Cu1-Cl3 2.3300(4), Cu1-Cl1^{i} 2.7605(4), N2-C7 1.491(2), N2-C6 1.4940(19), C6-C5 1.516(2), O2-C5 1.426(2), O2-C8 1.4320(19), C7-C8 1.507(2); Cl2-Cu1-Cl1 128.117(16), Cl2-Cu1-Cl3 111.753(15), Cl1-Cu1-Cl3 114.503(15), Cl2-Cu1-Cl1^{i} 101.393(15), Cl1-Cu1-Cl1^{i} 95.042(13), Cl3-Cu1-Cl1^{i} 97.109(14), Cu1-Cl1-Cu1^{i} 84.957(13). Symmetry transformations used to generate equivalent atoms: (i) -x+1, -y+1, -z+1.

Table S3. Hydrogen bonds

D-H...A	d(D-H), Å	d(H...A), Å	d(D...A), Å	<(DHA), °
N2-H3...Cl3	0.87(2)	2.31(2)	3.1591(13)	166.5(18)
N(1)-H(2)...Cl3^{ii}	0.88(2)	2.34(2)	3.1798(13)	160.1(18)

N2-H4...Cl1^{iii}	0.87(2)	2.65(2)	3.2937(13)	131.6(17)
N1-H1...Cl2^{iv}	0.90(2)	2.27(2)	3.1345(13)	162.4(17)
N2-H4...Cl3^{v}	0.87(2)	2.67(2)	3.2853(13)	129.4(17)

Symmetry transformations used to generate equivalent atoms: (i) -x+1,-y+1,-z+1 (ii) x,-y+1/2,z-1/2 (iii) x-1,y,z (iv) -x+1,y-1/2,-z+1/2 (v) -x,-y+1,-z+1

2. Catalysis studies

Table S4. Optimization of the catalytic hydroamination-alkynylation reaction between phenylacetylene and morpholine using the copper(I) chloride complex **8** containing the sulfone ligand **4**.

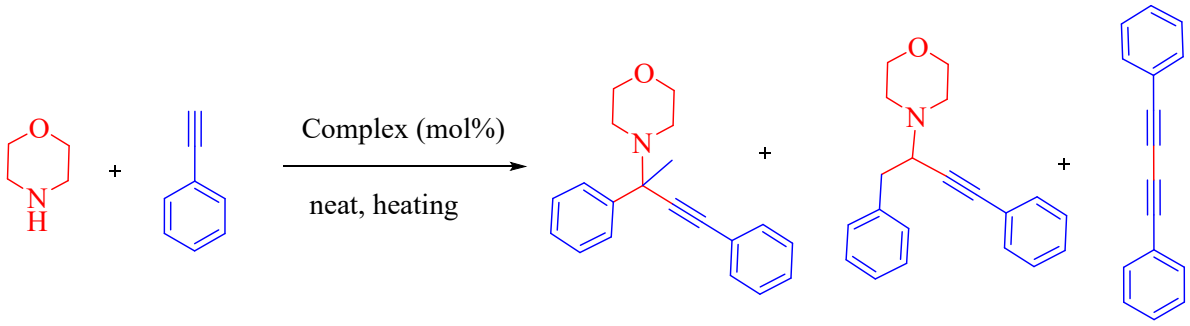

12a **12b** **12c**

Entry	Amine (equiv)	Alkyne (equiv)	Complex (mol%)	Temp. (°C)	Time (h)	Yield (%)[a]		
						12a	**12b**	**Diyne**
1	1	2	**8** (5)	80	14	8	30	-
2	1	2	**8** (2)	80	14	9	33	-
3	1	2	**8** (1.5)	80	14	4	45	-
4	1	2	**8** (1)	80	14	2	45	-
5	1	2	**8** (0.5)	80	14	8	27	-
6	1.5	4	**8** (1)	80	36	2	63	-
7	3	1	**8** (1)	80	14	2	14	-
8	1	6	**8** (5)	80	14	19	63	-
9	1	4	**8** (5)	80	14	16	62	-
10	1	4	**8** (1)	110	2	21	74	-
11	1	4	**8**(0.5)	110	12	3	50	-
12	1	4	**5** (1)	110	1.5	27	71	-

[a]Isolated yields based on morpholine.

The catalytic hydroamination-alkynylation reaction between morpholine and phenylacetylene in the presence of complex **8** under different conditions was optimized and summarized in Table S4. The reaction between morpholine and phenylacetylene in the 1:2 molar ratio in the presence of 5 mol% of complex **8** in a pressure tube at 80 °C for 14 h without exogeneous solvent under nitrogen atmosphere yielded a mixture of products from which compound **12a** (8%) and **12b** (30%) were isolated in a pure form by basic alumina column chromatography separation (entry1). When the loading of complex **8** was gradually decreased to 2, 1.5 and then to 1 mol% with other conditions remaining the same, the yield of the trisubstituted propargylamine (**12b**) increased to 45%, whereas the tetrasubstituted propargylamine (**12a**)

decreased to 2% yield (entry 2-4). The further decrease in the catalyst loading (0.5 mol%) resulted in the decreased isolated yield of 27% for **12b** (entry 5). When the alkyne/amine mole ratio is high (4:1.5) with 1 mol% of complex, the yield of **12b** is increased to 63% yield and that of **12a** remained almost the same (2%) (entry 6). Conversely, when the alkyne/amine ratio is low (1:3), the yield of **12b** also decreased (14%) with 2% yield of **12a** (entry 7). This is consistent with the structure of the product containing two phenylacetylene moieties. Subsequently, to improve the yield of product, the catalyst loading was increased to 5 mol% with alkyne/amine mole ratio of 6:1 or 4:1 at 80 °C (entry 8 and 9). Yet, the yield of the trisubstituted product did not improve beyond 63%. Remarkably, the yields of both products increased to 74% and 21% when the temperature of the reaction is increased to 110 °C with 1 mol% of catalyst (entry 10). Further, under the same conditions, when the catalyst loading is 0.5 mol%, the yield of the trisubstituted product is decreased to 50% (entry 11). Similar result was obtained with complex **5** (entry 12).

Catalytic hydroamination-alkynylation using $[Cu(CH_3CN)_4]BF_4$

Under dinitrogen atmosphere, an oven dried teflon-capped pressure tube equipped with a stirring bar was charged with *N*-phenylpiperazine (0.20 mL, 1.26 mmol), phenylacetylene (0.56 mL, 5.09 mmol), and $[Cu(CH_3CN)_4]BF_4$ (0.0396 g, 0.1258 mmol). After closing the tube with Teflon cap tightly, the bottom of the tube containing the reaction mixture was placed in a preheated oil bath at 110 °C and stirred for 24 h. Under dinitrogen atmosphere, the reaction was monitored by TLC to check if *N*-phenylpiperazine is completely consumed. After cooling down to room temperature, the reaction mixture was loaded onto a basic alumina column and eluted with ethyl acetate/hexane (v/v = 1/99) mixture. The solvent was evaporated from the first fraction using rotary evaporator and then dried under vacuum to obtain the tetrasubstituted propargylamine **17a**, and the second fraction of solvent gave the trisubstituted product **17b**. ^{1}H and ^{13}C NMR spectra were recorded to confirm their purity and structure. For **17a**: 0.402 g, 1.096 mmol, yield = 87%. For **17b**: 0.021 g, 0.057 mmol, yield = 5%.

Catalytic hydroamination-alkynylation using complex 11b

Under dinitrogen atmosphere, an oven dried teflon-capped pressure tube equipped with a stirring bar was charged with *N*-phenylpiperazine (0.20 mL, 1.26 mmol), phenylacetylene (0.56 mL, 5.09 mmol), and copper complex **11b** (0.0102 g, 0.0126 mmol). After closing the tube with Teflon cap tightly, the bottom of the tube containing the reaction mixture was placed in a

preheated oil bath at 110 °C and stirred for 12 h. Under dinitrogen atmosphere, the reaction was monitored by TLC to check if n-phenyl piperazine is completely consumed. After cooling down to room temperature, the reaction mixture was loaded onto a basic alumina column and eluted with ethyl acetate/hexane (*v*/*v* = 1/99) mixture. The solvent was evaporated from the first fraction using rotary evaporator and then dried under vacuum to obtain the tetrasubstituted propargylamine **17a**, and the second fraction of solvent gave the trisubstituted product **17b**. ^{1}H and ^{13}C NMR spectra were recorded to confirm their purity and structure. For **17a**: 0.321 g, 0.875 mmol, yield = 70%. For **17b**: 0.082g, 0.223 mmol., yield = 18%.

3. Substrate scope data

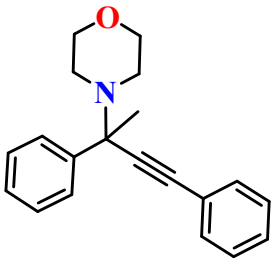

4-(2,4-diphenylbut-3-yn-2-yl)morpholine[4] 12a: 0.090 g, 0.309 mmol, yield = 27%. ^{1}H NMR ($CDCl_3$, 500 MHz): δ = 7.75 (d, *J*(HH) = 10.0, 2H, C_6H_5), 7.53 (t, *J*(HH) = 5.0, 2H, C_6H_5), 7.34-7.31 (m, 5H, C_6H_5), 7.25 (t, *J*(HH) = 5.0, 1H, C_6H_5), 3.71 (t, *J*(HH) = 5.0, 4H, morpholine CH_2), 2.71 (br s, 2H, morpholine CH_2), 2.48 (br s, 2H, morpholine CH_2), 1.66 (s, 3H, CH_3). ^{13}C{^{1}H} NMR ($CDCl_3$, 125.7 MHz): δ = 145.0, 132.0, 128.4, 128.4, 128.3, 127.4, 126.8, 123.3, 88.4, 88.3, 67.6, 63.5, 48.2, 30.6. HRMS (+ ESI): calcd *m/z* for $[M+H]^+$ $C_{20}H_{22}NO^+$: 292.1696, found: 292.1709.

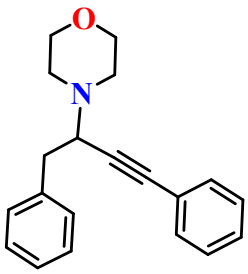

4-(1,4-diphenylbut-3-yn-2-yl)morpholine[5] 12b: 0.240 g, 0.823 mmol, yield = 71%. ^{1}H NMR ($CDCl_3$, 500 MHz): δ = 7.43-7.26 (m, 10H, C_6H_5), 3.85-3.75 (m, 5H, morpholine CH_2, CH),

3.13 (dd, *J*(HH) = 10.0, 5.0, 1H, CH_2), 3.04 (dd, *J*(HH) = 10.0, 5.0, 1H, CH_2), 2.87-2.83 (m, 2H, morpholine CH_2), 2.70-2.66 (m, 2H, morpholine CH_2). ^{13}C NMR ($CDCl_3$, 125.7 MHz, ppm) δ = 138.5, 131.7, 129.5, 128.3, 128.2, 128.1, 126.5, 123.1, 87.4, 86.4, 67.1, 60.2, 49.9, 39.6. HRMS (+ ESI): calcd *m/z* for $[M+H]^+$ $C_{20}H_{22}NO^+$: 292.1696, found: 292.1697.

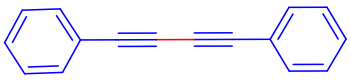

1,4-diphenylbuta-1,3-diyne[6] 12c: 0.170 g, 0.840 mmol, yield = 36%. ^{1}H NMR ($CDCl_3$, 500 MHz): δ = 7.54 (d, *J*(HH) = 5.0, 4H, C_6H_5), 7.38-7.33 (m, 6H, C_6H_5). ^{13}C{^{1}H} NMR ($CDCl_3$, 125.7 MHz): δ = 132.7, 129.3, 128.6, 122.0, 81.7, 74.1.

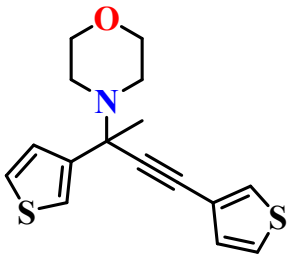

4-(2,4-di(thiophen-3-yl)but-3-yn-2-yl)morpholine 13a: 0.100 g, 0.330 mmol, yield = 28%. ^{1}H NMR ($CDCl_3$, 500 MHz): δ = 7.46 (d, *J*(HH) = 5.0, 1H, thiophene C*H*), 7.41 (d, *J*(HH) = 5.0, 1H, thiophene C*H*), 7.27-7.14 (m, 4H, thiophene C*H*), 3.69 (t, *J*(HH) = 5.0, 4H, morpholine CH_2), 2.68 (t, *J*(HH) = 5.0, 2H, morpholine CH_2), 2.45 (t, *J*(HH) = 5.0, 2H, morpholine CH_2), 1.67 (s, 3H, CH_3). HRMS (+ ESI): calcd *m/z* for $[M+H]^+$ $C_{16}H_{18}NOS_2^+$: 304.0825, found: 304.0819.

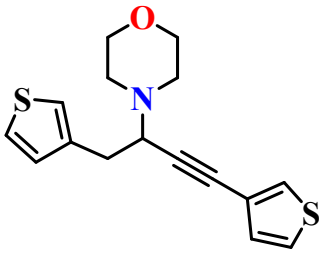

4-(1,4-di(thiophen-3-yl)but-3-yn-2-yl)morpholine 13b: 0.200 g, 0.660 mmol, yield = 57%. ^{1}H NMR ($CDCl_3$, 500 MHz): δ = 7.40 (d, *J*(HH) = 5.0, 1H, thiophene C*H*), 7.27-7.24 (m, 2H, thiophene C*H*), 7.17 (d, *J*(HH) = 5.0, 1H, thiophene C*H*), 7.10-7.08 (m, 2H, thiophene C*H*), 3.82-3.71 (m, 5H, morpholine CH_2 and CH), 3.07 (m, 2H, CH_2), 2.82-2.78 (m, 2H, morpholine

CH_2), 2.65-2.62 (m, 2H, morpholine CH_2). ^{13}C{^{1}H} NMR ($CDCl_3$, 125.7 MHz): δ = 138.7, 130.0, 128.9, 128.5, 125.3, 125.1, 122.1, 122.1, 86.1, 82.1, 67.1, 59.4, 49.8, 34.0.

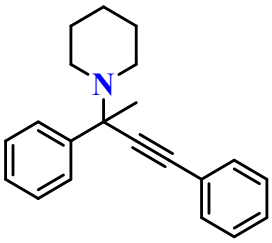

1-(2,4-diphenylbut-3-yn-2-yl)piperidine[7] 14a: 0.050 g, 0.173 mmol, yield = 18%. ^{1}H NMR ($CDCl_3$, 400 MHz): δ = 7.76 (d, *J*(HH) = 8.0, 2H, C_6H_5), 7.53 (d, *J*(HH) = 8.0, 2H, C_6H_5), 7.35-7.22 (m, 6H, C_6H_5), 2.67 (br s, 2H, piperidine CH_2), 2.42 (d, *J*(HH) = 8.0, 2H, piperidine CH_2), 1.65 (s, 3H, CH_3), 1.61 (br s, 2H, piperidine CH_2), 1.56 (br s, 2H, piperidine CH_2), 1.45 (d, *J*(HH) = 8.0, 2H, piperidine CH_2). ^{13}C{^{1}H} NMR ($CDCl_3$, 125.7 MHz): δ = 146.4, 132.0, 128.4, 128.2, 128.0, 127.0, 126.6, 123.8, 89.6, 87.6, 63.8, 48.9, 31.3, 26.7, 24.9.

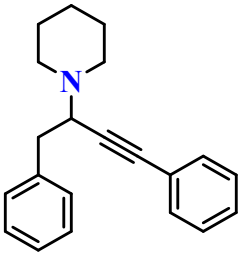

1-(1,4-diphenylbut-3-yn-2-yl)piperidine[5] 14b: 0.200 g, 0.691 mmol, yield = 71%. ^{1}H NMR ($CDCl_3$, 500 MHz): δ = 7.34-7.15 (m, 10H, C_6H_5), 3.67 (q, *J*(HH) = 5.0, 1H, C*H*), 3.01-2.94 (m, 2H, CH_2), 2.72 (br s, 2H, piperidine CH_2), 2.53 (br s, 2H, piperidine CH_2), 1.64-1.57 (m, 4H, piperidine CH_2), 1.44-1.42 (m, 2H, piperidine CH_2). ^{13}C{^{1}H} NMR ($CDCl_3$, 125.7 MHz): δ = 139.0, 131.6, 129.6, 128.2, 128.1, 127.8, 126.3, 123.5, 87.3, 86.8, 60.8, 50.8, 40.1, 26.2, 24.6.

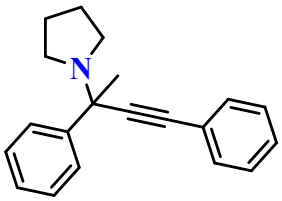

1-(2,4-diphenylbut-3-yn-2-yl)pyrrolidine[8] 15a: 0.100 g, 0.363 mmol, yield = 30%. ^{1}H NMR ($CDCl_3$, 500 MHz): δ = 7.78 (d, *J*(HH) = 10.0, 2H, C_6H_5), 7.52 (t, *J*(HH) = 5.0, 2H, C_6H_5), 7.35-7.30 (m, 5H, C_6H_5), 7.25 (t, *J*(HH) = 7.5, 1H, C_6H_5), 2.77 (d, *J*(HH) = 5.0, 2H, pyrrolidine

CH_2), 2.62 (q, J(HH) = 5.0, 2H, pyrrolidine CH_2), 1.78 (t, J(HH) = 7.5, 4H, pyrrolidine CH_2), 1.73 (s, 3H, CH_3). ^{13}C{^{1}H} NMR ($CDCl_3$, 125.7 MHz): δ = 145.7, 132.0, 128.4, 128.2, 128.1, 127.2, 126.6, 123.6, 89.5, 87.5, 62.9, 48.6, 32.4, 24.0.

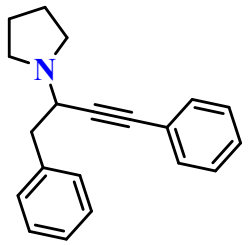

1-(1,4-diphenylbut-3-yn-2-yl)pyrrolidine[5] 15b: 0.200 g, 0.726 mmol, yield = 61%. ^{1}H NMR ($CDCl_3$, 500 MHz): δ = 7.33-7.17 (m, 10H, C_6H_5), 3.90 (q, J(HH) = 5.0, 1H, CH), 3.08 (m, 1H, CH_2), 2.93 (t, J(HH) = 10.0, 1H, CH_2), 2.80 (d, J(HH) = 5.0, 2H, pyrrolidine CH_2), 2.74 (d, J(HH) = 10.0, 2H, pyrrolidine CH_2), 1.79 (t, J(HH) = 7.5, 4H, pyrrolidine CH_2). ^{13}C{^{1}H} NMR ($CDCl_3$, 125.7 MHz): δ = 138.8, 131.7, 129.5, 128.2, 128.2, 127.9, 126.4, 123.4, 87.5, 86.5, 57.1, 49.8, 41.8, 23.6.

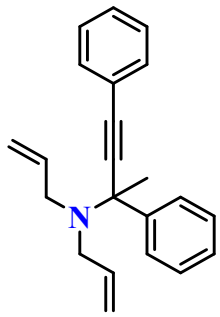

N,N-diallyl-2,4-diphenylbut-3-yn-2-amine 16a: 0.040 g, 0.132 mmol, yield = 16%. ^{1}H NMR ($CDCl_3$, 500 MHz): δ = 7.83 (d, J(HH) = 10.0, 2H, C_6H_5), 7.55 (d, J(HH) = 5.0, 2H, C_6H_5), 7.36 (t, J(HH) = 7.5, 5H, C_6H_5), 7.27 (t, J(HH) = 5.0, 1H, C_6H_5), 6.00-5.96 (m, 2H, CH), 5.18 (d, J(HH) = 15.0, 2H, CH_2), 5.06 (d, J(HH) = 10.0, 2H, CH_2), 3.35 (dd, J(HH) = 10.0, 15.0, 2H, CH_2), 3.26 (d, J(HH) = 15.0, 2H, CH_2), 1.70 (s, 3H, CH_3). ^{13}C{^{1}H} NMR ($CDCl_3$, 125.7 MHz): δ = 146.7, 138.0, 131.8, 130.2, 128.5, 128.3, 128.1, 127.2, 126.6, 115.6, 91.1, 86.9, 64.1, 53.5, 32.5.

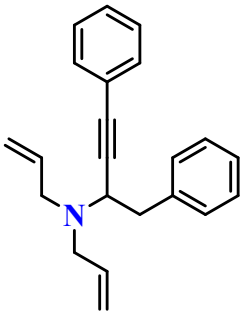

N,N-diallyl-1,4-diphenylbut-3-yn-2-amine[5] 16b: 0.200 g, 0.663 mmol, yield = 82%. ^{1}H NMR ($CDCl_3$, 500 MHz): δ = 7.36 (d, *J*(HH) = 5.0, 2H, C_6H_5), 7.26 (t, *J*(HH) = 5.0, 7H, C_6H_5), 7.19 (q, *J*(HH) = 5.0, 1H, C_6H_5), 5.79(q, *J*(HH) = 5.0, 10.0, 2H, C*H*), 5.18 (d, *J*(HH) = 15.0, 2H, CH_2), 5.09 (d, *J*(HH) = 10.0, 2H, CH_2), 3.95 (t, *J*(HH) = 7.5, 1H, C*H*), 3.38 (q, *J*(HH) = 5.0, 2H, CH_2), 3.05 (dd, *J*(HH) = 5.0, 15.0, 2H, CH_2), 3.01-2.94 (m, 2H, CH_2). ^{13}C{^{1}H} NMR ($CDCl_3$, 125.7 MHz): δ = 138.9, 136.5, 131.8, 129.7, 128.3, 128.2, 128.0, 126.4, 123.6, 117.3, 87.7, 86.2, 55.4, 54.2, 40.6.

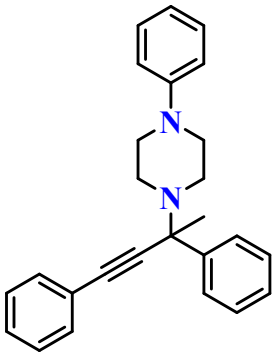

1-(2,4-diphenylbut-3-yn-2-yl)-4-phenylpiperazine 17a: 0.321 g, 0.875 mmol, yield = 70% (using complex **11b**) and 0.402 g, 1.096 mmol, yield 87% (using $[Cu(CH_3CN)_4][BF_4]$) ^{1}H NMR ($CDCl_3$, 500 MHz): δ = 7.79 (d, *J*(HH) = 5.5, 2H, C_6H_5), 7.52 (t, *J*(HH) = 5.0, 2H, C_6H_5), 7.34 (t, *J*(HH) = 7.5, 2H, C_6H_5), 7.30-7.21 (m, 6H, C_6H_5), 6.91 (d, *J*(HH) = 10.0, 2H, C_6H_5), 6.82 (t, *J*(HH) = 7.5, 1H, C_6H_5), 3.22-3.15 (m, 4H, piperazine CH_2), 2.90 (br d, *J*(HH) = 5.0, 2H, piperazine CH_2), 2.66 (t, *J*(HH) = 5.0, 2H, piperazine CH_2), 1.72 (s, 3H, CH_3). ^{13}C{^{1}H} NMR ($CDCl_3$, 125.7 MHz): δ = 151.5, 145.3, 132.0, 129.2, 128.4, 128.4, 128.2, 127.3, 126.6, 123.3, 119.6, 115.9, 88.5, 88.3, 63.3, 49.6, 47.7, 31.1.

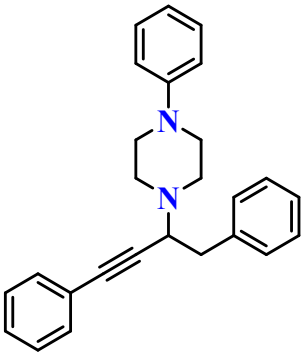

1-(1,4-diphenylbut-3-yn-2-yl)-4-phenylpiperazine 17b: 0.400 g, 1.091 mmol, yield = 87%. ^{1}H NMR ($CDCl_3$, 400 MHz): δ = 7.37-7.21 (m, 12H, C_6H_5), 6.95 (d, *J*(HH) = 5.0, 2H, C_6H_5), 6.85 (t, *J*(HH) = 7.5, 1H, C_6H_5), 3.80 (q, *J*(HH) = 5.0, 1H, C*H*), 3.28-3.23 (m, 4H, piperazine CH_2), 3.12-3.08 (m, 1H, CH_2), 3.03 (s, 1H, CH_2), 3.01-2.96 (m, 2H, piperazine CH_2), 2.81-2.77 (m, 2H, piperazine CH_2). ^{13}C{^{1}H} NMR ($CDCl_3$, 125.7 MHz): δ = 151.6, 138.8, 131.8, 129.7, 129.3, 128.4, 128.2, 126.7, 123.3, 119.9, 116.3, 87.5, 86.6, 60.1, 49.7, 49.5, 40.1.

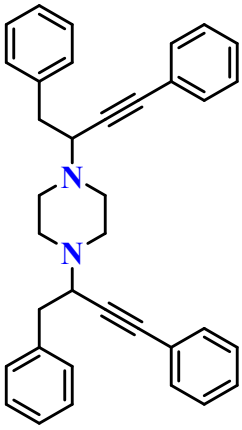

1,4-bis(1,4-diphenylbut-3-yn-2-yl)piperazine 18: 0.400 g, 0.808 mmol, yield = 70%. ^{1}H NMR ($CDCl_3$, 400 MHz): δ = 7.36-7.21 (m, 20H, C_6H_5), 3.77-3.72 (m, 2H, C*H*), 3.08 (t, *J*(HH) = 4.0, 2H, CH_2), 3.06-2.88 (m, 6H, CH_2), 2.78-2.71 (m, 4H, piperazine CH_2). ^{13}C{^{1}H} NMR ($CDCl_3$, 125.7 MHz): δ = 138.9, 131.9, 129.8, 128.4, 128.1, 126.6, 123.5, 87.4, 86.9, 60.1, 49.6, 40.1.

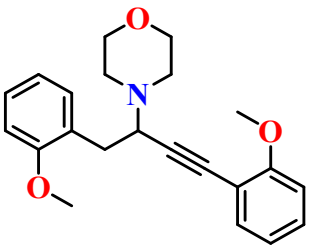

4-(1,4-bis(2-methoxyphenyl)but-3-yn-2-yl)morpholine 19: 0.368 g, 1.05 mmol, yield = 90%. ^{1}H NMR ($CDCl_3$, 500 MHz): δ = 7.33-7.22 (m, 4H, C_6H_5), 6.92-6.83 (m, 4H, C_6H_5), 3.92-3.89 (m, 1H, C*H*), 3.84 (s, 3H, CH_3), 3.83 (s, 3H, CH_3), 3.80-3.74 (m, 4H, morpholine CH_2), 3.22-3.18 (m, 1H, CH_2), 2.93-2.84 (m, 3H, morpholine CH_2, CH_2), 2.71-2.68 (m, 2H, morpholine CH_2). ^{13}C{^{1}H} NMR ($CDCl_3$, 125.7 MHz): δ = 160.2, 157.9, 133.7, 131.8, 129.4, 127.8, 126.9, 120.5, 120.3, 112.9, 110.9, 110.3, 91.5, 82.9, 67.4, 58.4, 55.9, 55.4, 50.0, 34.0. HRMS (+ ESI): calcd *m/z* for $[M+H]^+$ $C_{22}H_{26}NO_3^+$: 352.1907, found: 352.1915.

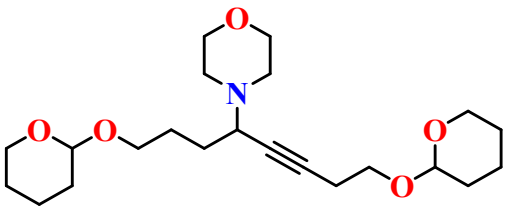

4-(1,8-bis((tetrahydro-2H-pyran-2-yl)oxy)oct-5-yn-4-yl)morpholine 20: 0.300 g, 0.760 mmol, yield = 65%. ^{1}H NMR ($CDCl_3$, 400 MHz): δ = 4.63 (s, 1H, C*H*), 4.54 (s, 1H, C*H*), 3.86-3.69 (m, 8H, CH_2), 3.51-3.34 (m, 4H, morpholine CH_2), 3.23 (d, *J*(HH) = 16.0, 1H, C*H*), 2.60-2.47 (m, 6H, CH_2), 1.79-1.50 (m, 16H, CH_2). ^{13}C{^{1}H} NMR ($CDCl_3$, 125.7 MHz): δ = 99.1, 98.9, 83.2, 78.2, 67.3, 67.2, 66.2, 62.4, 62.2, 57.7, 52.4, 49.7, 47.8, 47.1, 30.9, 30.7, 29.8, 26.9, 25.6, 25.6, 20.3, 19.7, 19.5. HRMS (+ ESI): calcd *m/z* for $[M+Na]^+$ $C_{22}H_{37}NO_5Na^+$: 418.2564, found: 418.2559.

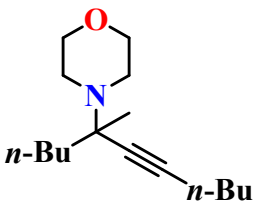

4-(5-methylundec-6-yn-5-yl)morpholine[4] 21: 0.280 g, 1.11 mmol, yield = 96%. ^{1}H NMR ($CDCl_3$, 500 MHz): δ = 3.68 (t, *J*(HH) = 5.0, 4H, morpholine CH_2), 2.57-2.54 (m, 4H, morpholine CH_2), 2.15 (t, *J*(HH) = 10.0, 2H, CH_2), 1.54 (m, 2H, CH_2), 1.44 (m, 2H, CH_2), 1.39-1.35 (m, 4H, CH_2), 1.28-1.25 (m, 2H, CH_2), 1.21 (s, 3H, CH_3), 0.87 (t, *J*(HH) = 5.0, 6H, CH_3).

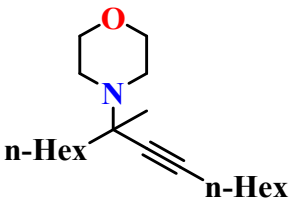

4-(7-methylpentadec-8-yn-7-yl)morpholine[4] 22: 0.322 g, 1.05 mmol, yield = 90%. ^{1}H NMR ($CDCl_3$, 500 MHz): δ = 3.63 (t, *J*(HH) = 5.0, 4H, morpholine C*H*$_2$), 2.54-2.49 (m, 4H, morpholine C*H*$_2$), 2.11 (t, *J*(HH) = 5.0, 2H, C*H*$_2$), 1.51-1.48 (m, 2H, C*H*$_2$), 1.43-1.39 (m, 2H, CH_2), 1.34-1.31 (m, 4H, CH_2), 1.21 (br s, 10H, C*H*$_2$), 1.17 (s, 3H, C*H*$_3$), 0.81 (q, *J*(HH) = 5.0, 6H, C*H*$_3$).

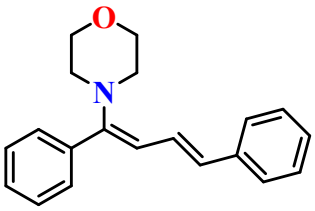

4-((1Z,3E)-1,4-diphenylbuta-1,3-dien-1-yl)morpholine[9] 23: 0.290 g, 0.995 mmol, yield = 86%. ^{1}H NMR ($CDCl_3$, 500 MHz): δ = 7.50-7.45 (m, 5H, C_6H_5), 7.27-7.25 (m, 4H, C_6H_5), 7.15 (t, *J*(HH) = 5.0, 1H, C_6H_5), 6.74 (dd, *J*(HH) = 15.0, 10.0, 1H, C*H*), 6.47 (d, *J*(HH) = 15.0, 1H, C*H*), 5.69 (d, *J*(HH) = 10.0, 1H, C*H*), 3.80 (t, *J*(HH) = 5.0, 4H, morpholine C*H*$_2$), 2.98 (t, *J*(HH) = 5.0, 4H, morpholine C*H*$_2$). ^{13}C{^{1}H} NMR ($CDCl_3$, 125.7 MHz): δ = 152.6, 138.8, 137.0, 130.4, 128.6, 128.5, 128.5, 128.0, 126.5, 126.1, 125.7, 106.7, 67.0, 49.6.

4. NMR, HRMS and IR Spectra

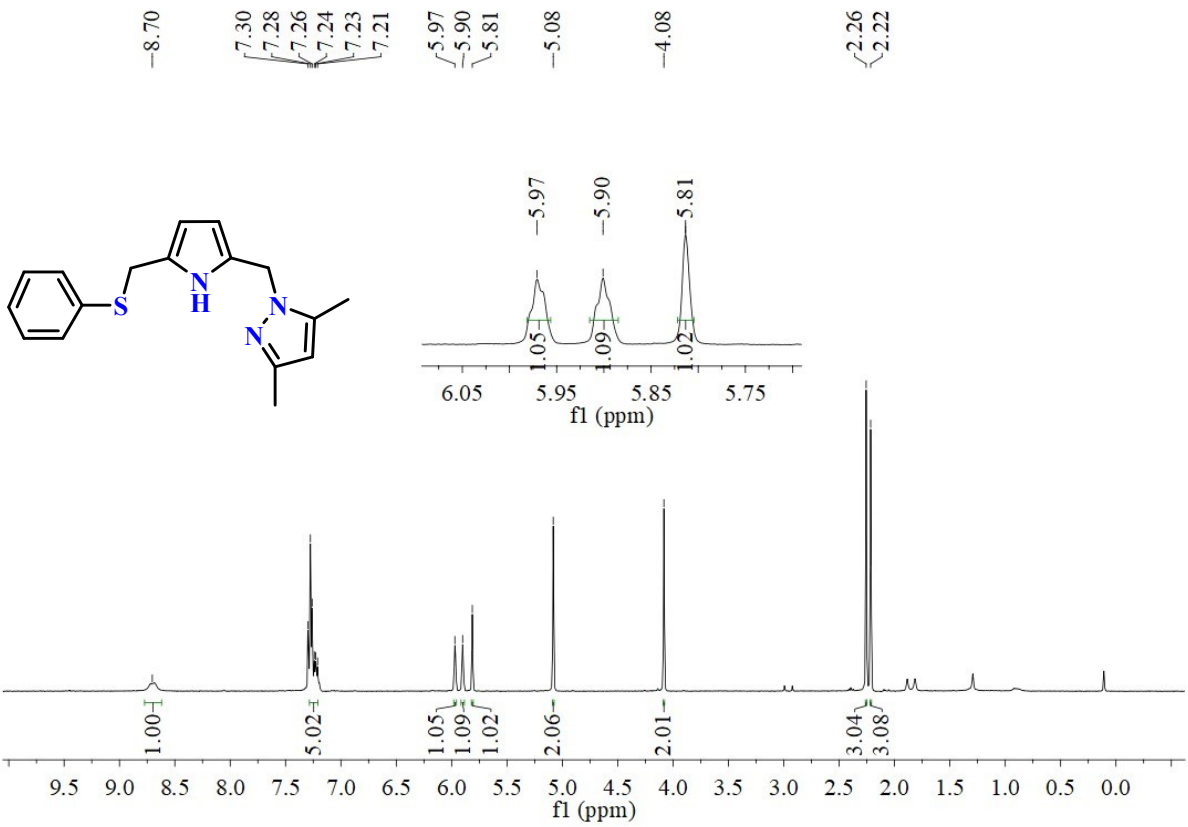

Figure S9. ^{1}H NMR (25 °C, 500 MHz) spectrum of sulfane ligand **2** in $CDCl_3$.

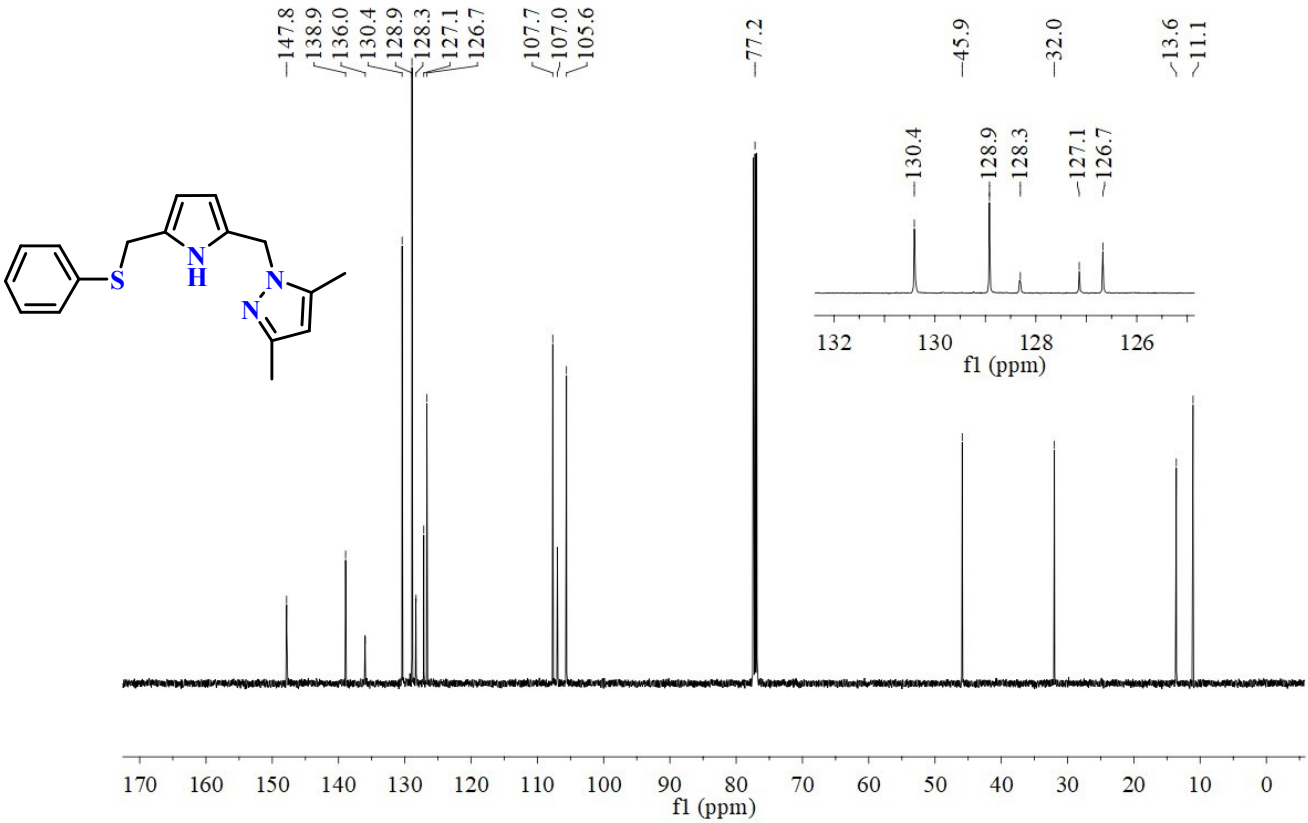

Figure S10. ^{13}C{^{1}H} NMR (25 °C, 125.7 MHz) spectrum of the sulfane ligand **2** in $CDCl_3$.

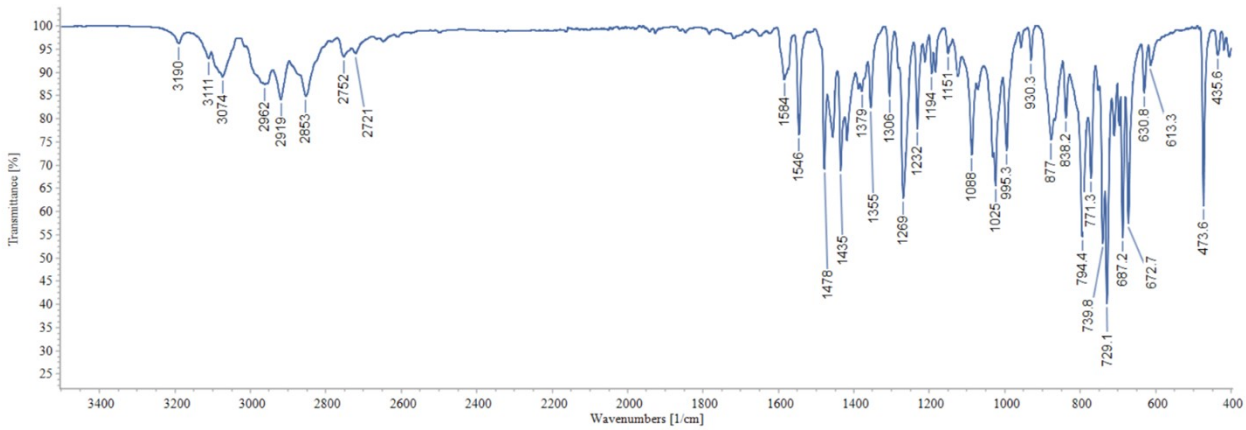

Figure S11. The ATR spectrum of the sulfane ligand **2**.

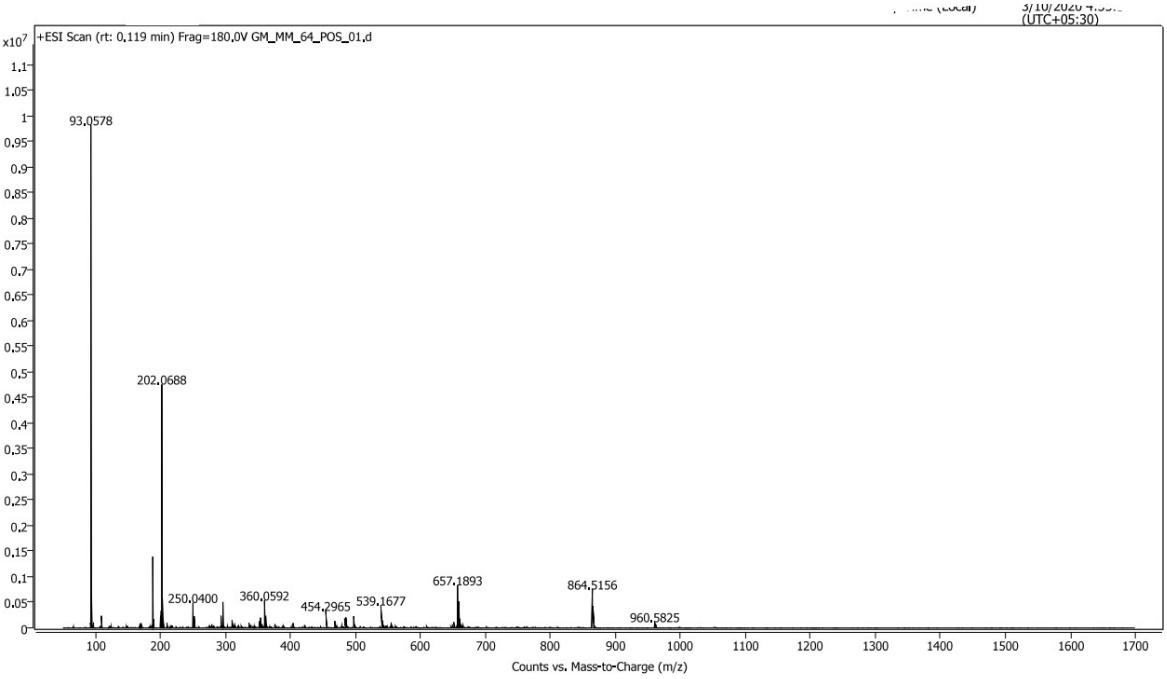

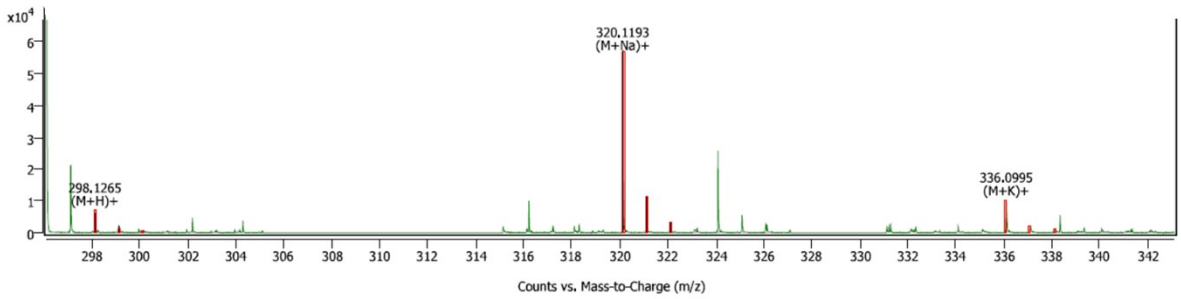

Compound ID Table

Name	Formula	Species	RT	RT Diff	Mass	CAS	ID Source	Score	Score (Lib)	Score (Tgt)
	C17 H19 N3 S	(M+H)+ (M+Na)+ (M+K)+	0.126		297.1300		FBF	99.14		99.14

Figure S12. HRMS (ESI+) spectrum of the sulfane ligand **2**.

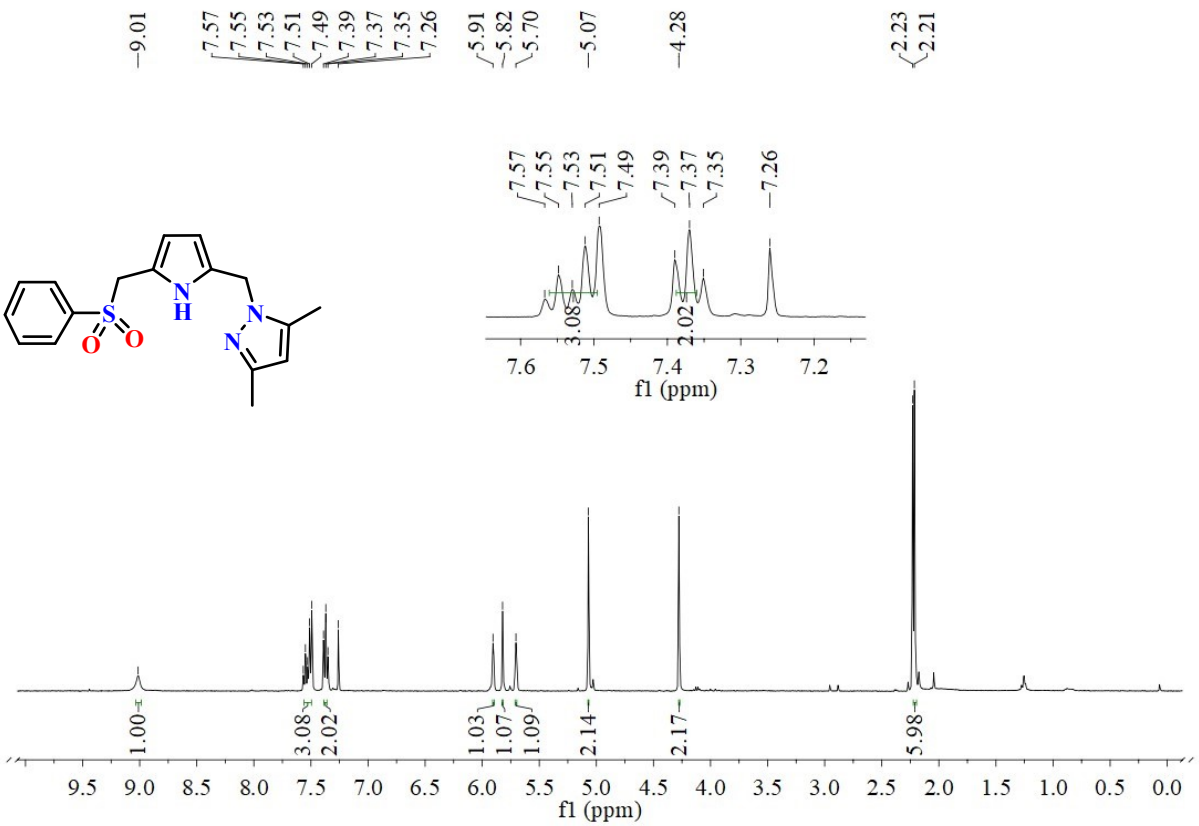

Figure S13. ^{1}H NMR (25 °C, 400 MHz) spectrum of the sulfone ligand **4** in $CDCl_3$.

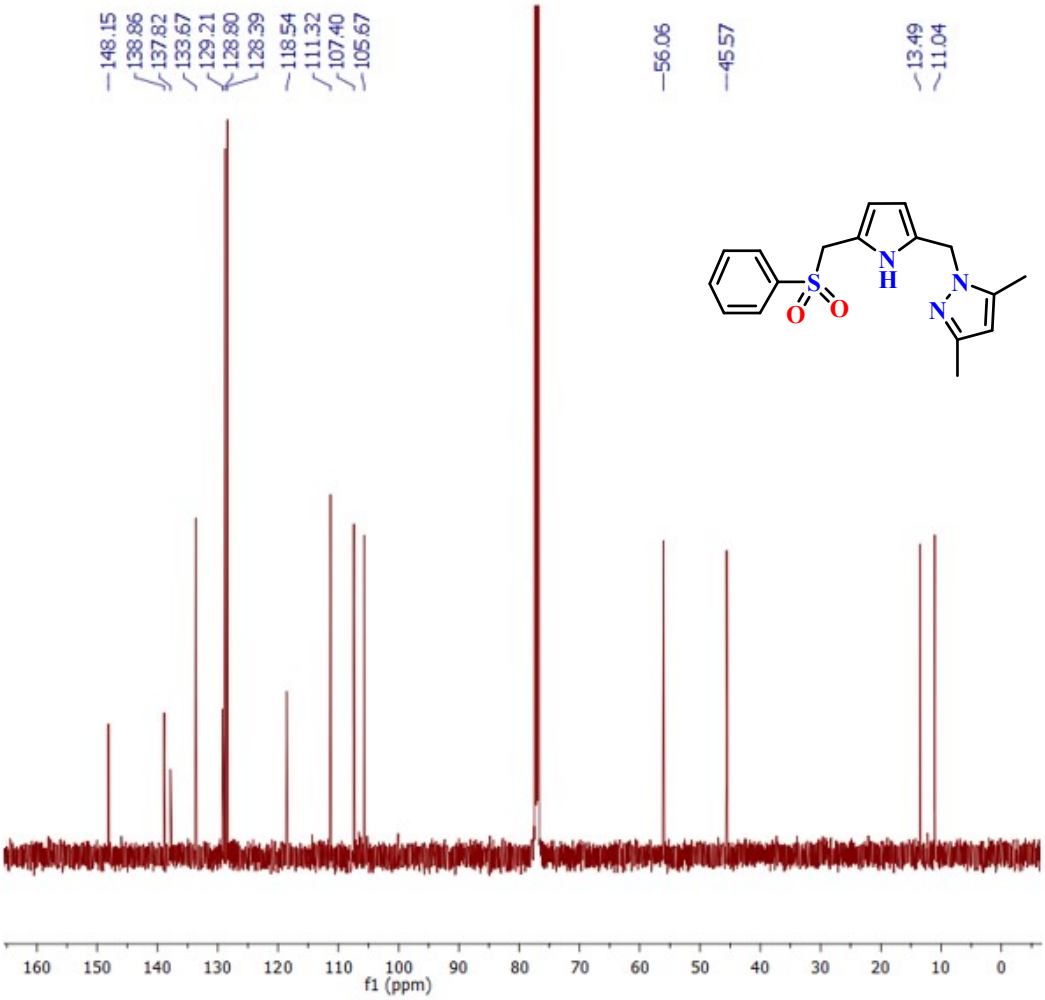

Figure S14. $^{13}C\{^{1}H\}$ NMR (25 °C, 125.7 MHz) spectrum of the sulfone ligand **4** in $CDCl_3$.

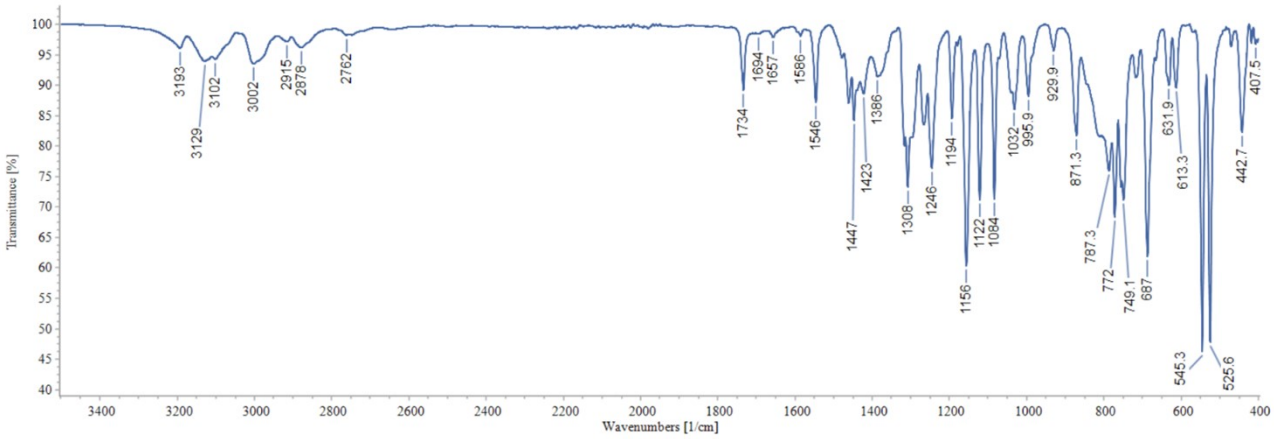

Figure S15. The ATR spectrum of the sulfone ligand **4**.

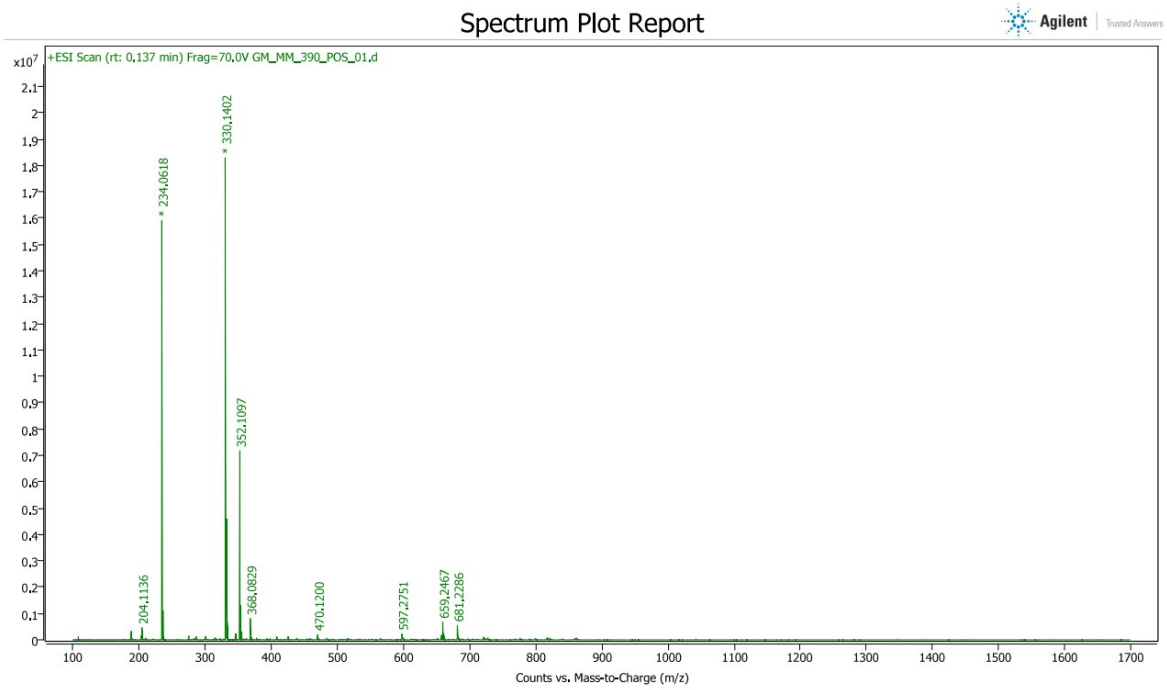

Figure S16. HRMS (ESI+) spectrum of the sulfone ligand **4**.

Species	*m/z*, Found	*m/z,* Calculated
$[M+H]^+$	330.1402	330.1271
$[M+Na]^+$	352.1097	352.1090
$[M+K]^+$	368.0829	368.0830

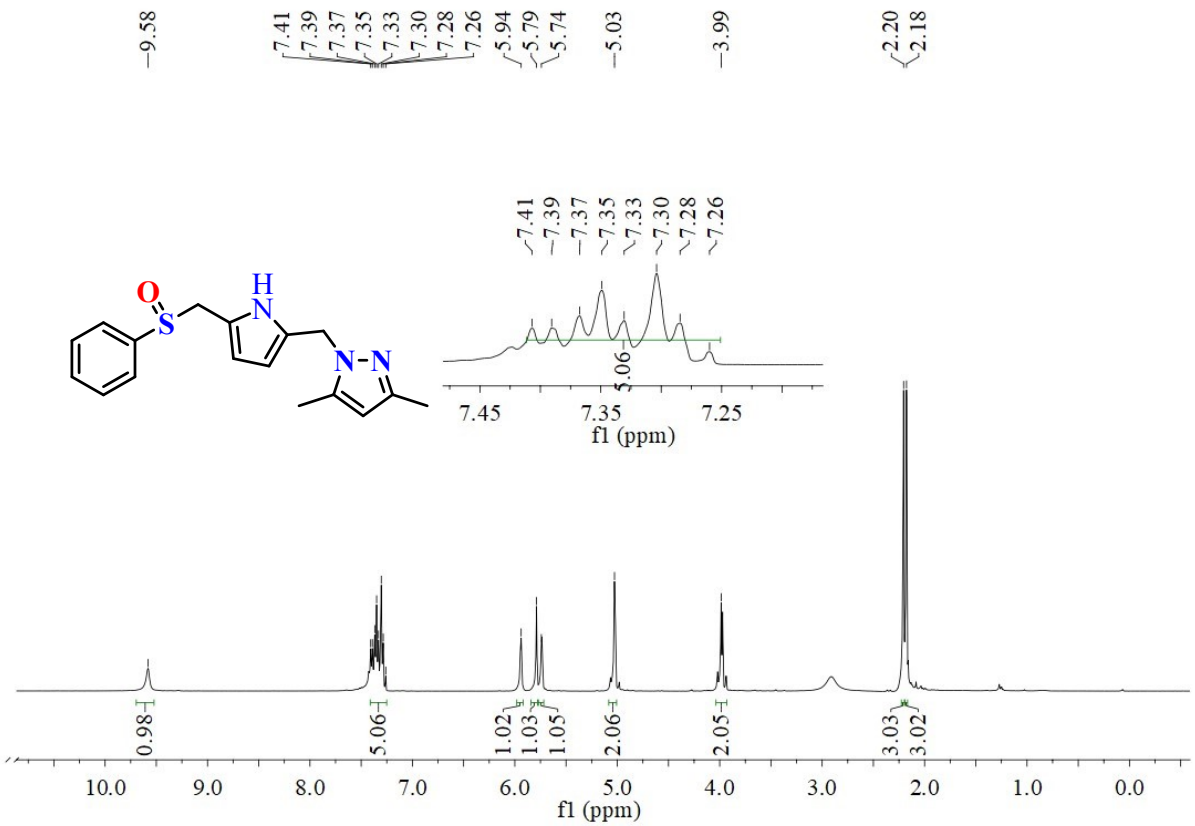

Figure S17. ^{1}H NMR (25 °C, 400 MHz) spectrum of the sulfoxide **3** in $CDCl_3$.

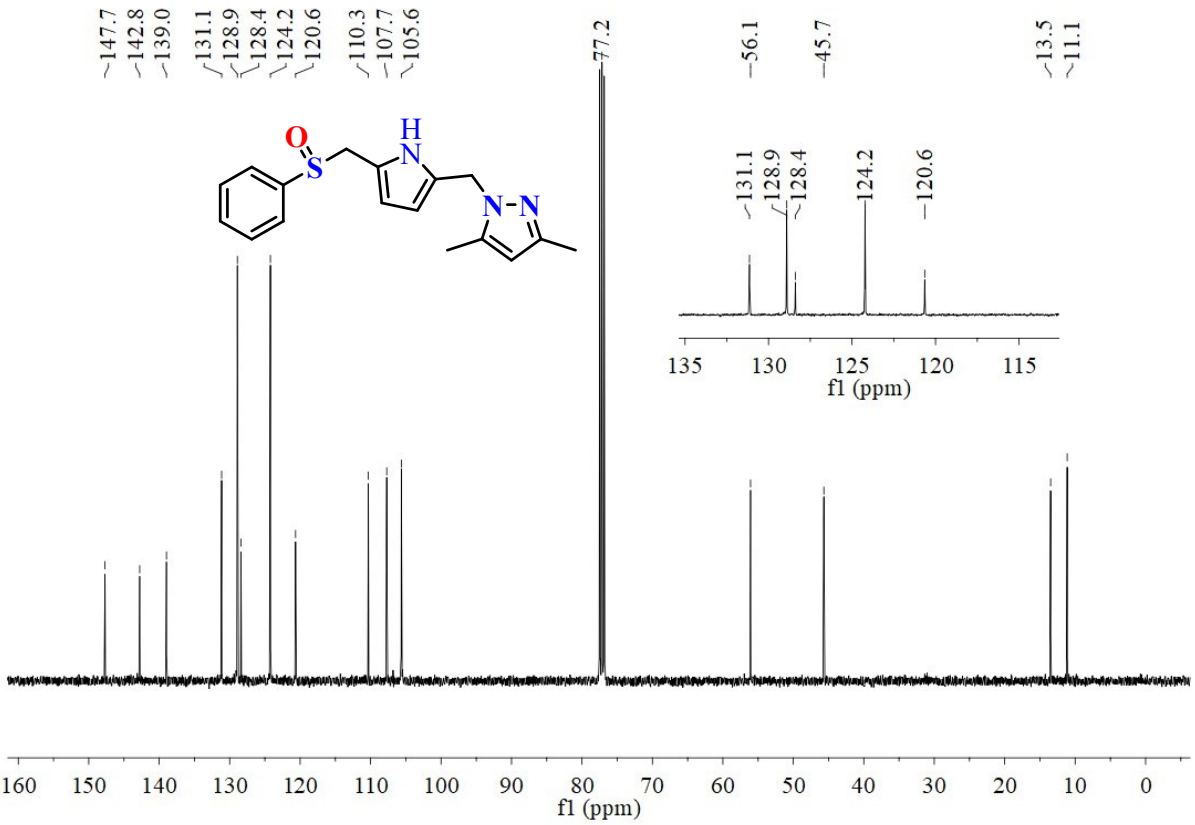

Figure S18. ^{13}C{^{1}H} NMR (25 °C, 125.7 MHz) spectrum of the sulfoxide **3** in $CDCl_3$.

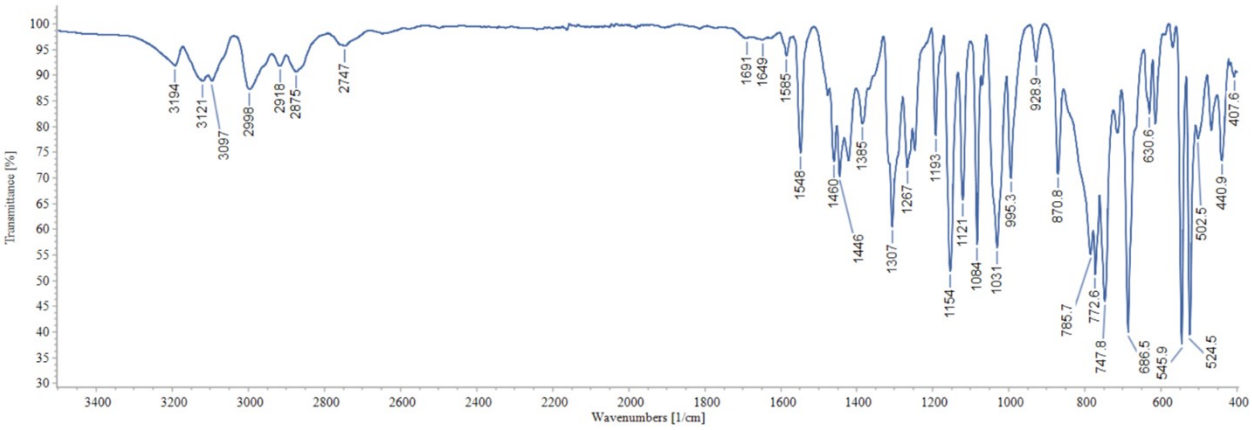

Figure S19. The ATR spectrum of the sulfoxide **3**.

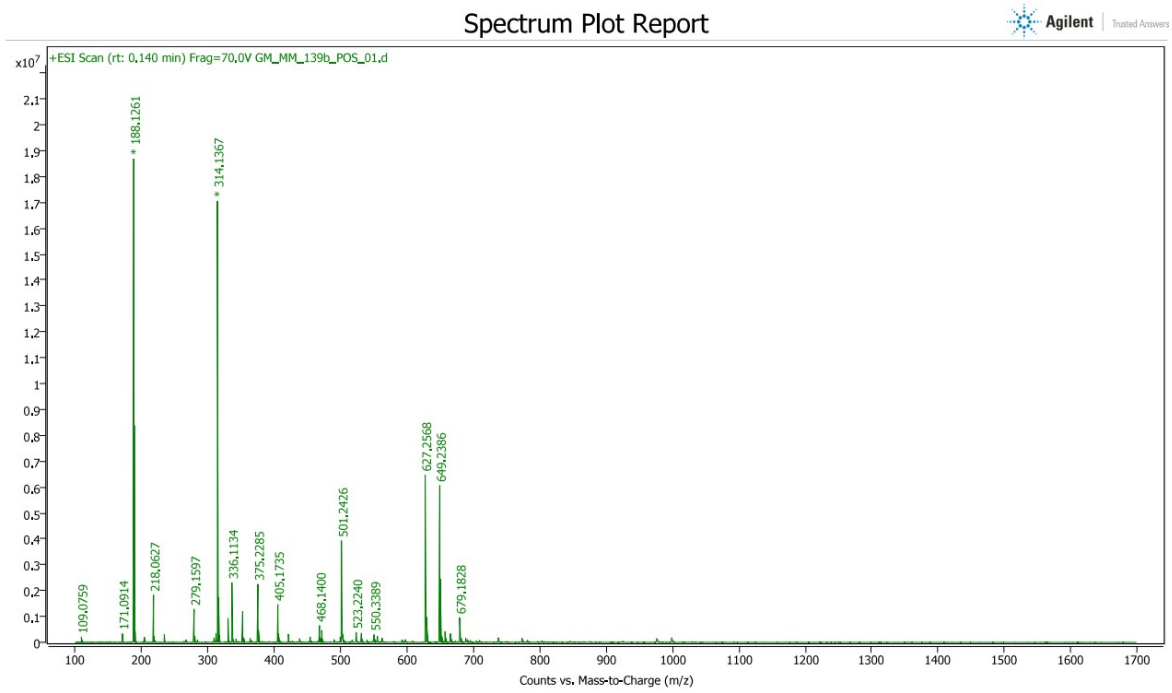

Figure S20. HRMS (ESI+) spectrum of the sulfoxide **3**.

Species	*m/z*, Found	*m/z,* Calculated
$[M+H]^+$	314.1367	314.1322
$[M+Na]^+$	336.1134	336.1141

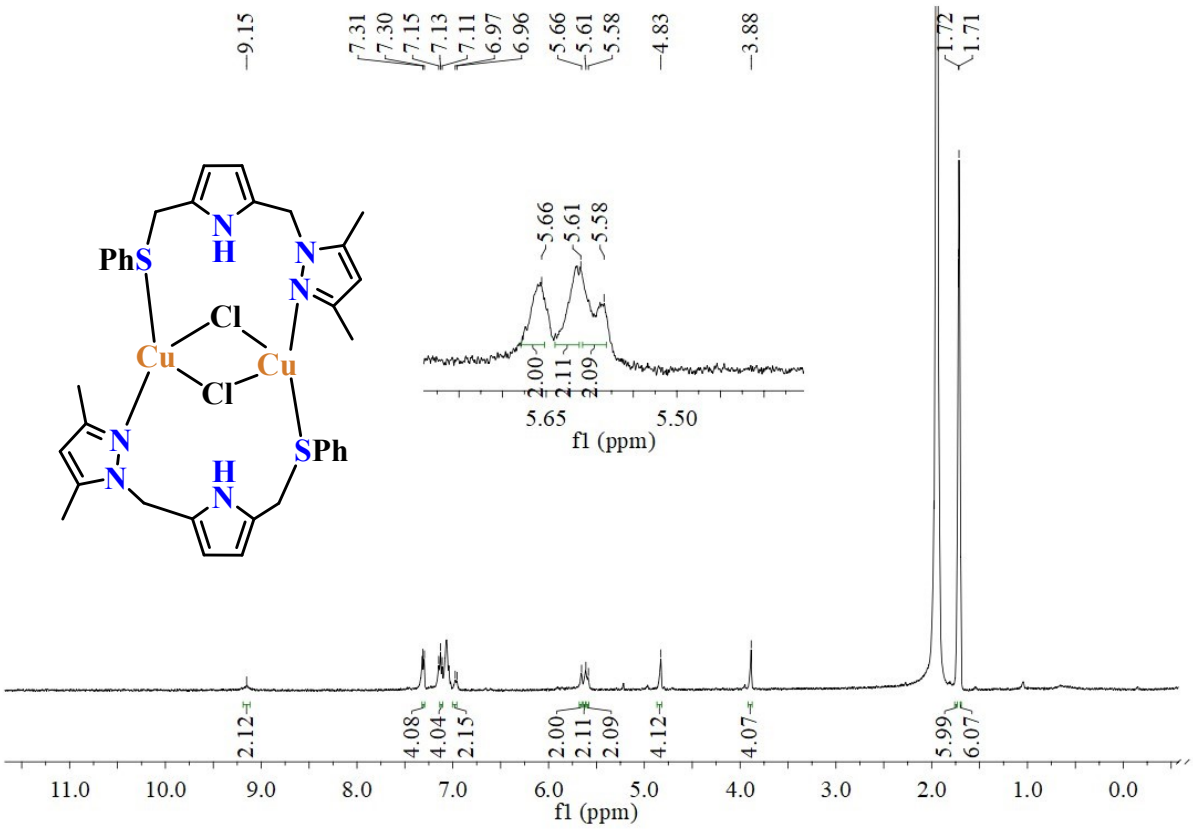

Figure S21. ^{1}H NMR (25 °C, 400 MHz) spectrum of complex **5** [Cu(μ-Cl){C_4H_3N-2-(CH_2Me_2pz)-5-(CH_2SPh)-κ^2-*S*,*N*}]$_2$ in CD_3CN.

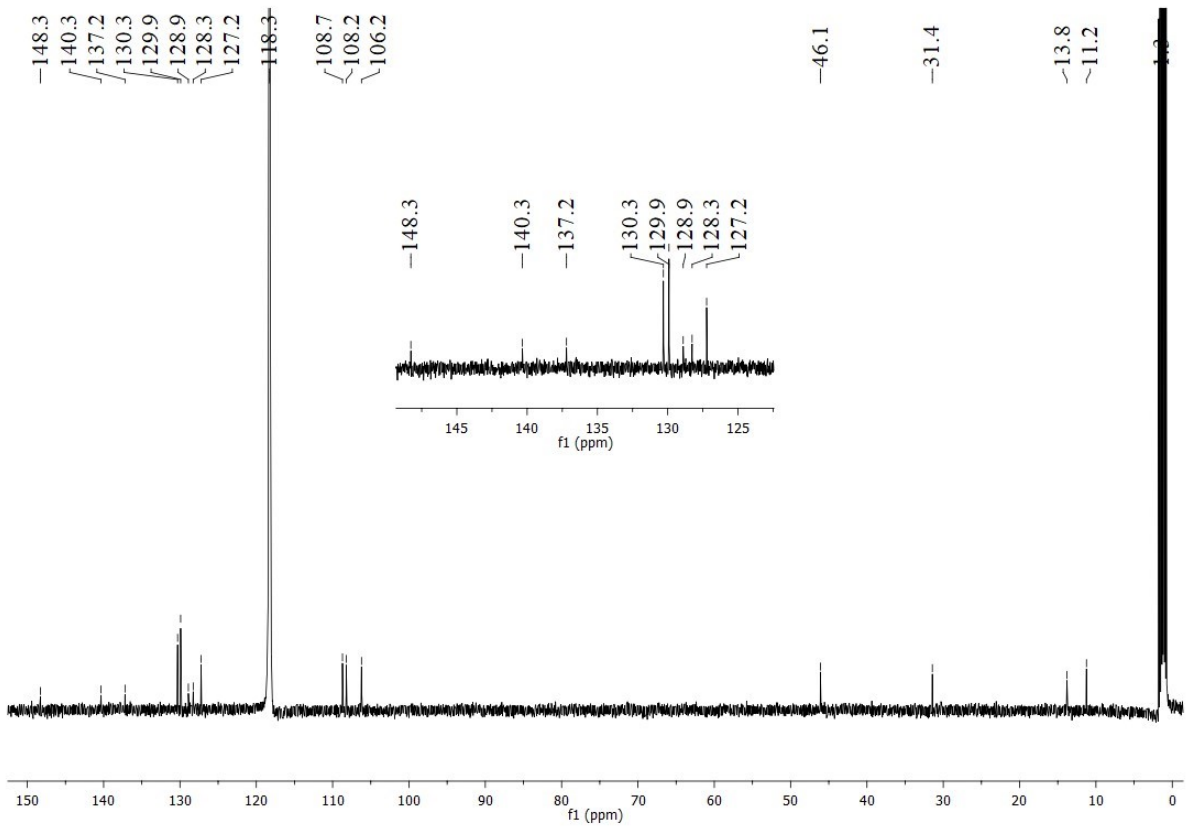

Figure S22. $^{13}C\{^{1}H\}$ NMR (25 °C, 125.7 MHz) spectrum of complex **5** [Cu(μ-Cl){C_4H_3N-2-(CH_2Me_2pz)-5-(CH_2SPh)-κ^2-*S*,*N*}]$_2$ in CD_3CN.

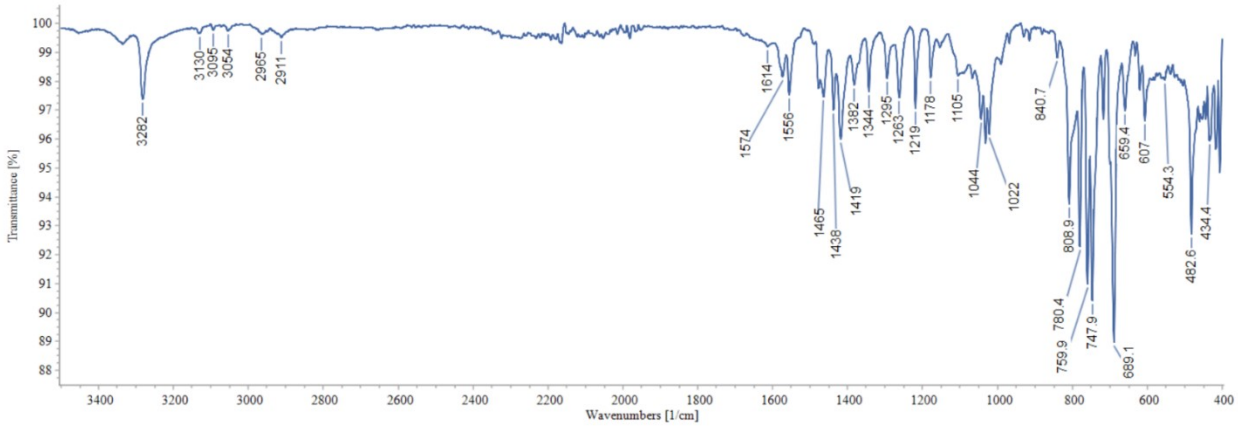

Figure S23. The ATR spectrum of complex **5** [Cu(μ-Cl){C_4H_3N-2-(CH_2Me_2pz)-5-(CH_2SPh)-κ^2-*S*,*N*}]$_2$.

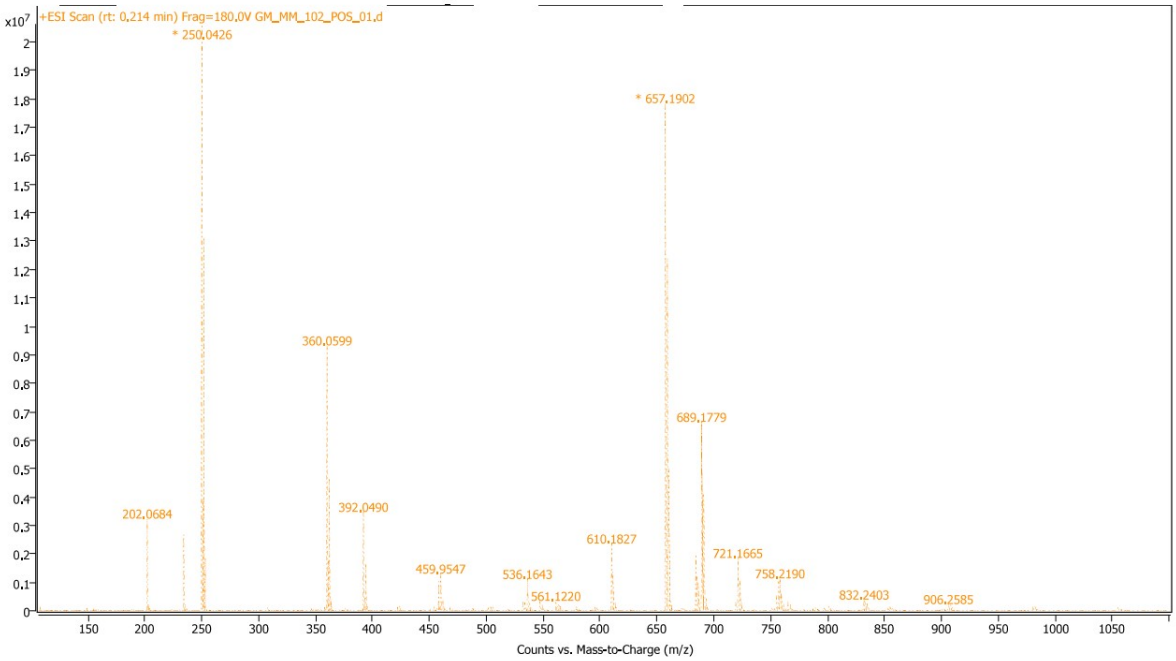

Figure S24. HRMS (ESI+) spectrum of complex **5** [Cu(μ-Cl){C_4H_3N-2-(CH_2Me_2pz)-5-(CH_2SPh)-κ^2-*S*,*N*}]$_2$.

Species	*m*/*z*, Found	*m*/*z,* Calculated
[M-$CuCl_2$]$^+$	657.1902	657.1895
[Cu(ligand **2**)$_2$(MeOH)]$^+$	689.1779	689.2158
[Cu(ligand **2**)]$^+$	360.0599	360.0596

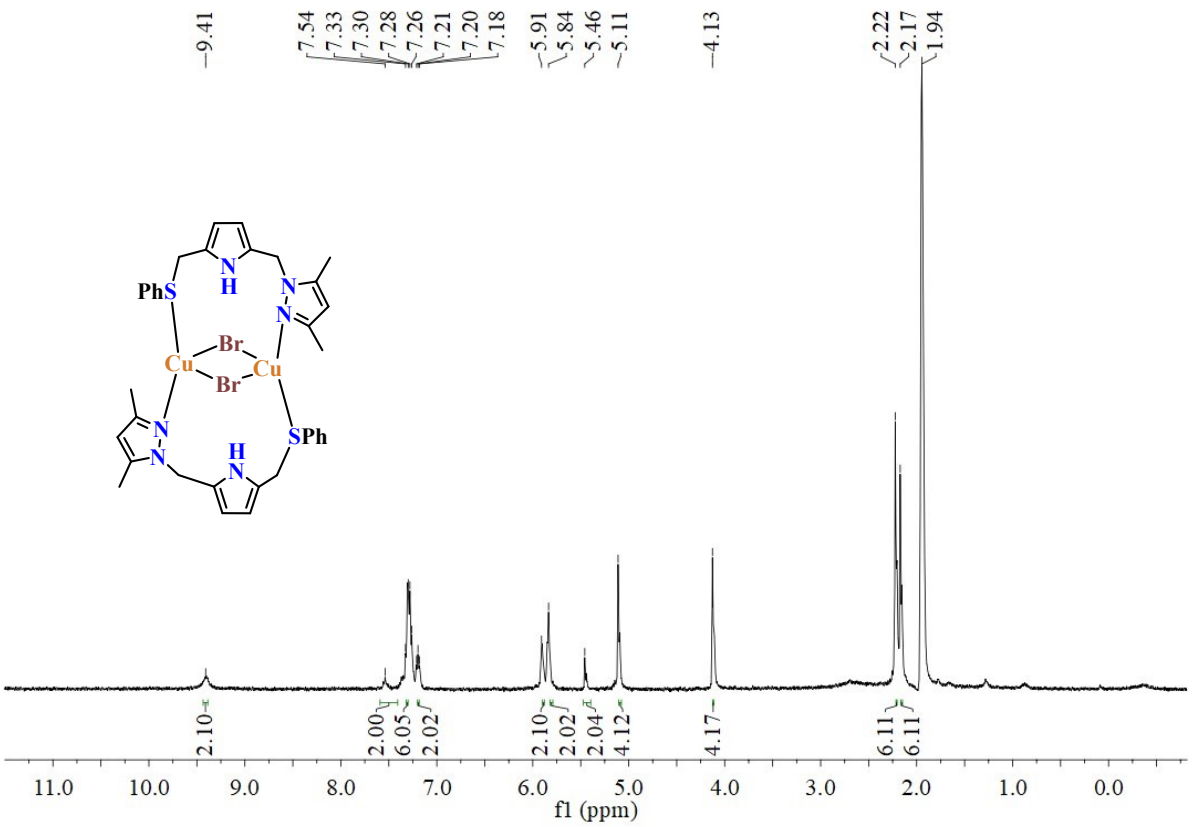

Figure S25. ^{1}H NMR (25 °C, 400 MHz) spectrum of complex **6** [Cu(μ-Br){C_4H_3N-2-(CH_2Me_2pz)-5-(CH_2SPh)-κ^2-*S*,*N*}]$_2$ in CD_3CN.

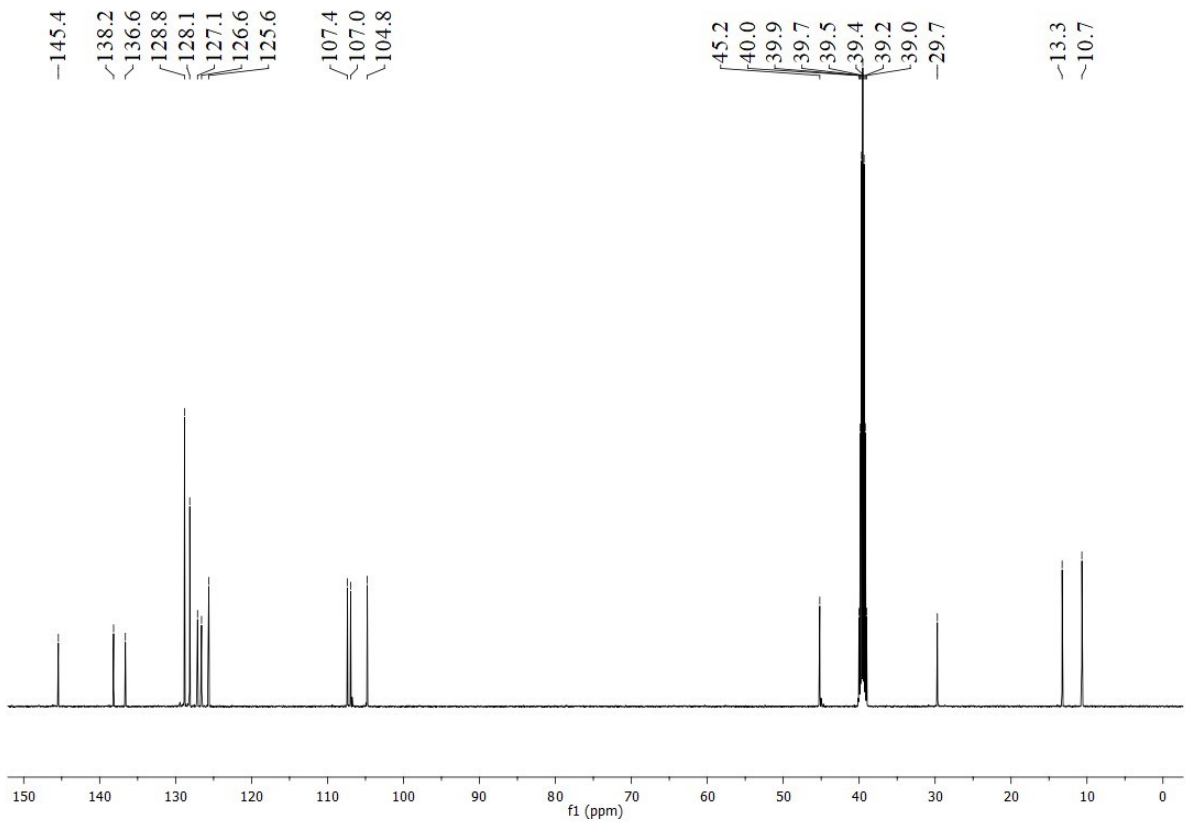

Figure S26. $^{13}C\{^{1}H\}$ NMR (25 °C, 125.7 MHz) spectrum of complex **6** [Cu(μ-Br){C_4H_3N-2-(CH_2Me_2pz)-5-(CH_2SPh)-κ^2-*S*,*N*}]$_2$ in DMSO-d_6.

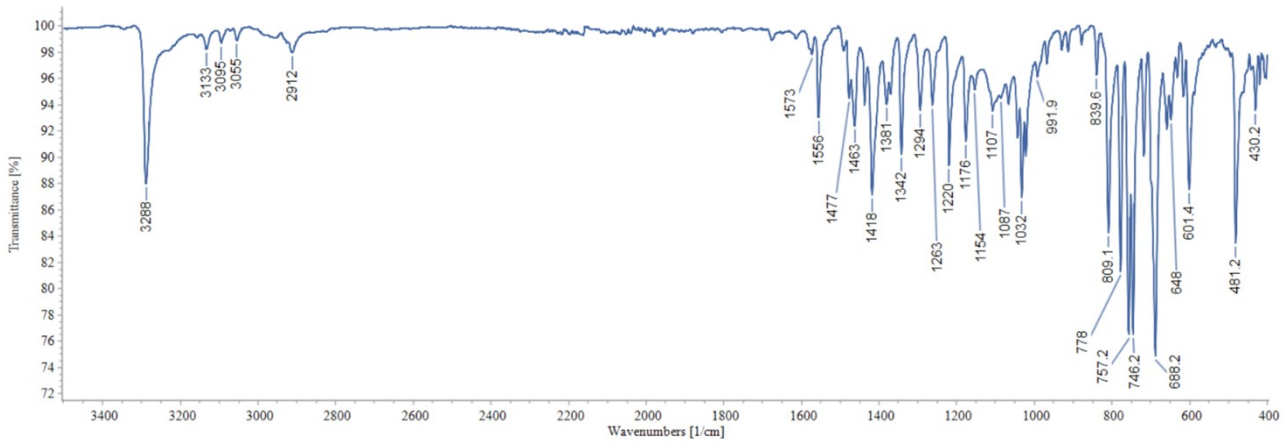

Figure S27. The ATR spectrum of complex **6** [Cu(μ-Br){C_4H_3N-2-(CH_2Me_2pz)-5-(CH_2SPh)-κ^2-*S*,*N*}]$_2$.

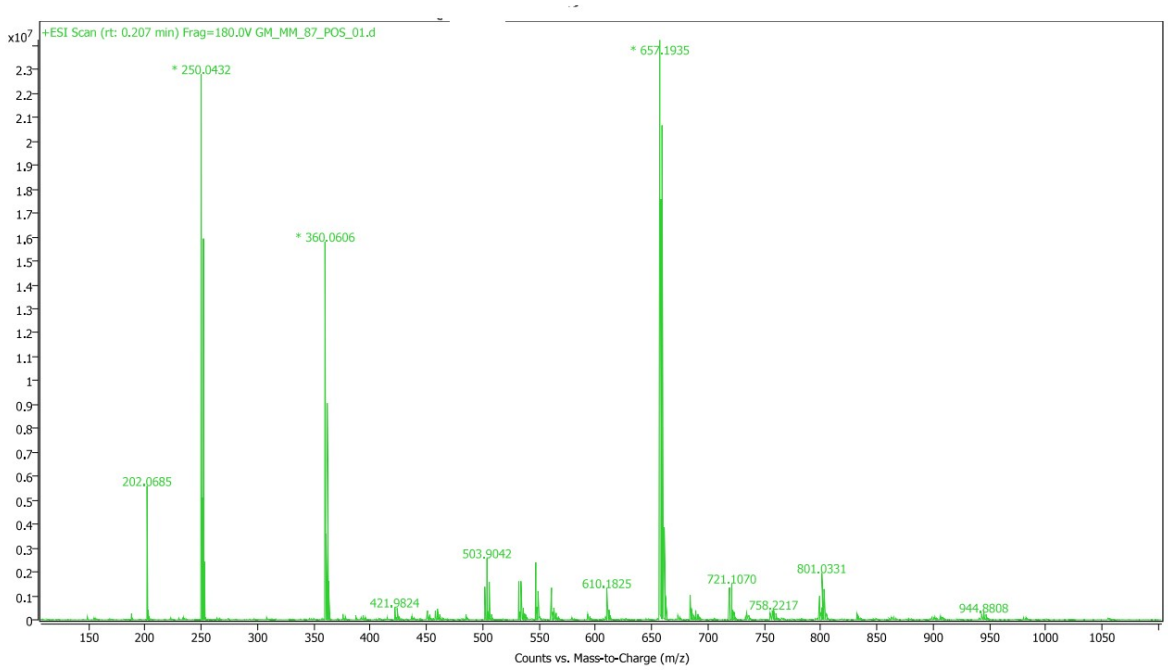

Figure S28. HRMS (ESI+) spectrum of complex **6** [Cu(μ-Br){C_4H_3N-2-(CH_2Me_2pz)-5-(CH_2SPh)-κ^2-*S*,*N*}]$_2$.

Species	*m*/*z*, Found	*m*/*z,* Calculated
[M-$CuCl_2$]$^+$	657.1935	657.1895
[Cu(ligand **2**)$_2$(MeOH)]$^+$	689.1779	689.2158
[Cu(ligand **2**)]$^+$	360.0606	360.0596

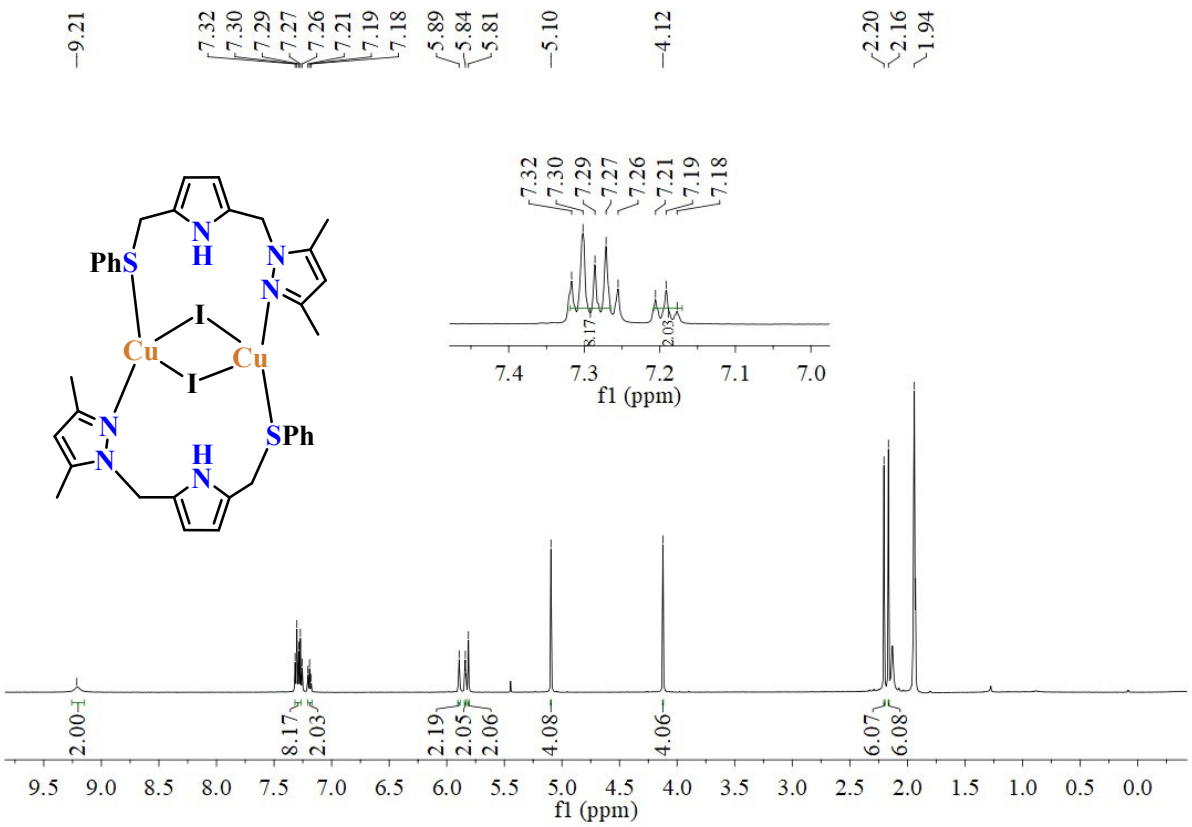

Figure S29. ^{1}H NMR (25 °C, 500 MHz) spectrum of complex **7** [Cu(μ-I){C_4H_3N-2-(CH_2Me_2pz)-5-(CH_2SPh)-κ^2-*S*,*N*}]$_2$ in CD_3CN.

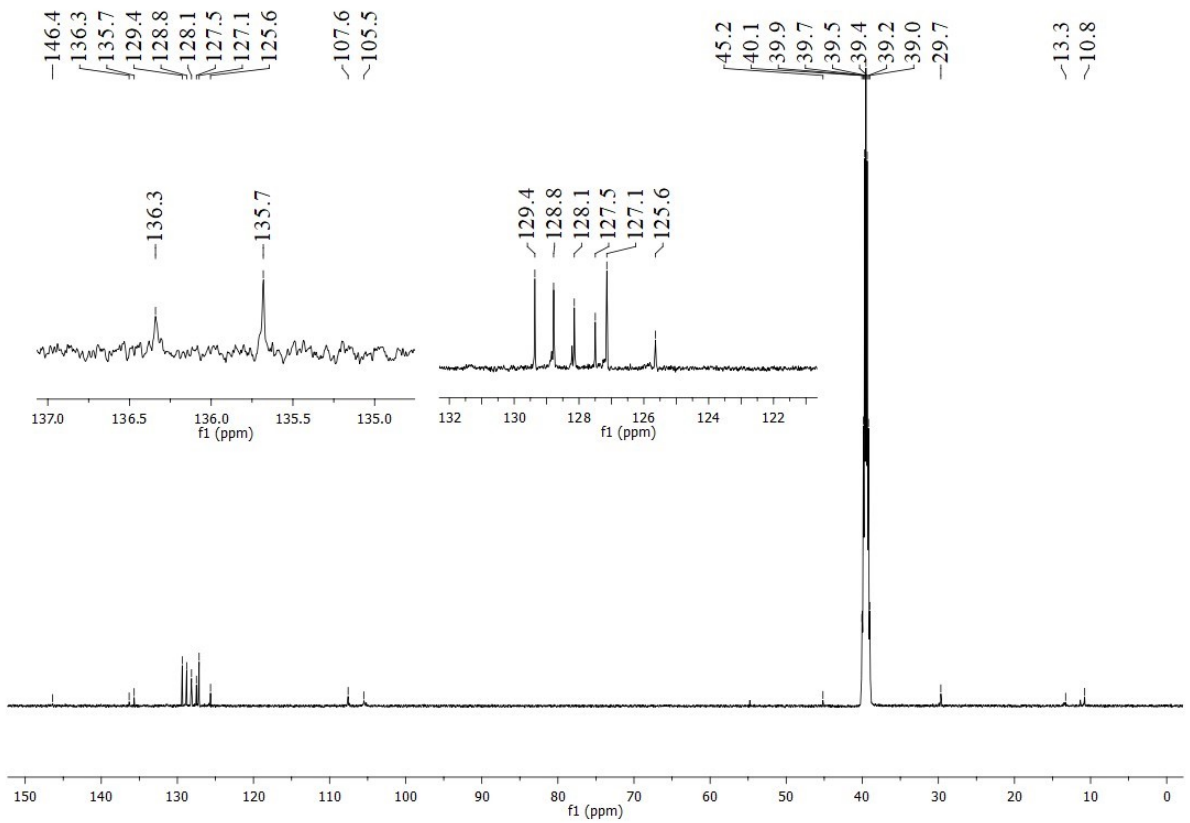

Figure S30. $^{13}C\{^{1}H\}$ NMR (25 °C, 125.7 MHz) spectrum of complex **7** [Cu(μ-I){C_4H_3N-2-(CH_2Me_2pz)-5-(CH_2SPh)-κ^2-*S*,*N*}]$_2$ in DMSO-d_6.

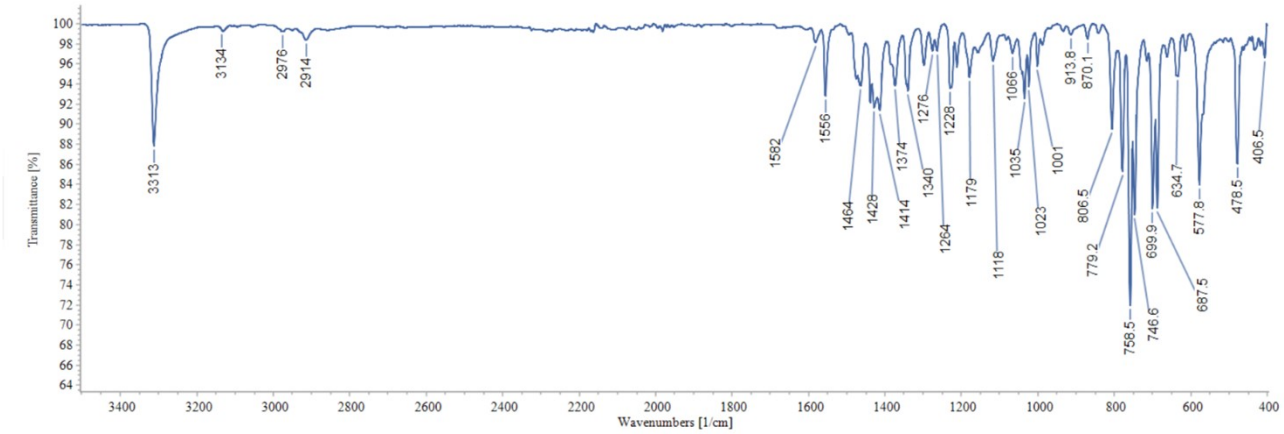

Figure S31. The ATR spectrum of complex **7** [Cu(μ-I){C_4H_3N-2-(CH_2Me_2pz)-5-(CH_2SPh)-κ^2-*S*,*N*}]$_2$.

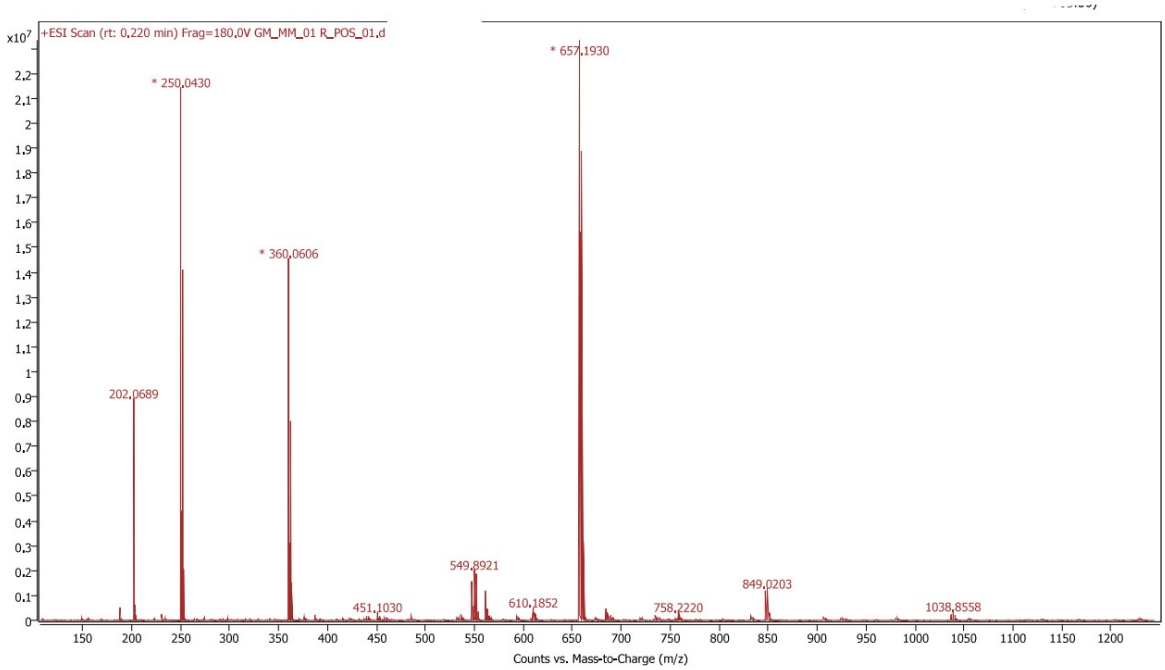

Figure S32. HRMS (ESI+) spectrum of complex **7** [Cu((μ-I){C_4H_3N-2-(CH_2Me_2pz)-5-(CH_2SPh)-κ^2-*S*,*N*}]$_2$.

Species	*m*/*z*, Found	*m*/*z*, Calculated
[M-$CuCl_2$]$^+$	657.1930	657.1895
[Cu(ligand **2**)]$^+$	360.0606	360.0596

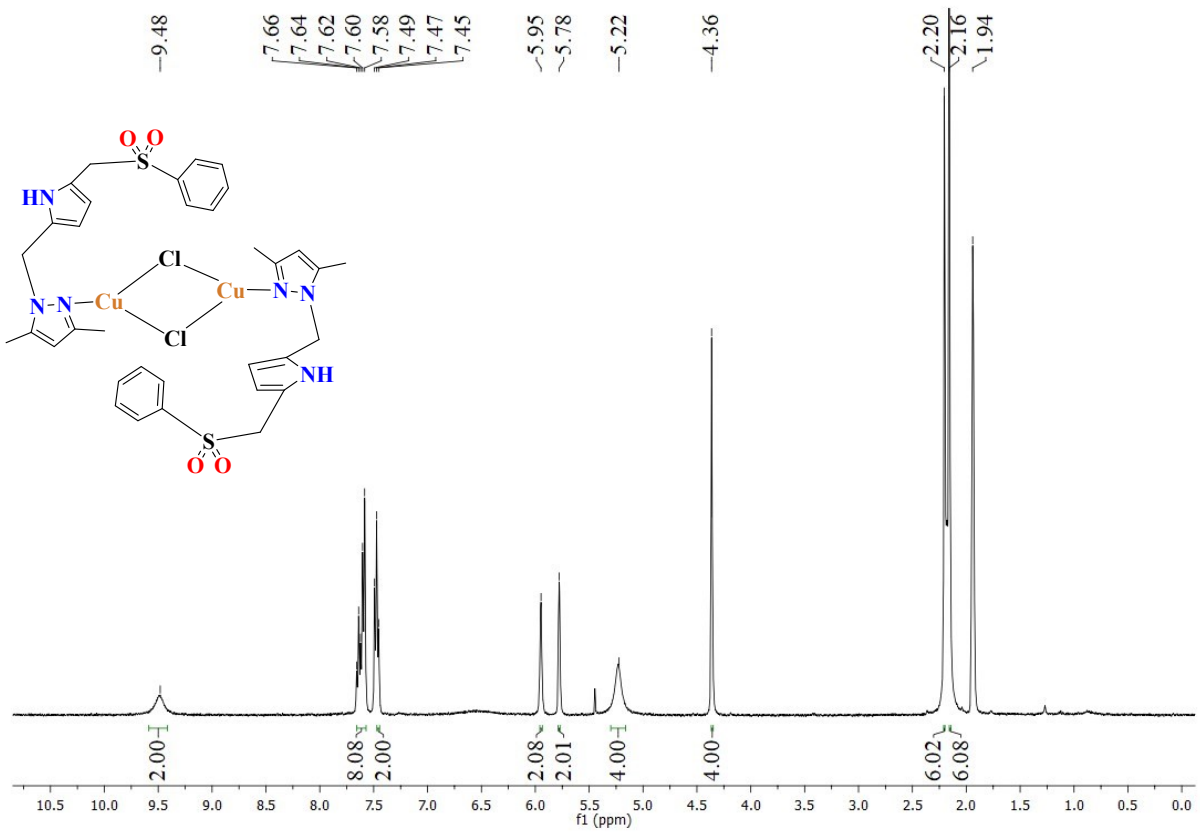

Figure S33. ^{1}H NMR (25 °C, 400 MHz) spectrum of complex **8** [Cu(μ-Cl){C_4H_3N-2-(CH_2Me_2pz)-5-(CH_2SO_2Ph)-κ^1-*N*}]$_2$ in CD_3CN.

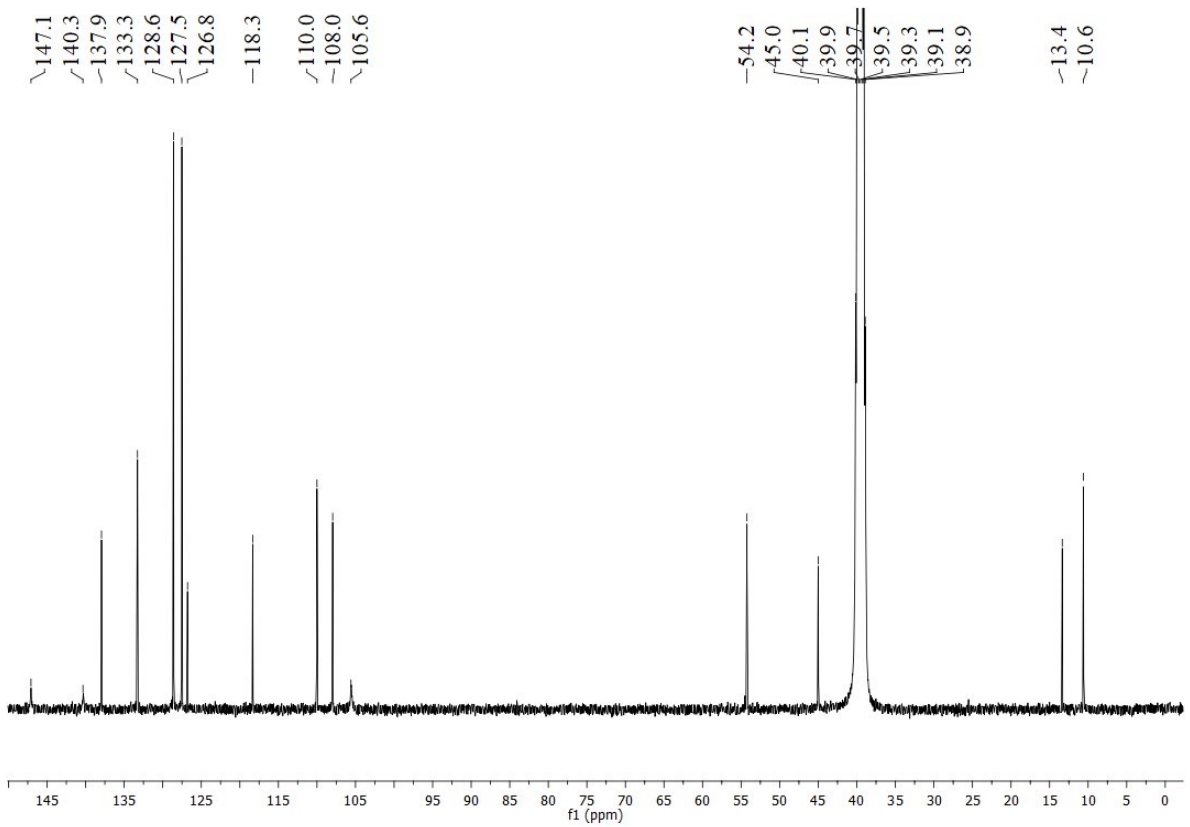

Figure S34. $^{13}C\{^{1}H\}$ NMR (25 °C, 100.6 MHz) spectrum of complex **8** [Cu(μ-Cl){C_4H_3N-2-(CH_2Me_2pz)-5-(CH_2SO_2Ph)-κ^1-N}]$_2$ in DMSO-d_6.

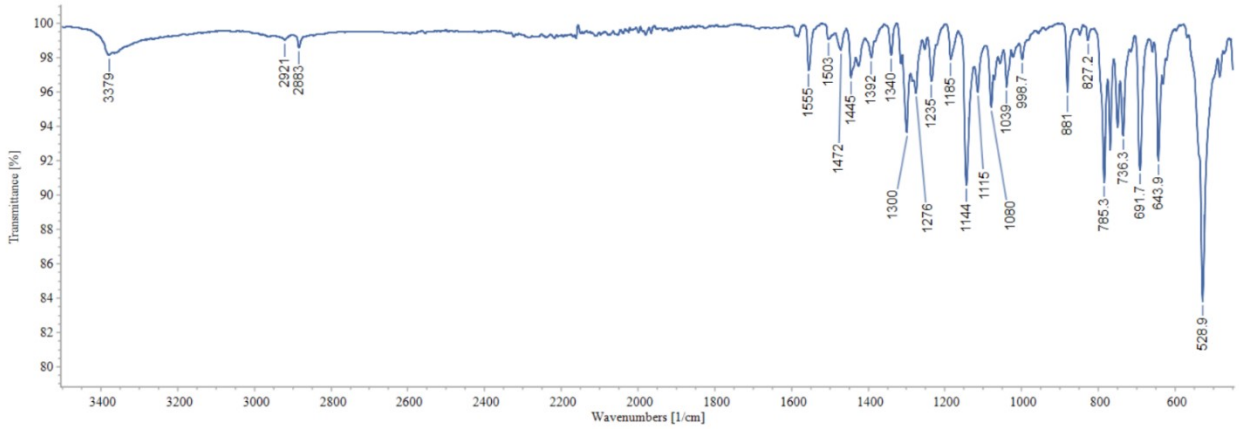

Figure S35. The ATR spectrum of complex **8** [Cu(μ-Cl){C_4H_3N-2-(CH_2Me_2pz)-5-(CH_2SO_2Ph)-κ^1-N}]$_2$.

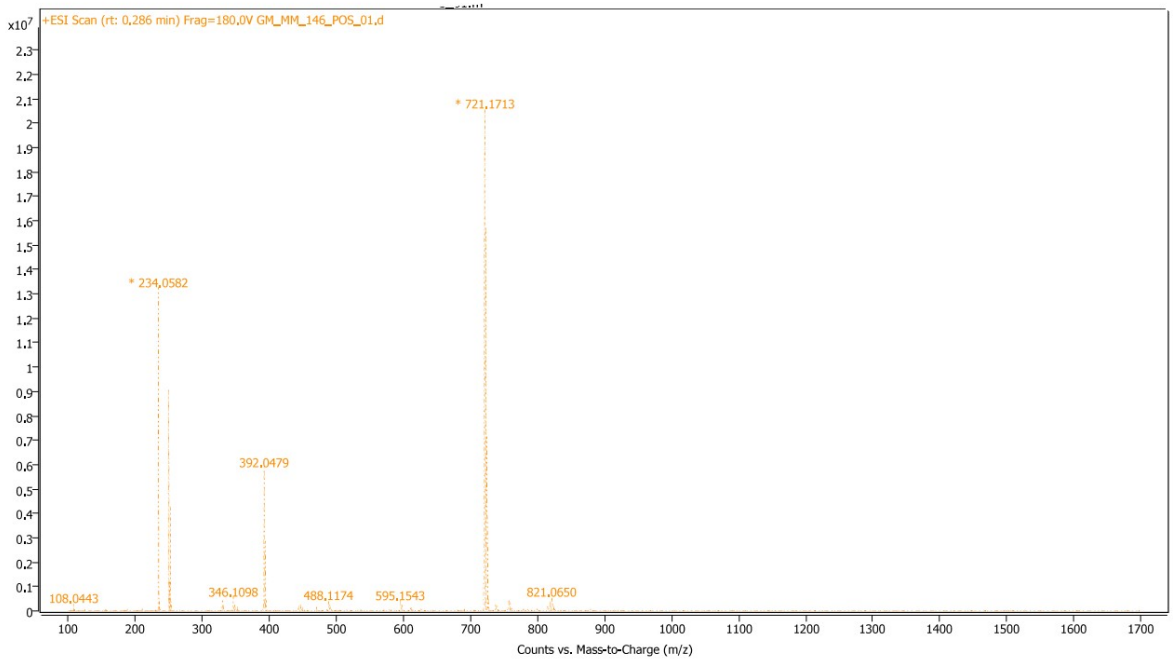

Figure S36. HRMS (ESI+) spectrum of complex **8** [Cu(μ-Cl){C_4H_3N-2-(CH_2Me_2pz)-5-(CH_2SO_2Ph)-κ^1-*N*}]$_2$.

Species	*m/z*, Found	*m/z,* Calculated
[Cu{C_4H_3N-2-(CH_2Me_2pz)-5-(CH_2SO_2Ph)-κ^1-*N*}$_2$]$^+$ (Cu(ligand **4**)$_2^+$)	721.1713	721.1692
[Cu{C_4H_3N-2-(CH_2Me_2pz)-5-(CH_2SO_2Ph)-κ^1-*N*}]$^+$ (Cu(ligand **4**)$^+$)	392.0479	392.0494
[Cu(CH_3OH)$_3$ {C_4H_3N-2-(CH_2Me_2pz)-5-(CH_2SO_2Ph)-κ^1-*N*}]$^+$ (Cu(CH_3OH)$_3$(ligand **4**)$^+$)	488.1174	488.1280

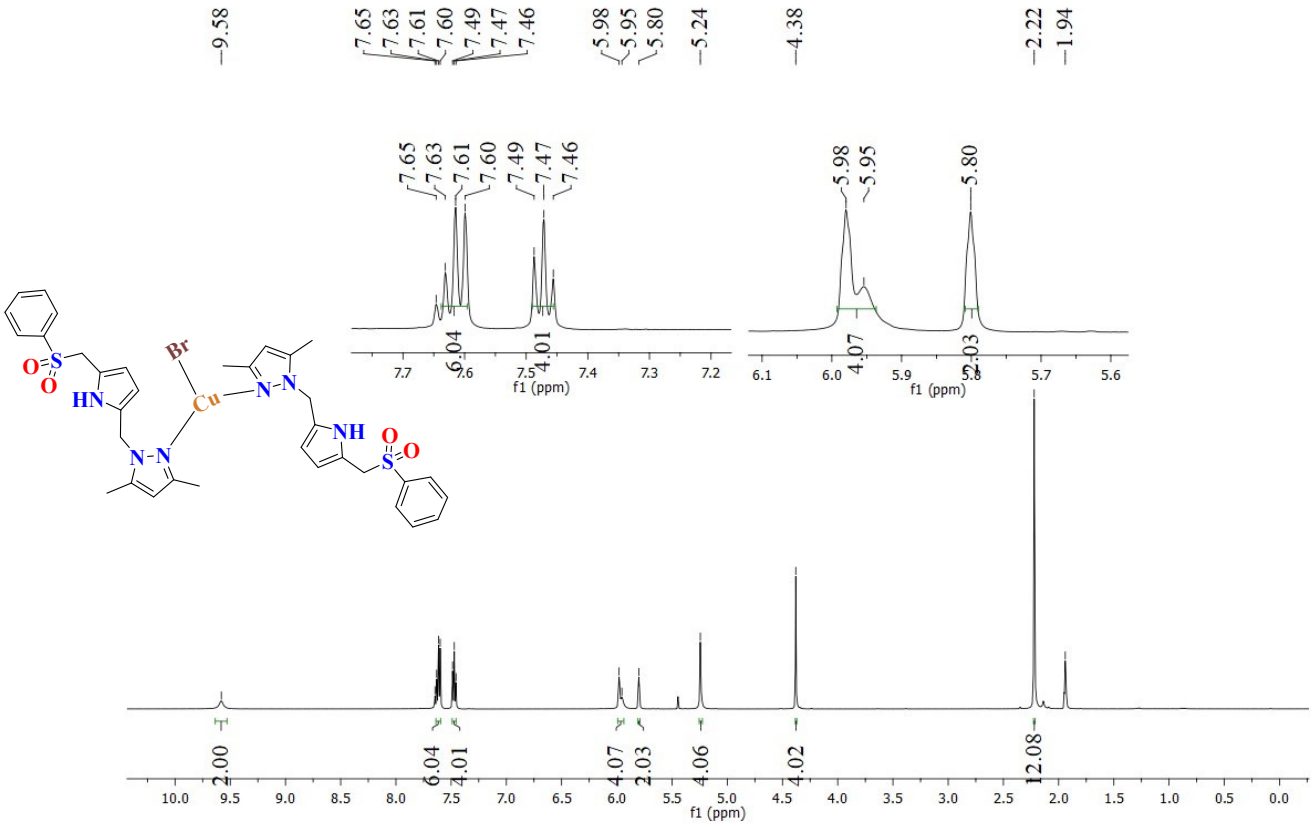

Figure S37. ^{1}H NMR (25 °C, 500 MHz) spectrum of complex **9** [CuBr{C_4H_3N-2-(CH_2Me_2pz)-5-(CH_2SO_2Ph)-κ^1-N}$_2$] in CD_3CN.

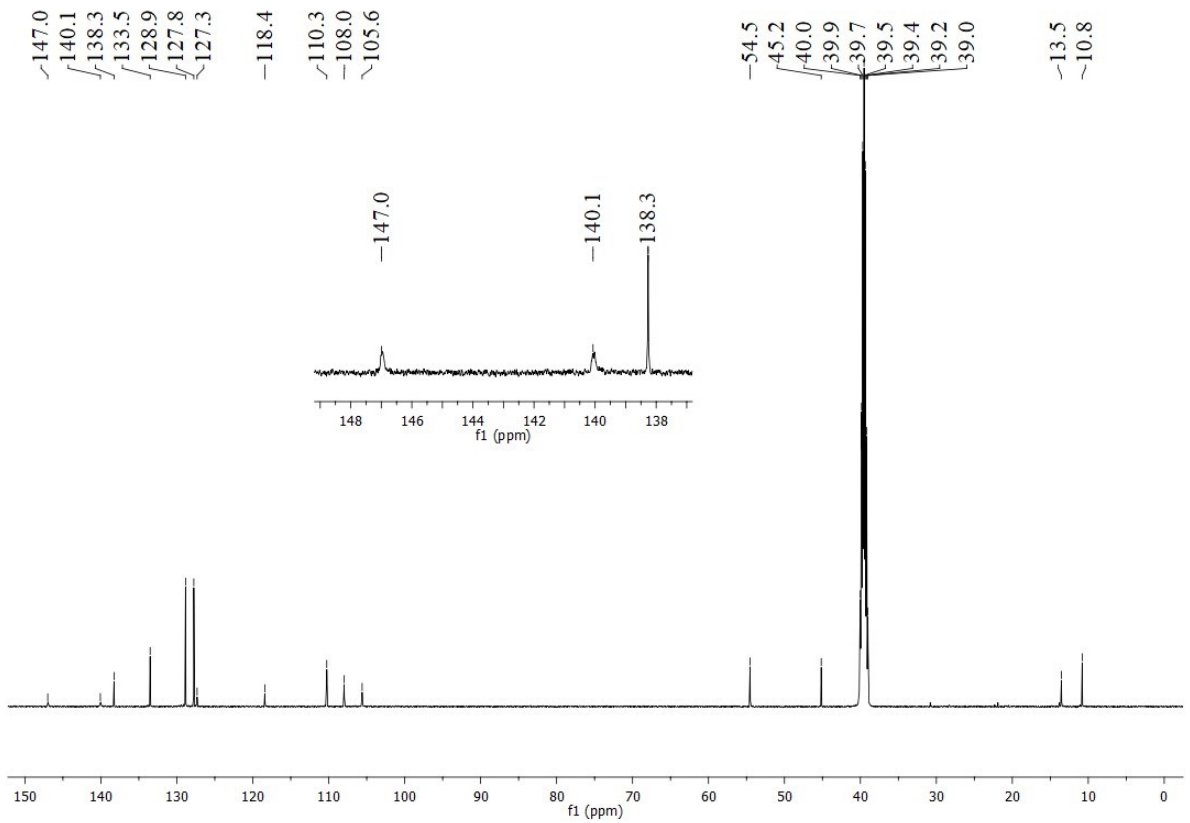

Figure S38. $^{13}C\{^{1}H\}$ NMR (25 °C, 125.7 MHz) spectrum of complex **9** [CuBr{C_4H_3N-2-(CH_2Me_2pz)-5-(CH_2SO_2Ph)-κ^1-N}$_2$] in DMSO-d_6.

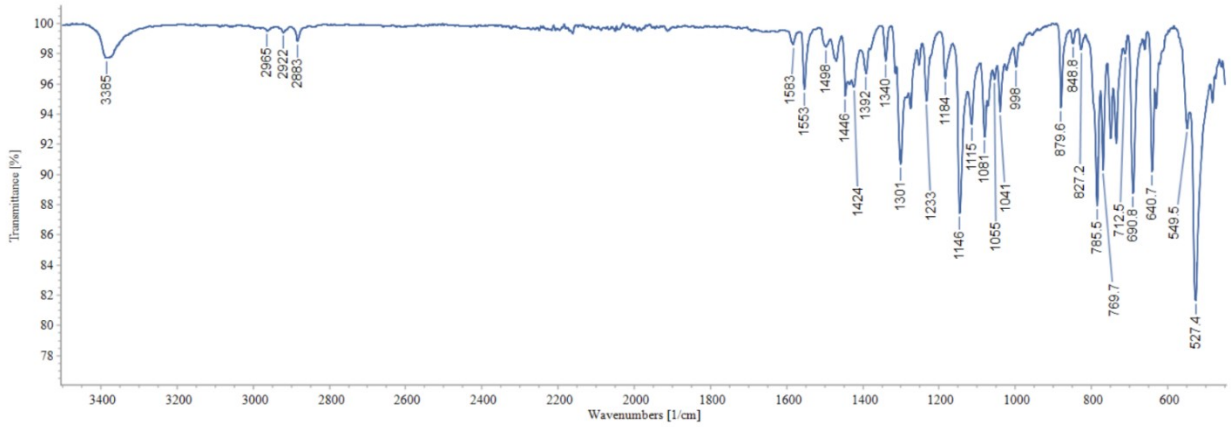

Figure S39. The ATR spectrum of complex **9** [CuBr{C_4H_3N-2-(CH_2Me_2pz)-5-(CH_2SO_2Ph)-κ^1-N}$_2$].

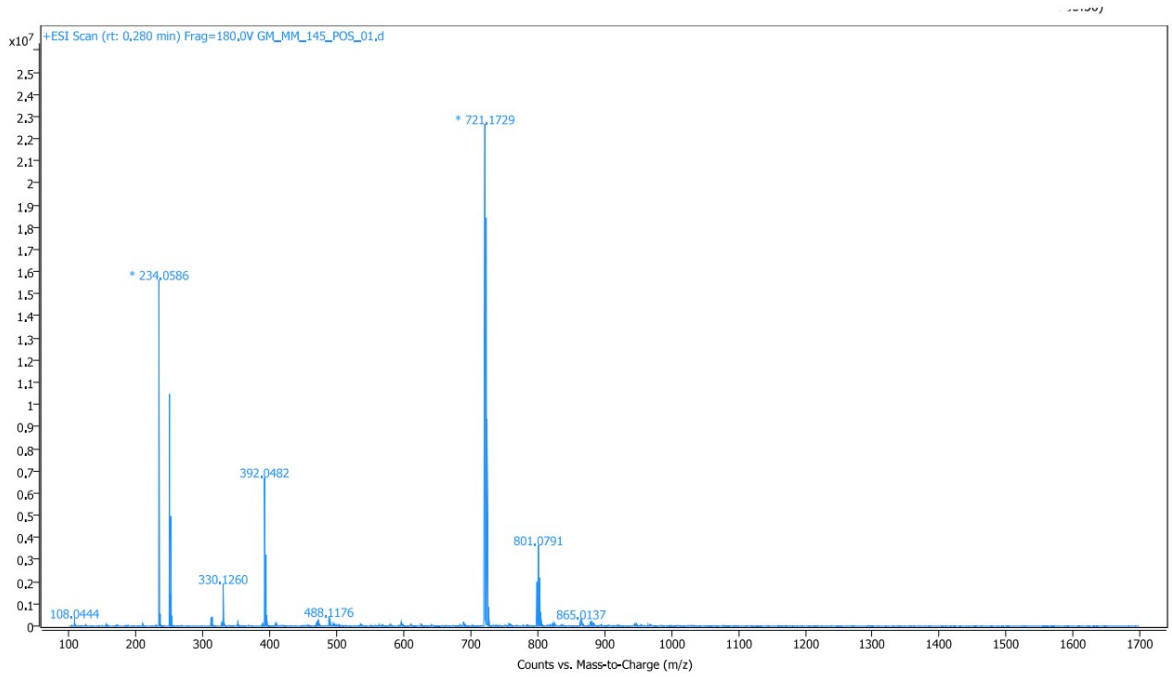

Figure S40. HRMS (ESI+) spectrum of complex **9** [CuBr{C_4H_3N-2-(CH_2Me_2pz)-5-(CH_2SO_2Ph)-κ^1-*N*}$_2$].

Species	*m/z*, Found	*m/z,* Calculated
[Cu{C_4H_3N-2-(CH_2Me_2pz)-5-(CH_2SO_2Ph)-κ^1-*N*}$_2$]$^+$ (Cu(ligand **4**)$_2^+$)	721.1729	721.1692
[Cu{C_4H_3N-2-(CH_2Me_2pz)-5-(CH_2SO_2Ph)-κ^1-*N*}]$^+$ (Cu(ligand **4**)$^+$)	392.0482	392.0494
[Cu(CH_3OH)$_3$ {C_4H_3N-2-(CH_2Me_2pz)-5-(CH_2SO_2Ph)-κ^1-*N*}]$^+$ (Cu(CH_3OH)$_3$(ligand **4**)$^+$)	488.1176	488.1280

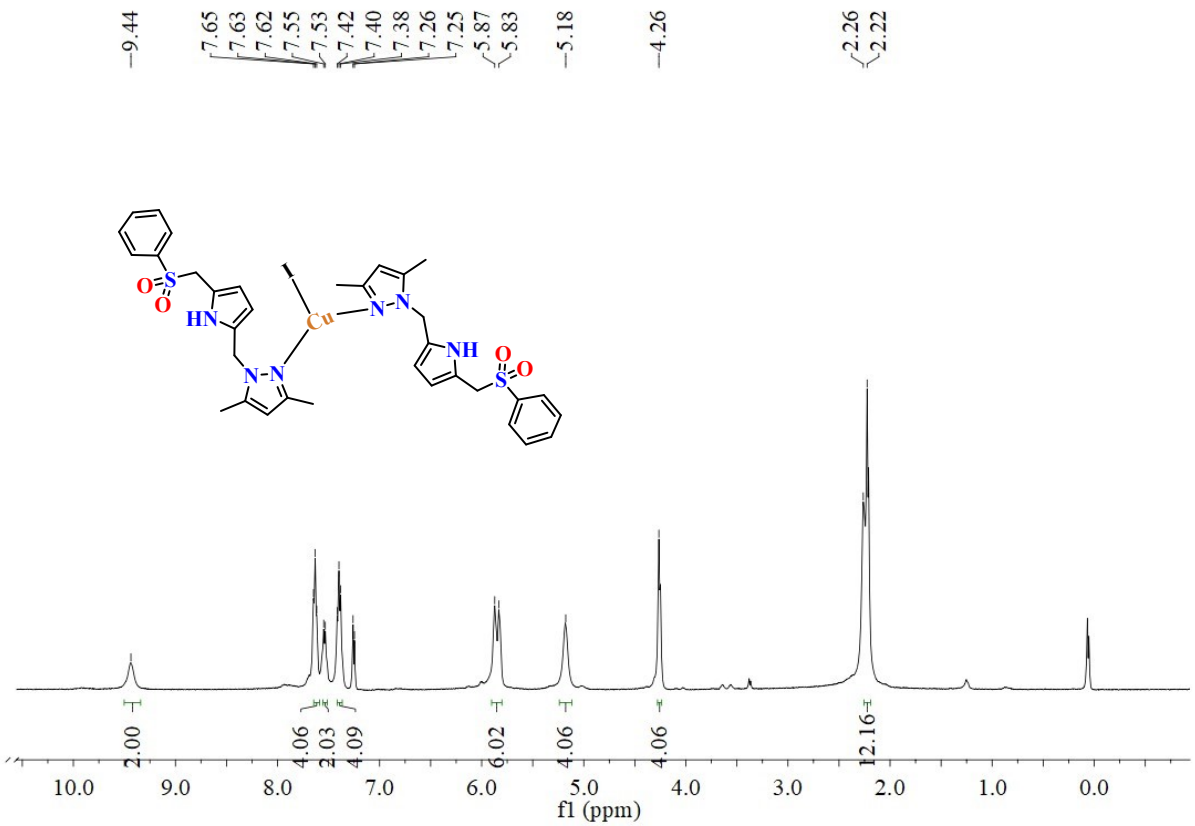

Figure S41. ^{1}H NMR (25 °C, 400 MHz) spectrum of complex **10** [CuI{C_4H_3N-2-(CH_2Me_2pz)-5-(CH_2SO_2Ph)-κ^1-N}$_2$] in $CDCl_3$.

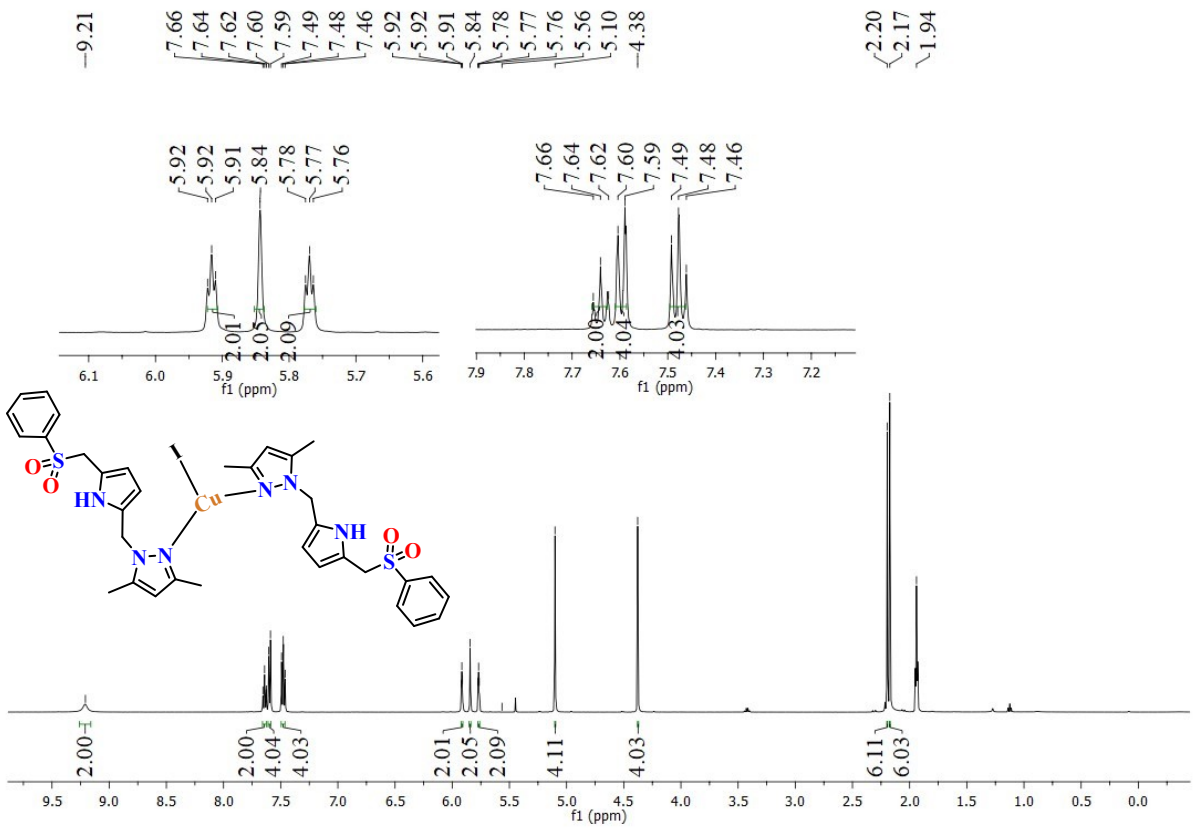

Figure S42. ^{1}H NMR (25 °C, 500 MHz) spectrum of complex **10** [CuI{C_4H_3N-2-(CH_2Me_2pz)-5-(CH_2SO_2Ph)-κ^1-N}$_2$] in CD_3CN.

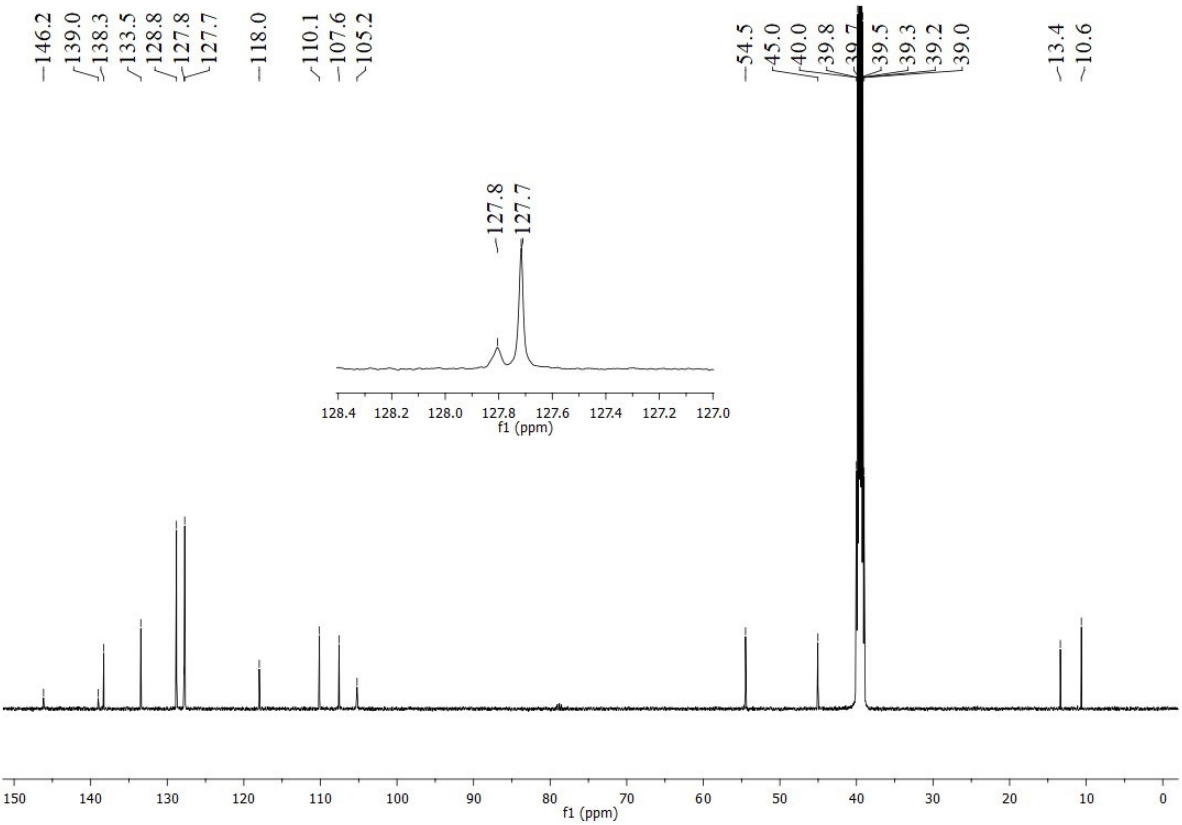

Figure S43. $^{13}C\{^{1}H\}$ NMR (25 °C, 125.7 MHz) spectrum of complex **10** [CuI{C_4H_3N-2-(CH_2Me_2pz)-5-(CH_2SO_2Ph)-κ^1-N}$_2$] in DMSO-d_6.

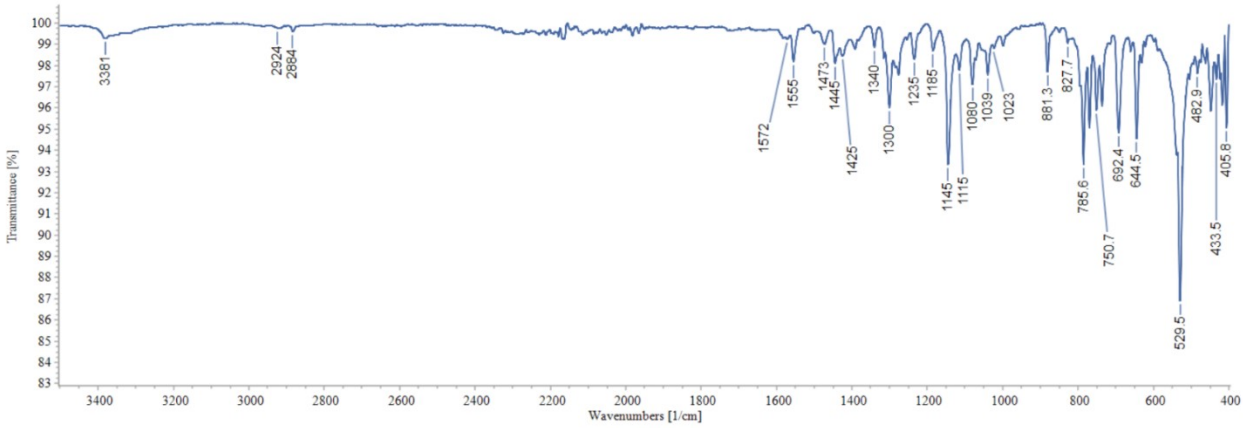

Figure S44. The ATR spectrum of complex **10** [CuI{C_4H_3N-2-(CH_2Me_2pz)-5-(CH_2SO_2Ph)-κ^1-N}$_2$].

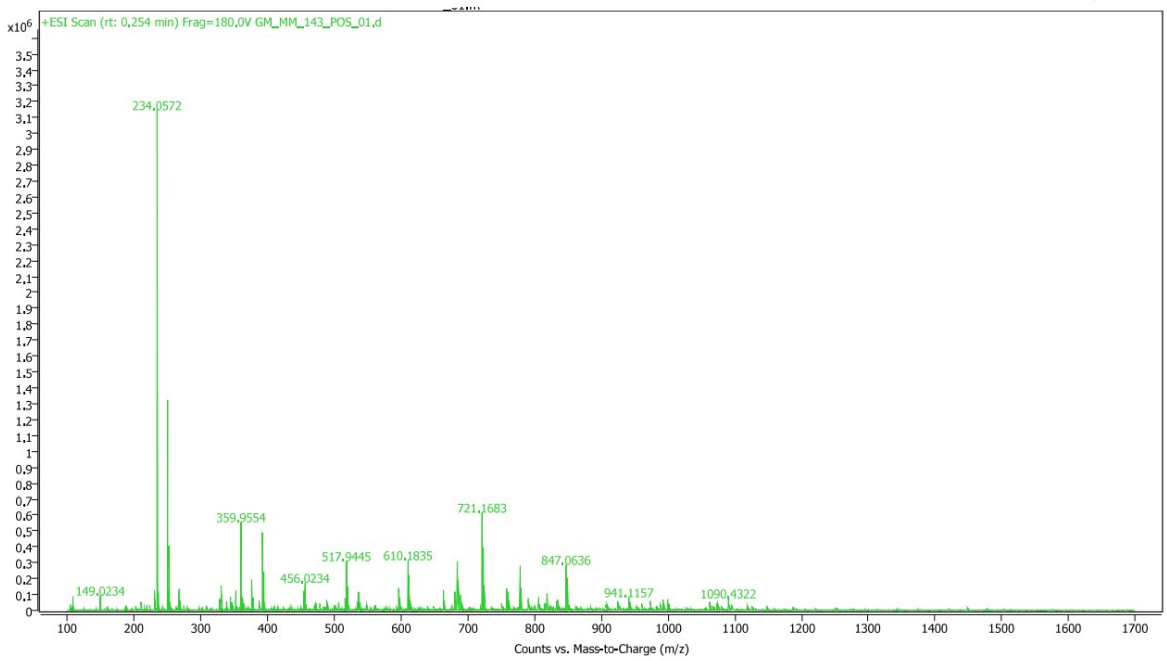

Figure S45. HRMS (ESI+) spectrum of complex **10** [CuI{C_4H_3N-2-(CH_2Me_2pz)-5-(CH_2SO_2Ph)-κ^1-N}$_2$].

Species	*m/z*, Found	*m/z,* Calculated
[Cu{C_4H_3N-2-(CH_2Me_2pz)-5-(CH_2SO_2Ph)-κ^1-N}$_2$]$^+$ (Cu(ligand **4**)$_2^+$)	721.1683	721.1692

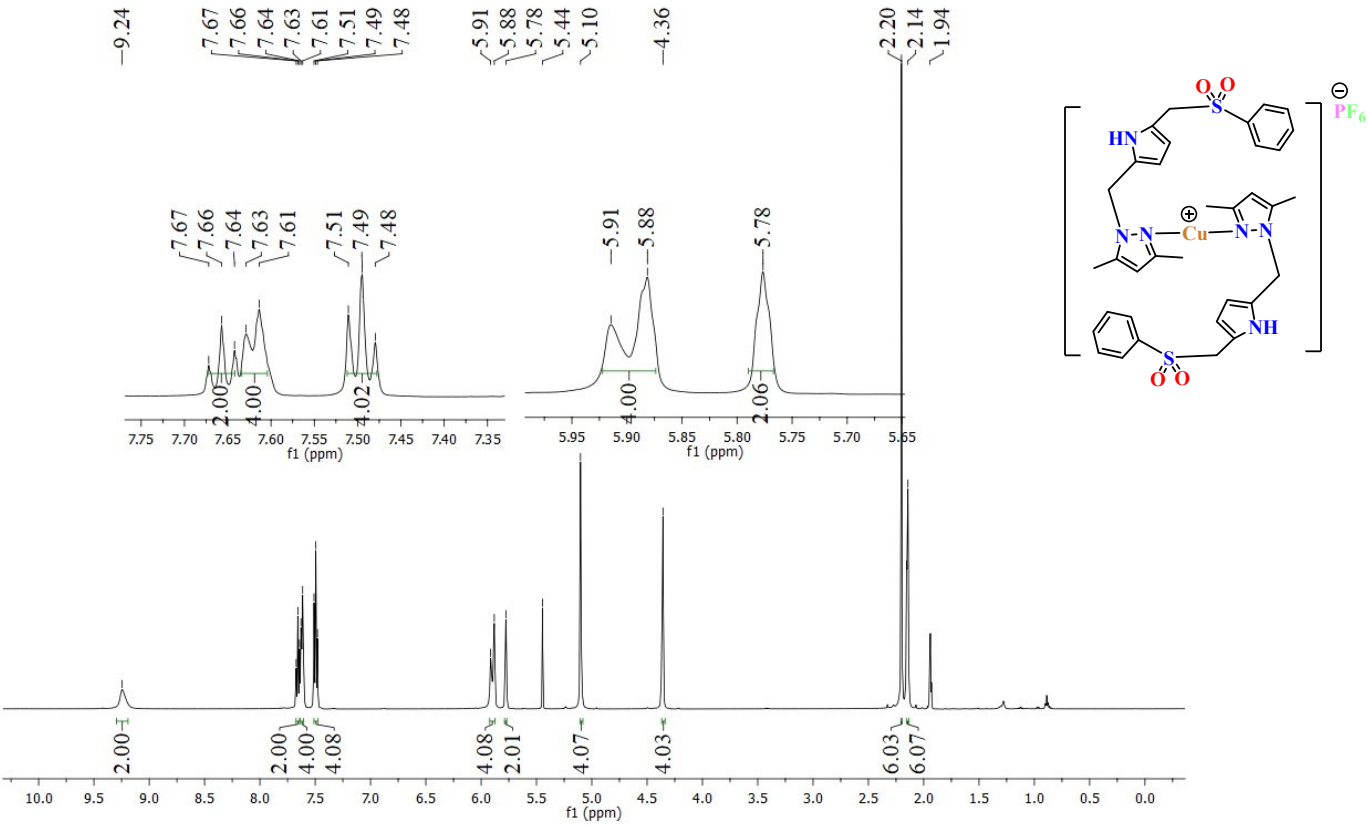

Figure S46. ^{1}H NMR (25 °C, 500 MHz) spectrum of complex **11a** [Cu{C_4H_3N-2-(CH_2Me_2pz)-5-(CH_2SO_2Ph)-κ^1-*N*}$_2$]PF_6 in CD_3CN.

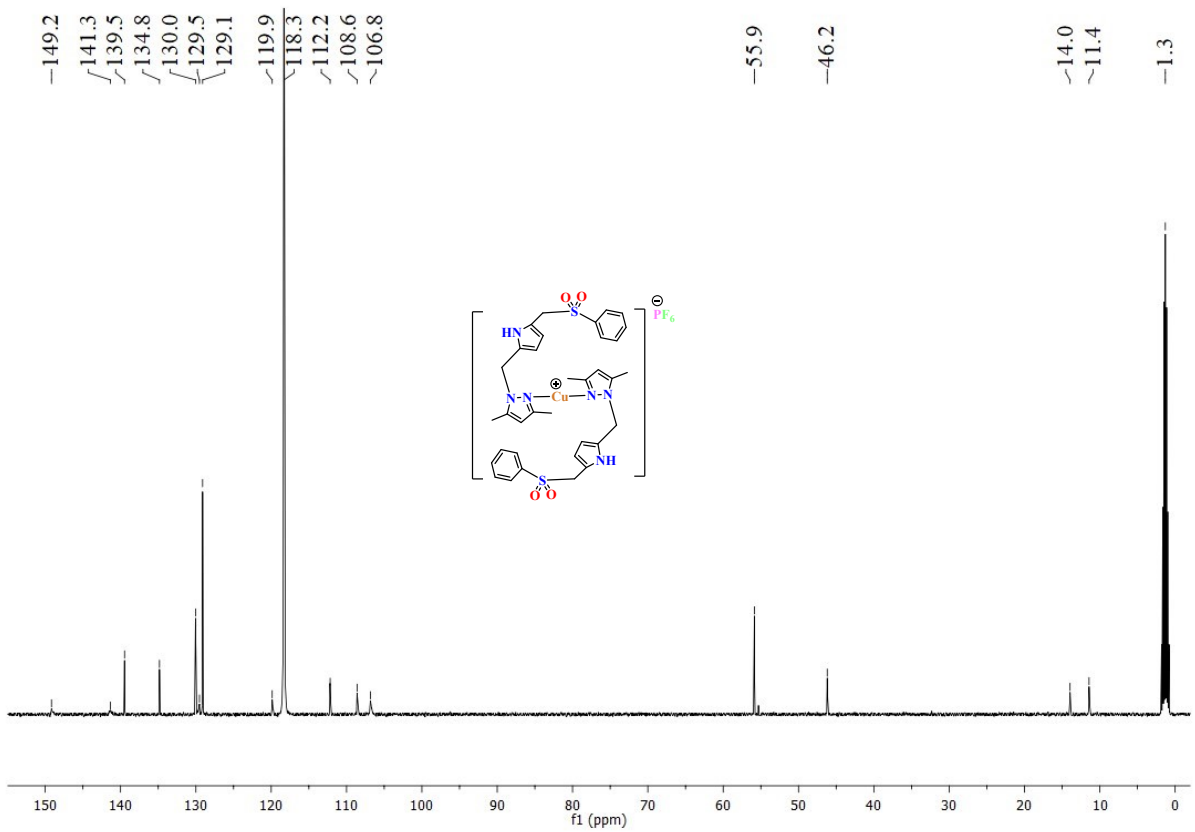

Figure S47. $^{13}C\{^{1}H\}$ NMR (25 °C, 125.7 MHz) spectrum of the complex **11a** [Cu{C_4H_3N-2-(CH_2Me_2pz)-5-(CH_2SO_2Ph)-κ^1-N}$_2$]PF_6 in CD_3CN.

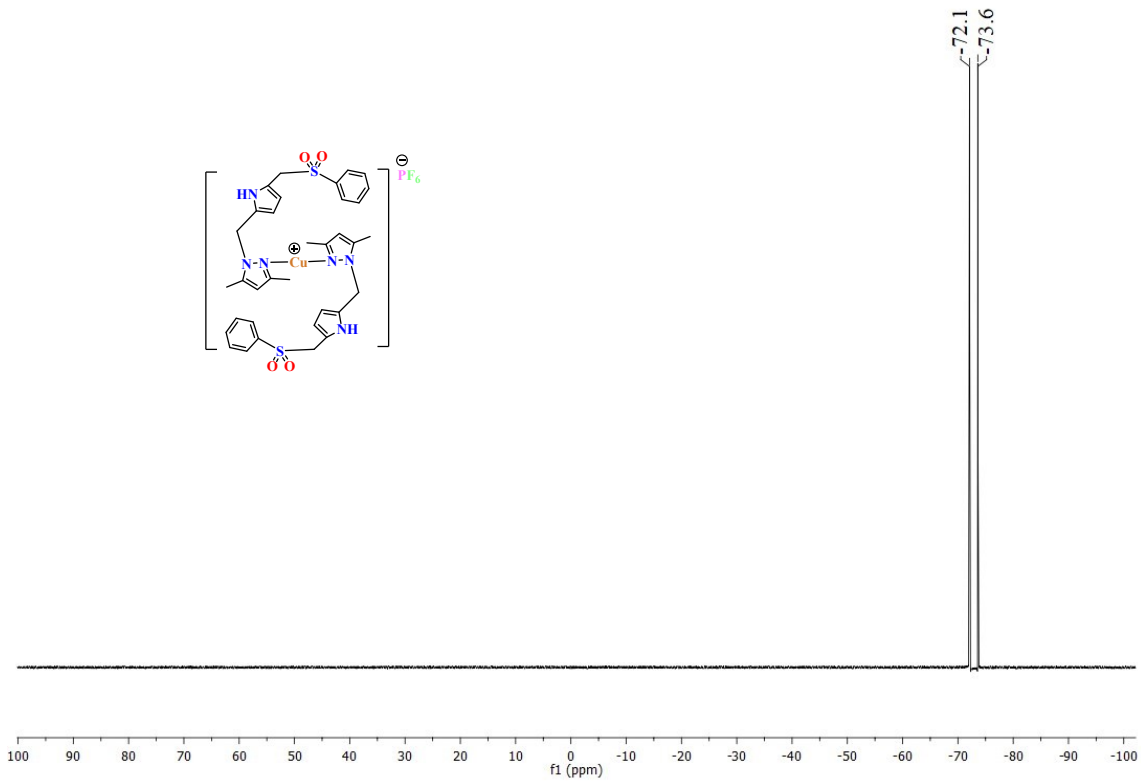

Figure S48. ^{19}F NMR (25 °C, 470.59 MHz) spectrum of complex **11a** [Cu{C_4H_3N-2-(CH_2Me_2pz)-5-(CH_2SO_2Ph)-κ^1-N}$_2$]PF_6 in CD_3CN.

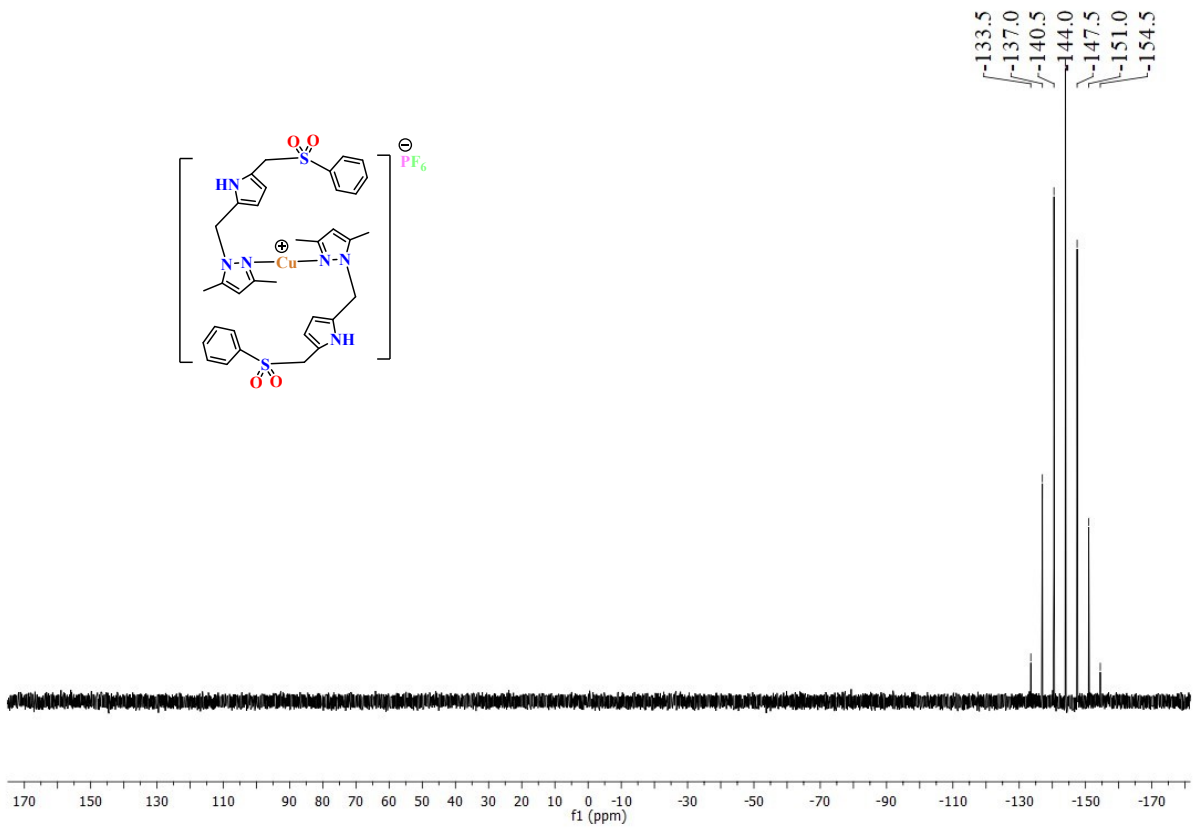

Figure S49. $^{31}P\{^{1}H\}$ NMR (25 °C, 202.46 MHz) spectrum of complex **11a** [Cu{C_4H_3N-2-(CH_2Me_2pz)-5-(CH_2SO_2Ph)-κ^1-N}$_2$]PF_6 in CD_3CN.

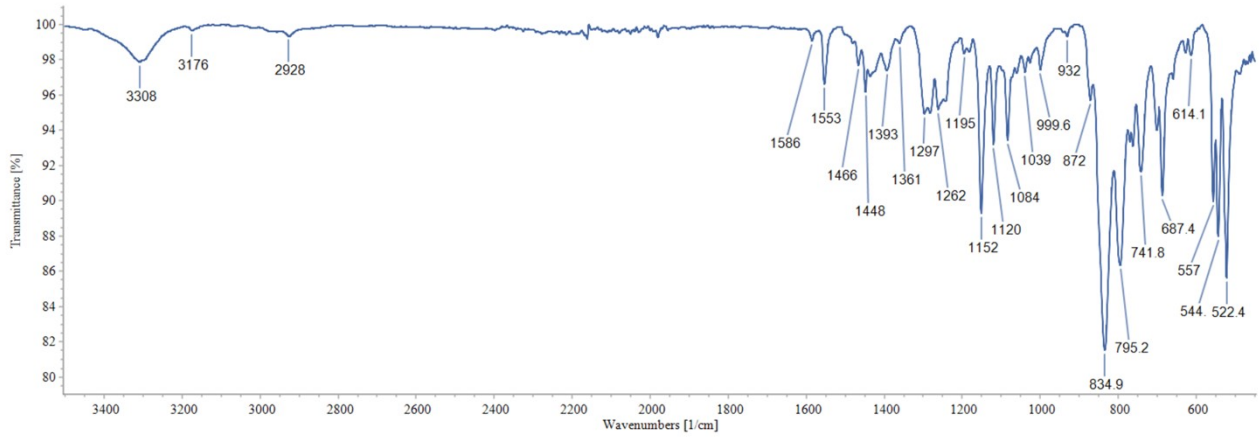

Figure S50. The ATR spectrum of complex **11a** [Cu{C_4H_3N-2-(CH_2Me_2pz)-5-(CH_2SO_2Ph)-κ^1-N}$_2$]PF_6.

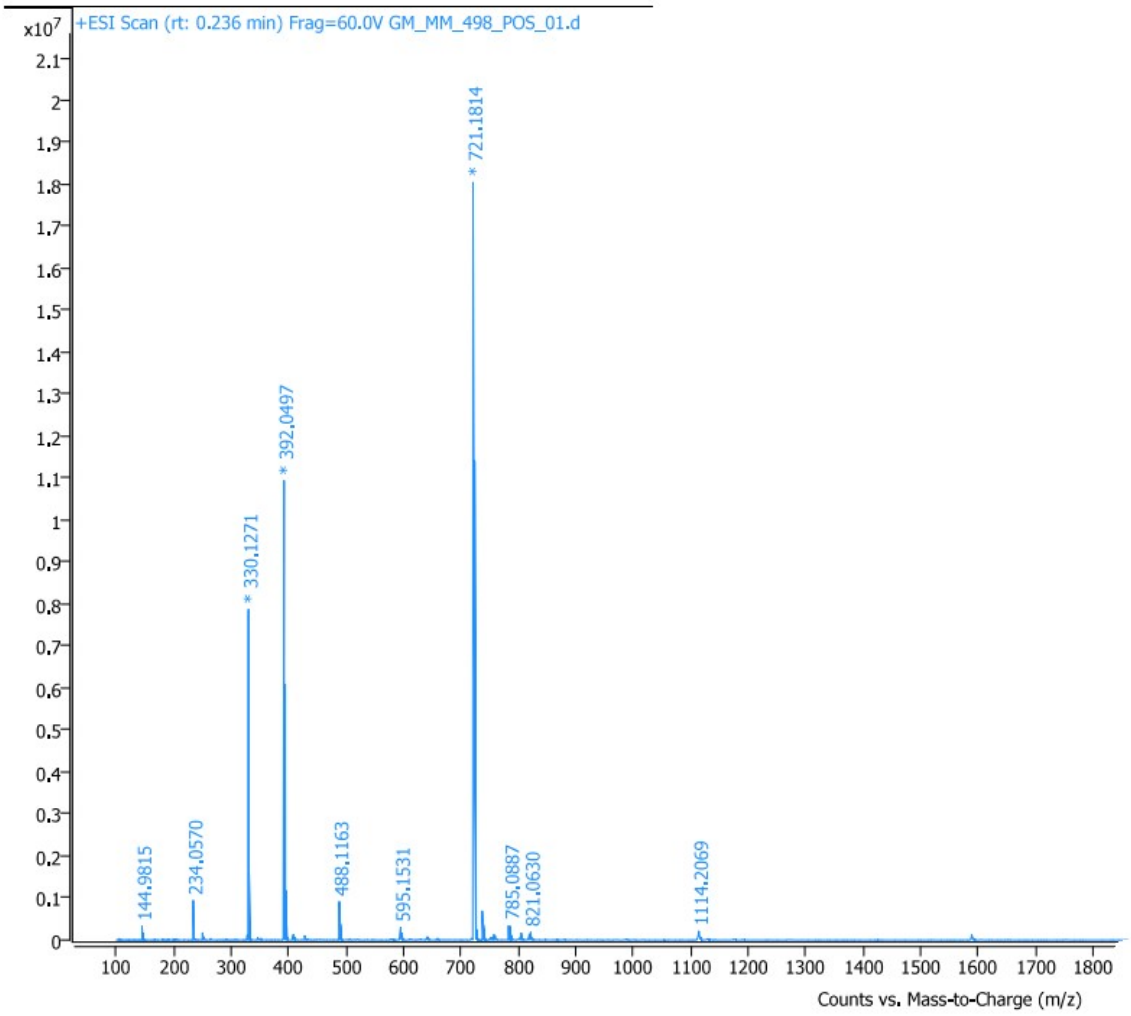

Figure S51. HRMS (ESI+) spectrum of complex **11a** [Cu{C_4H_3N-2-(CH_2Me_2pz)-5-(CH_2SO_2Ph)-κ^1-*N*}$_2$]PF_6.

Species	*m/z*, Found	*m/z,* Calculated
[Cu{C_4H_3N-2-(CH_2Me_2pz)-5-(CH_2SO_2Ph)-κ^1-*N*}$_2$]$^+$ (Cu(ligand **4**)$_2^+$)	721.1814	721.1692
[Cu{C_4H_3N-2-(CH_2Me_2pz)-5-(CH_2SO_2Ph)-κ^1-*N*}]$^+$ (Cu(ligand **4**)$^+$)	392.0497	392.0494
[Cu(CH_3OH)$_3$ {C_4H_3N-2-(CH_2Me_2pz)-5-(CH_2SO_2Ph)-κ^1-*N*}]$^+$ (Cu(CH_3OH)$_3$(ligand **4**)$^+$)	488.1163	488.1280

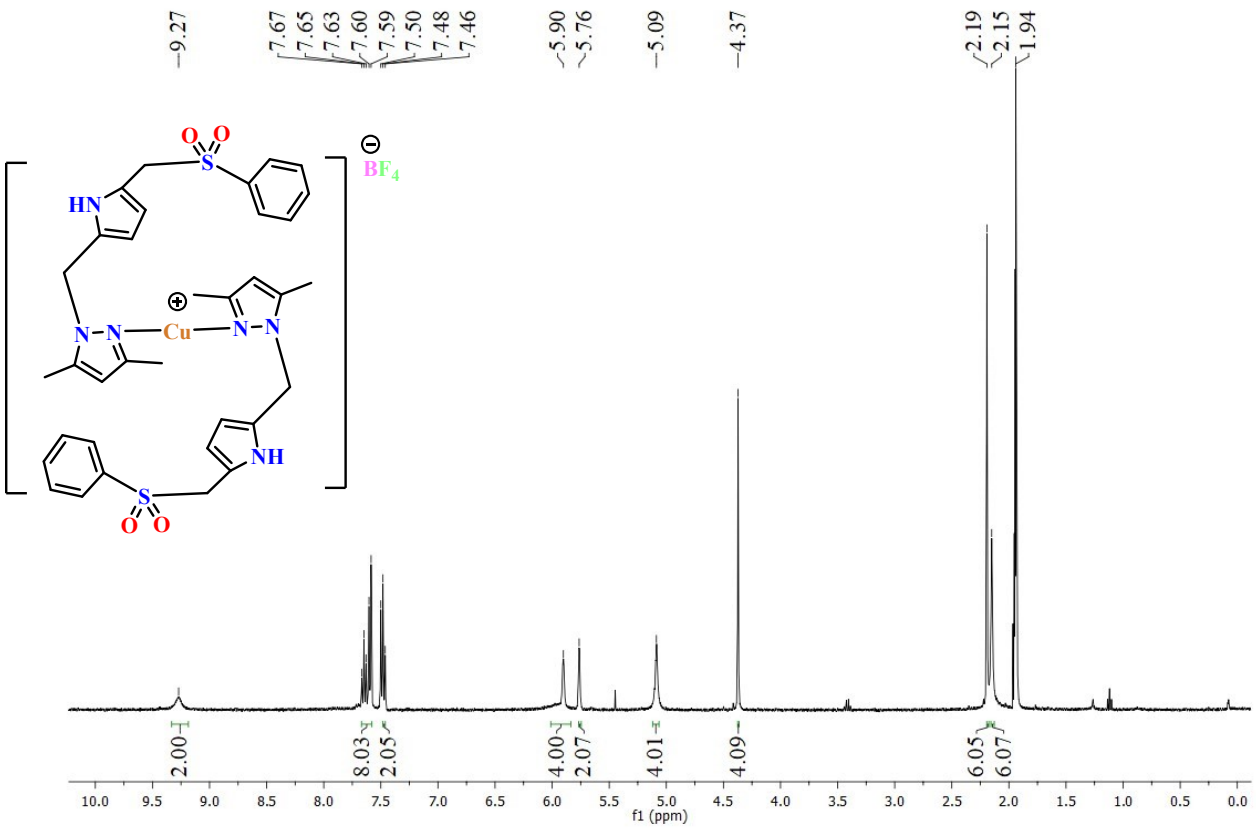

Figure S52. ^{1}H NMR (25 °C, 400 MHz) spectrum of complex **11b** in CD_3CN.

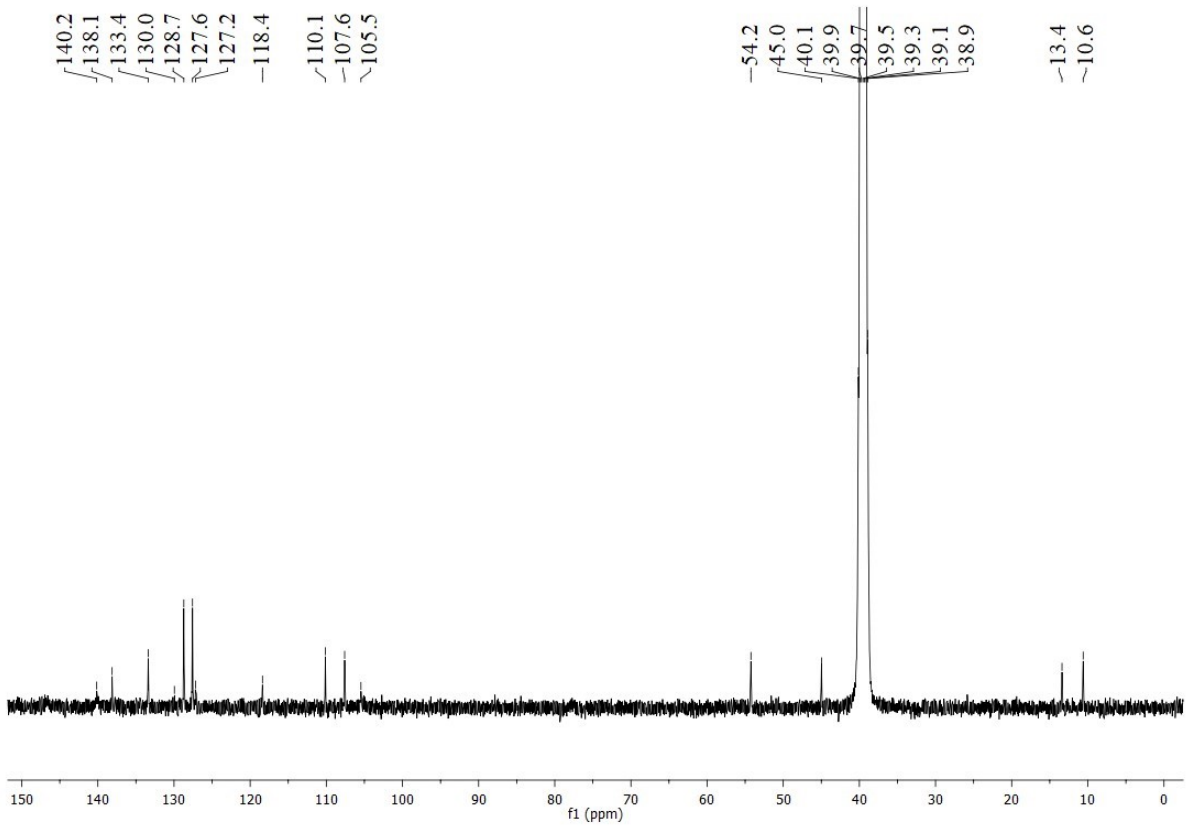

Figure S53. ^{13}C{^{1}H} NMR (25 °C, 100.6 MHz) spectrum of the complex **11b** [Cu{C_4H_3N-2-(CH_2Me_2pz)-5-(CH_2SO_2Ph)-κ^1-N}$_2$]BF_4 in DMSO-d_6.

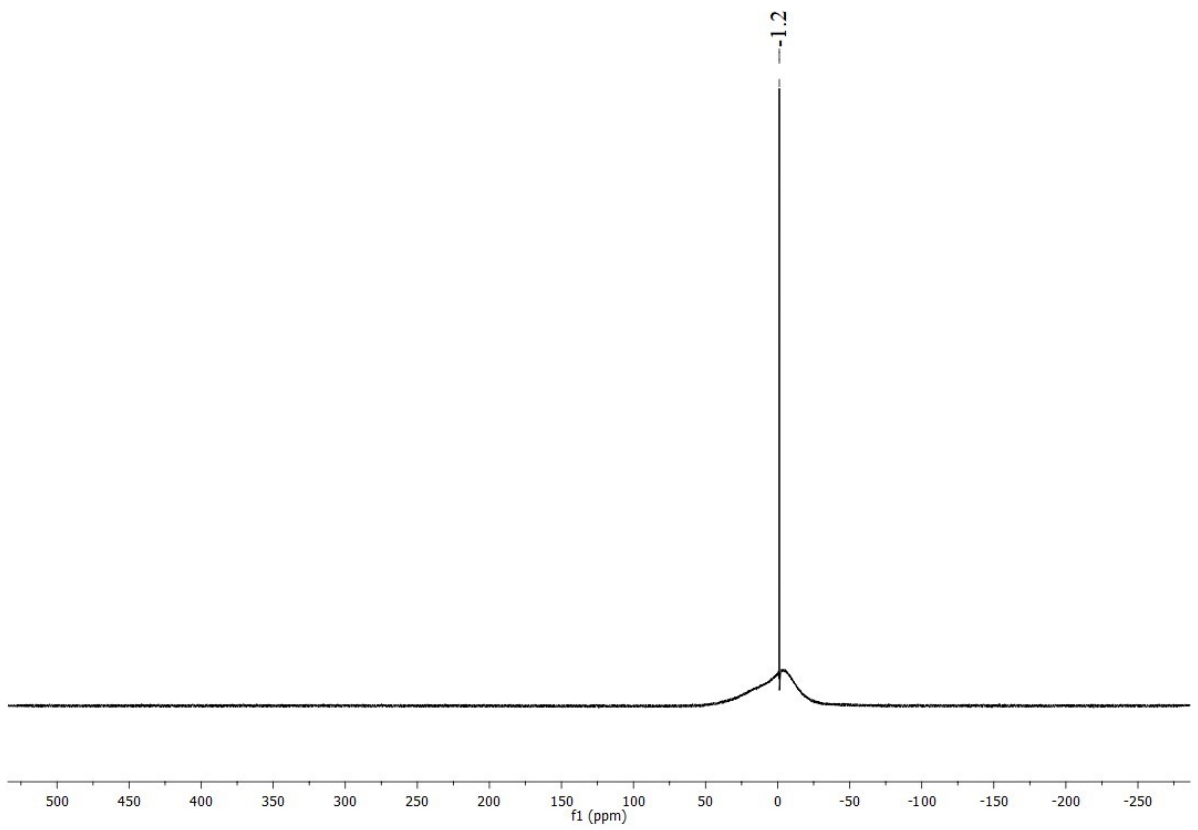

Figure S54. ^{11}B NMR (25 °C, 160.46 MHz) spectrum of complex **11b** [Cu{C_4H_3N-2-(CH_2Me_2pz)-5-(CH_2SO_2Ph)-κ^1-N}$_2$]BF_4 in CD_3CN.

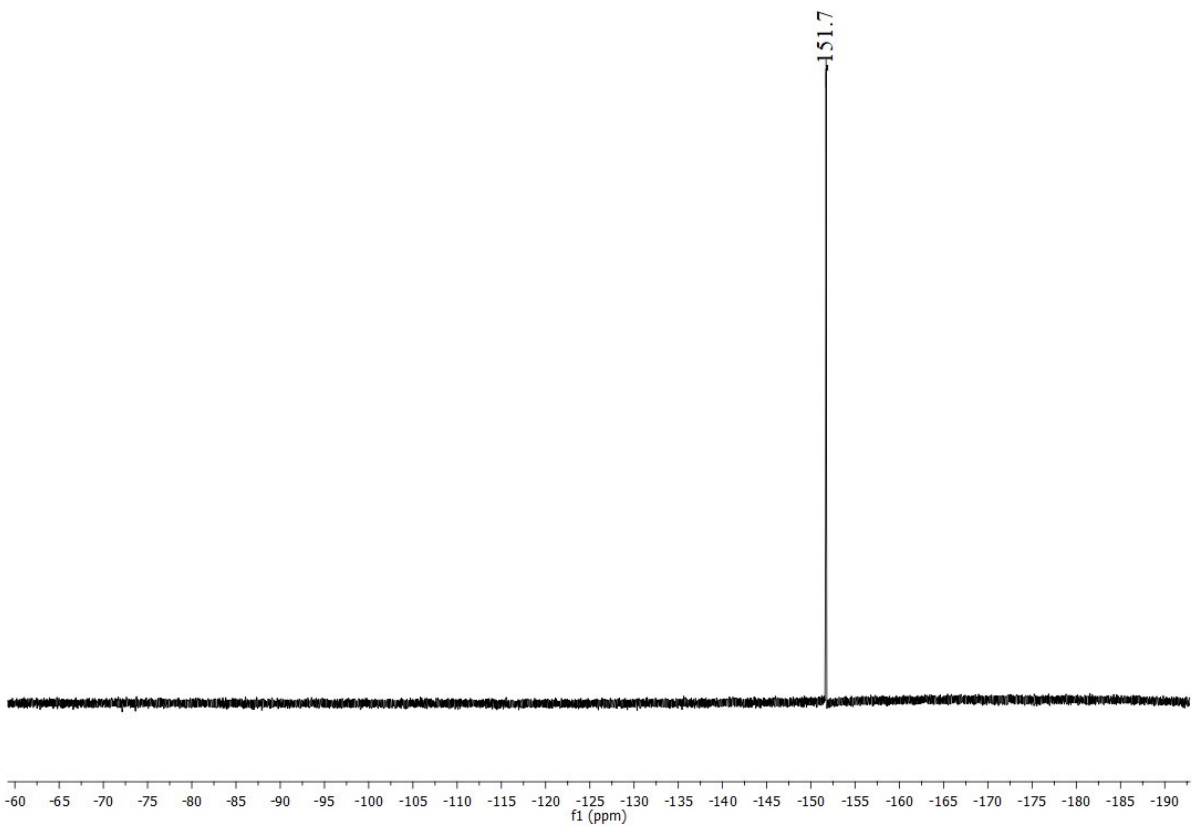

Figure S55. ^{19}F NMR (25 °C, 470.59 MHz) spectrum of complex **11b** [Cu{C_4H_3N-2-(CH_2Me_2pz)-5-(CH_2SO_2Ph)-κ^1-N}$_2$]BF_4 in CD_3CN.

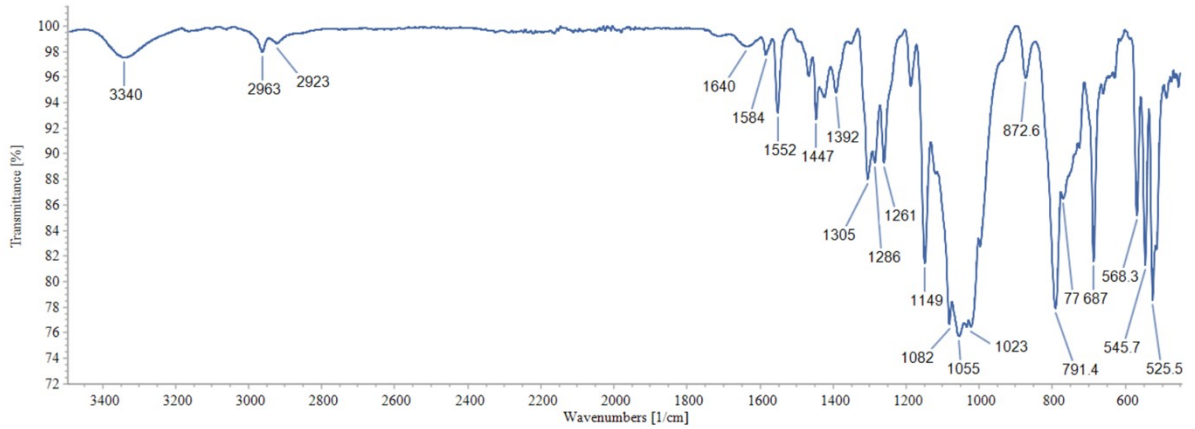

Figure S56. The ATR spectrum of complex **11b**.

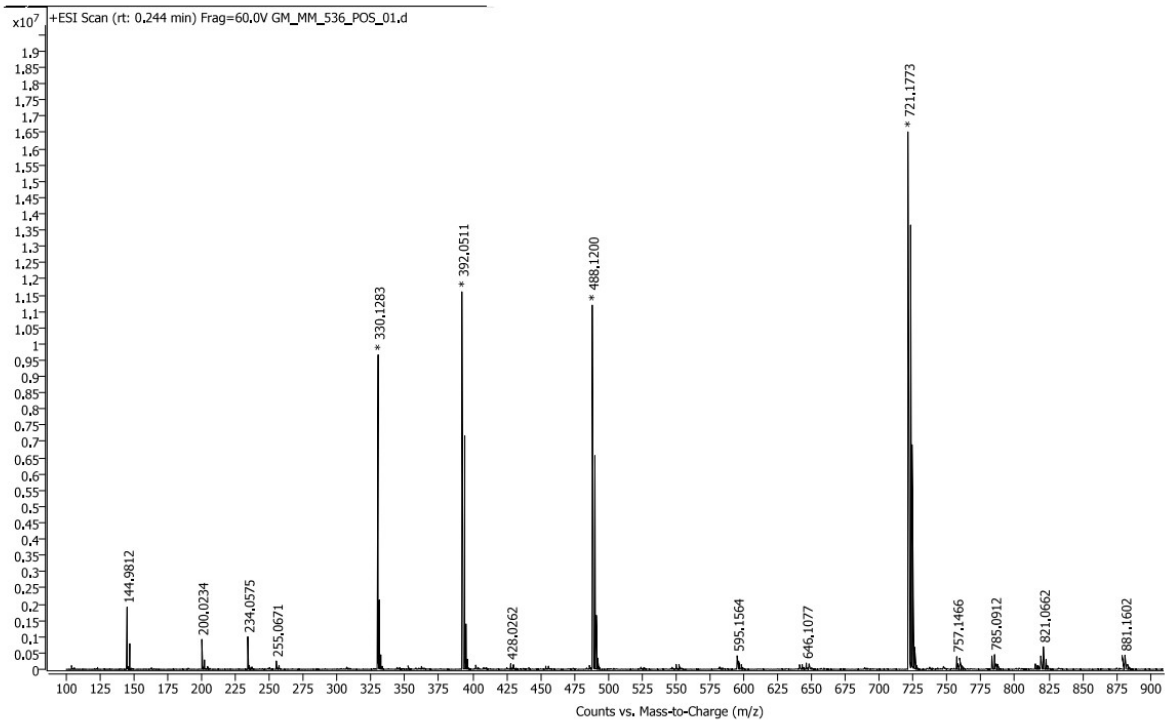

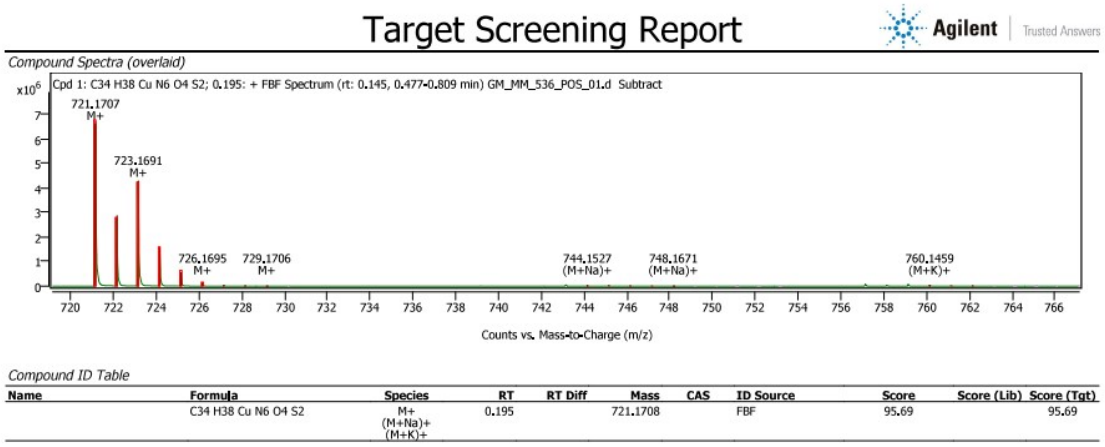

Target Screening Report

Agilent Trusted Answers

Compound Spectra (overlaid)

Cpd 1: C34 H38 Cu N6 O4 S2; 0.195: + FBF Spectrum (rt: 0.145, 0.477-0.809 min) GM_MM_536_POS_01.d Subtract

x10^6

721.1707 M+

723.1691 M+

726.1695 M+

729.1706 M+

744.1527 (M+Na)+

748.1671 (M+Na)+

760.1459 (M+K)+

Counts vs. Mass-to-Charge (m/z)

Compound ID Table

Name	Formula	Species	RT	RT Diff	Mass	CAS	ID Source	Score	Score (Lib)	Score (Tgt)
	C34 H38 Cu N6 O4 S2	M+ (M+Na)+ (M+K)+	0.195		721.1708		FBF	95.69		95.69

Figure S57. HRMS (ESI+) spectrum of complex **11b**.

Species	*m/z*, Found	*m/z,* Calculated
$[Cu\{C_4H_3N\text{-}2\text{-}(CH_2Me_2pz)\text{-}5\text{-}(CH_2SO_2Ph)\text{-}\kappa^1\text{-}N\}_2]^+$ (Cu(ligand **4**)$_2^+$)	721.1773	721.1692
$[Cu\{C_4H_3N\text{-}2\text{-}(CH_2Me_2pz)\text{-}5\text{-}(CH_2SO_2Ph)\text{-}\kappa^1\text{-}N\}]^+$ (Cu(ligand **4**)$^+$)	392.0511	392.0494
$[Cu(CH_3OH)_3\{C_4H_3N\text{-}2\text{-}(CH_2Me_2pz)\text{-}5\text{-}(CH_2SO_2Ph)\text{-}\kappa^1\text{-}N\}]^+$ (Cu$(CH_3OH)_3$(ligand **4**)$^+$)	488.1200	488.1280

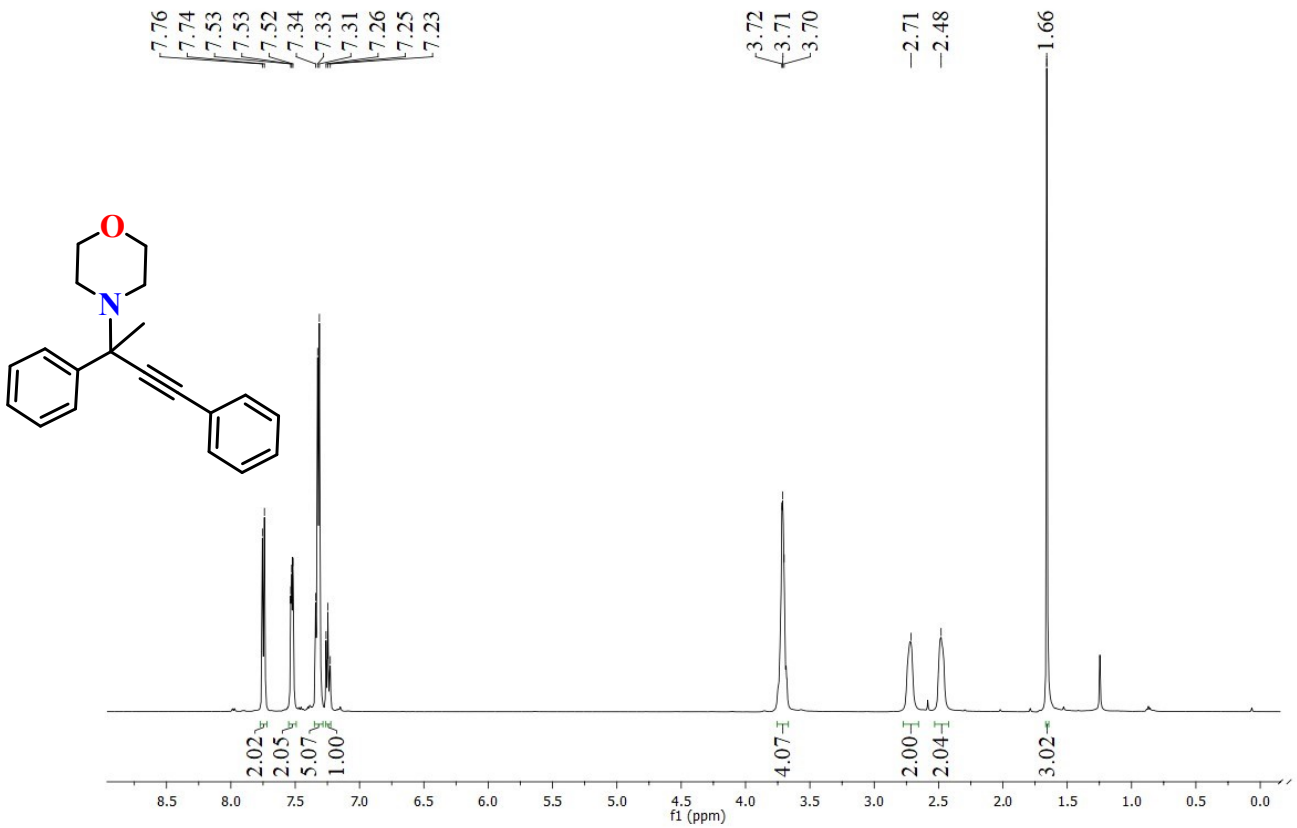

Figure S58. ^{1}H NMR (25 °C, 500 MHz) spectrum of tetrasubstituted propargylamine **12a** in $CDCl_3$.

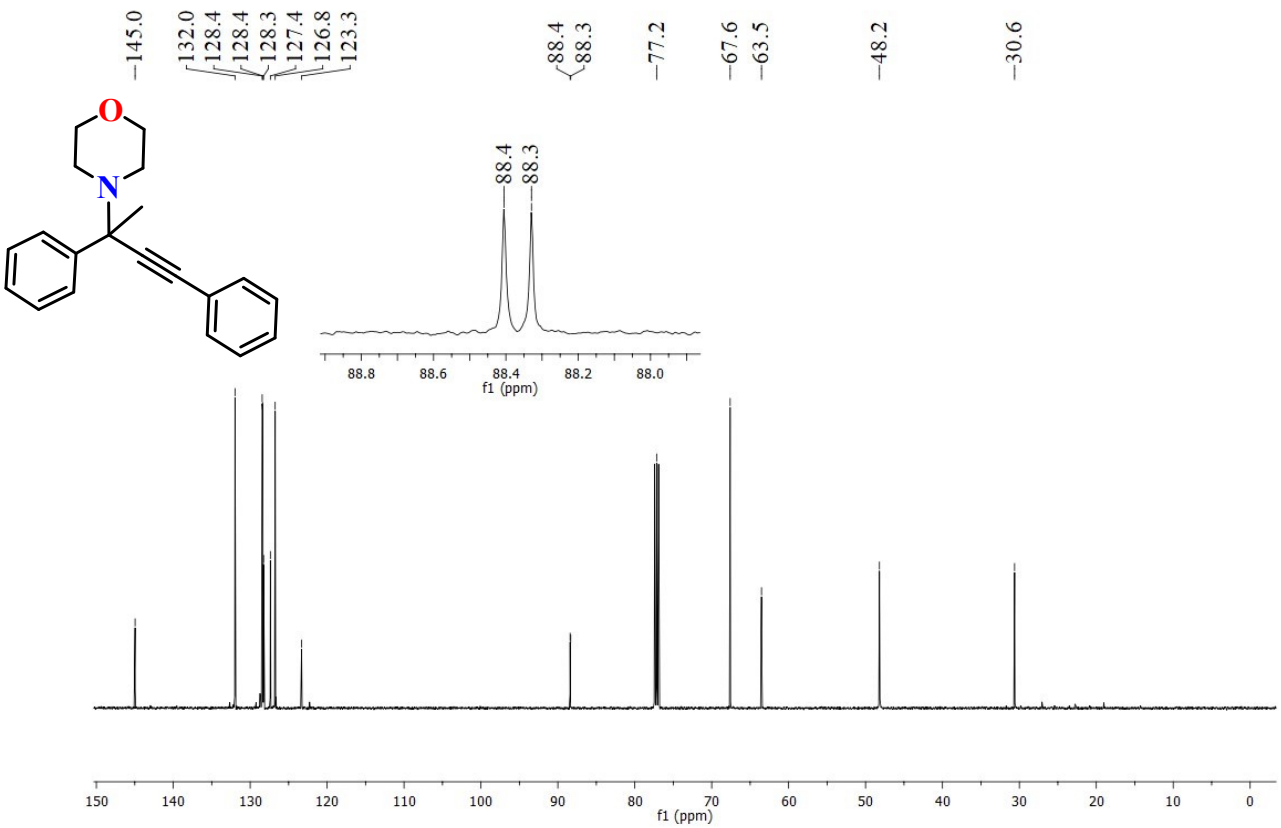

Figure S59. $^{13}C\{^{1}H\}$ NMR (25 °C, 125.7 MHz) spectrum of tetrasubstituted propargylamine **12a** in $CDCl_3$.

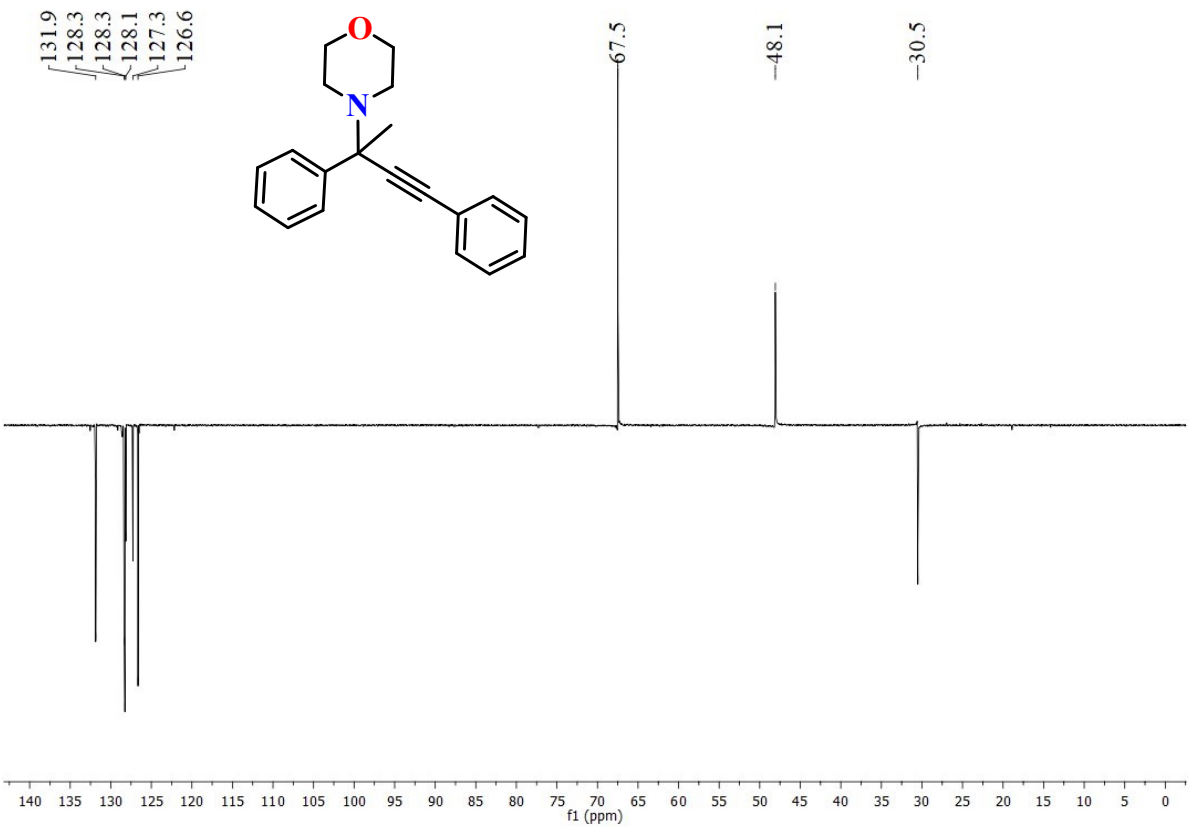

Figure S60. $^{13}C\{^{1}H\}$DEPT NMR (25 °C, 125.7 MHz) spectrum of tetrasubstituted propargylamine **12a** in $CDCl_3$.

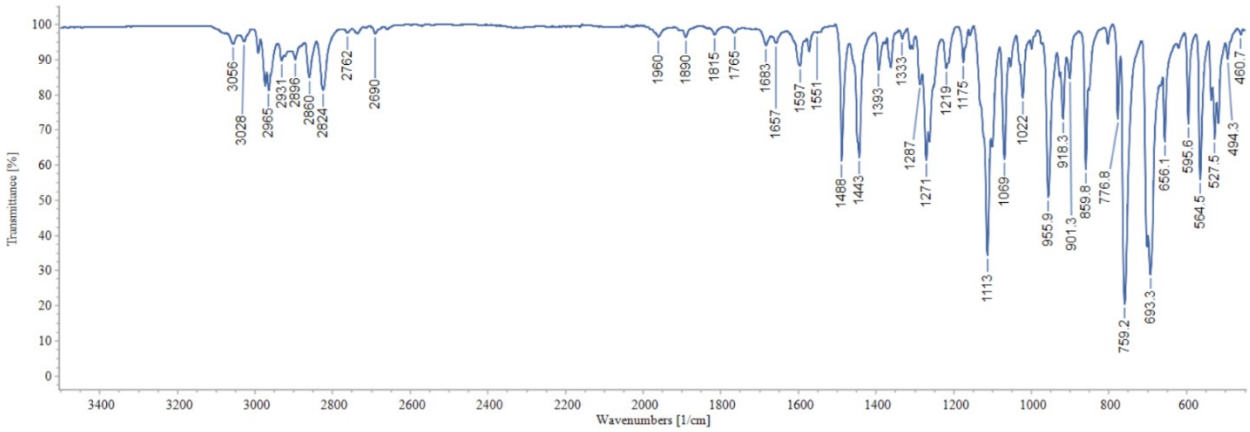

Figure S61. The ATR spectrum of tetra-substituted propargylamine **12a**.

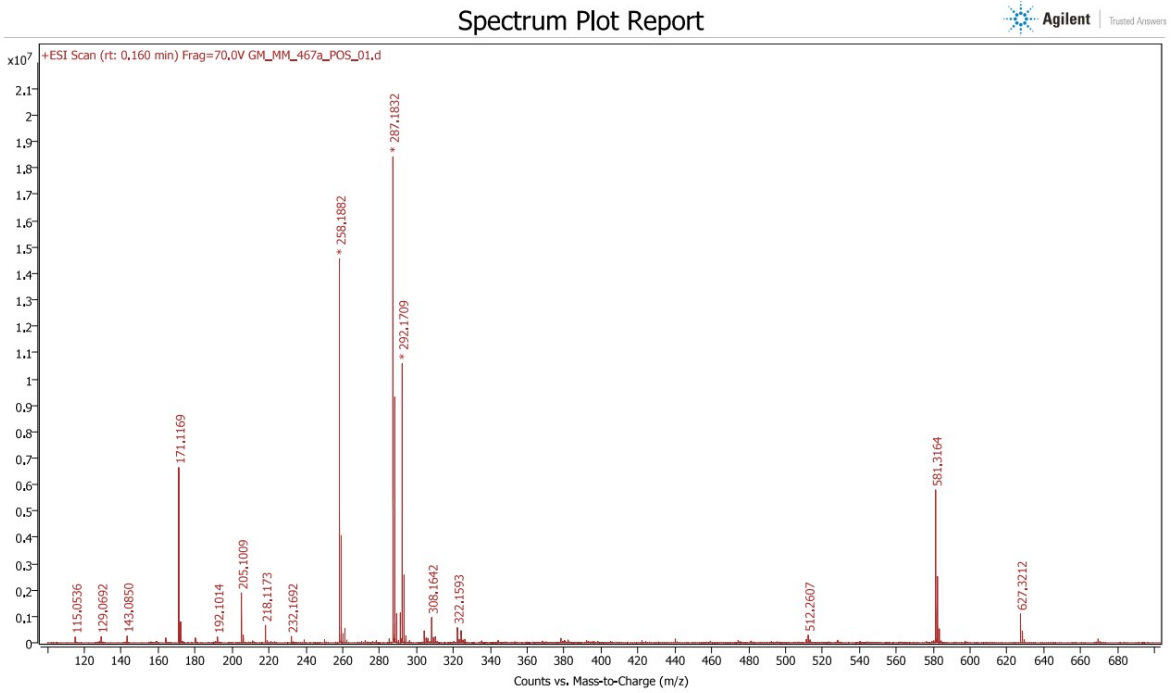

Figure S62. HRMS (ESI+) spectrum of tetrasubstituted propargylamine **12a**. $[M+H]^+$: Calc. 292.1696, found: 292.1709.

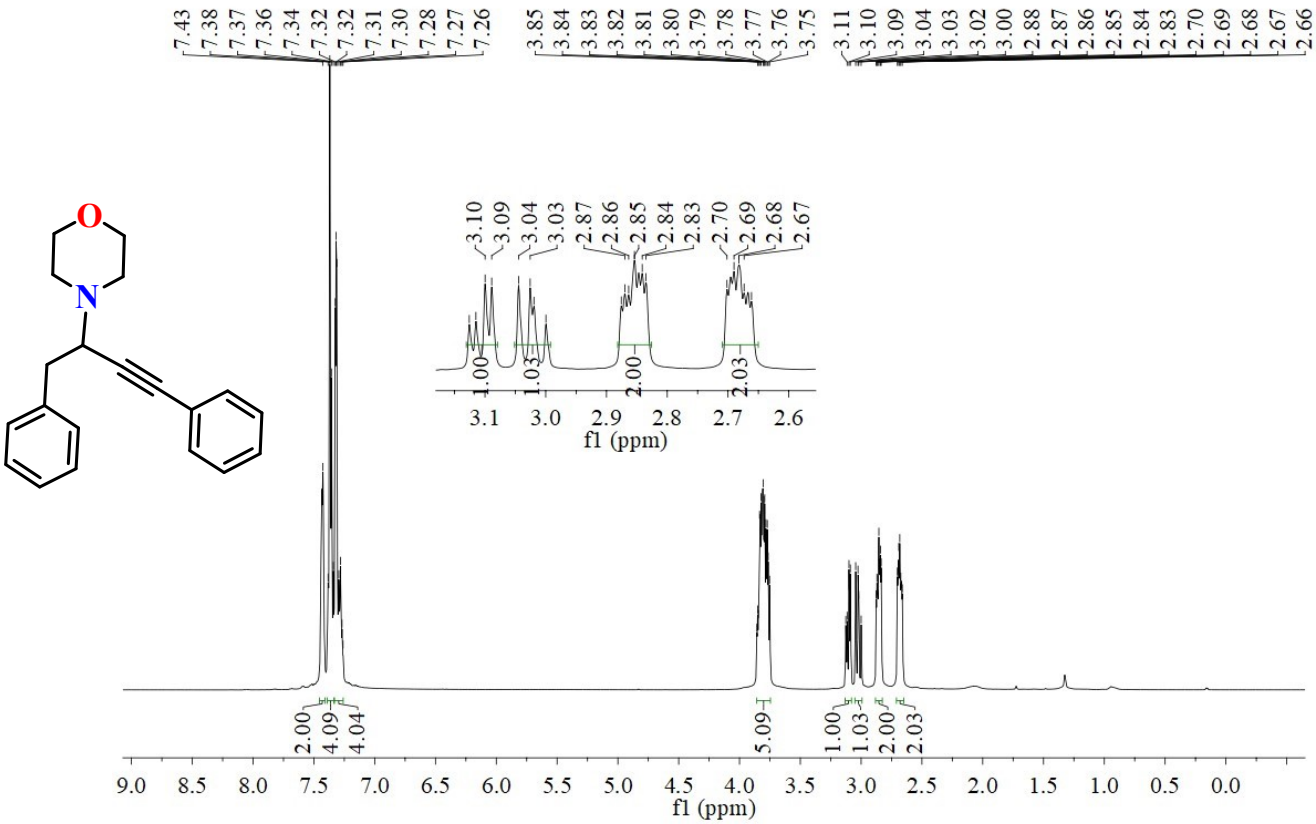

Figure S63. ^{1}H NMR (25 °C, 500 MHz) spectrum of trisubstituted propargylamine **12b** in $CDCl_3$.

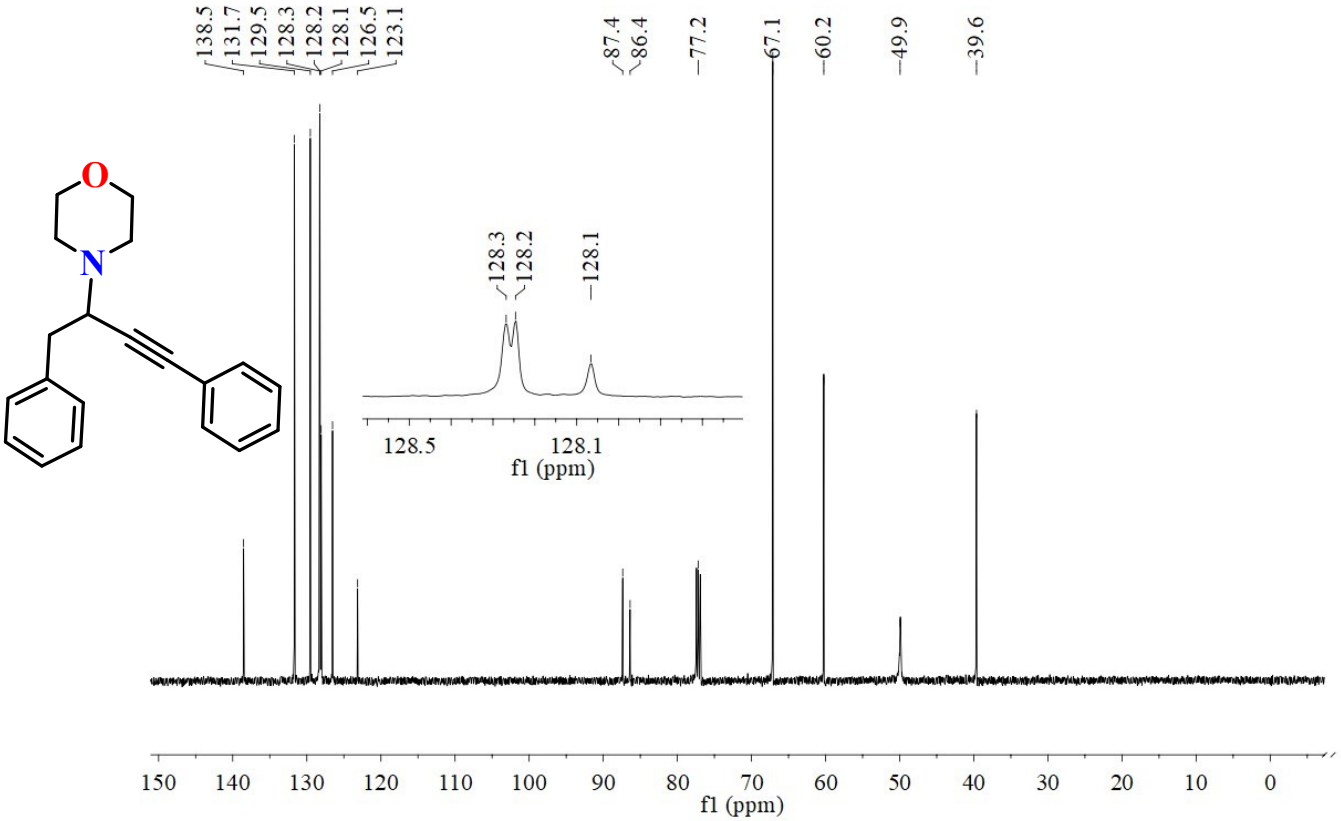

Figure S64. $^{13}C\{^{1}H\}$ NMR (25 °C, 125.7 MHz) spectrum of trisubstituted propargylamine **12b** in $CDCl_3$.

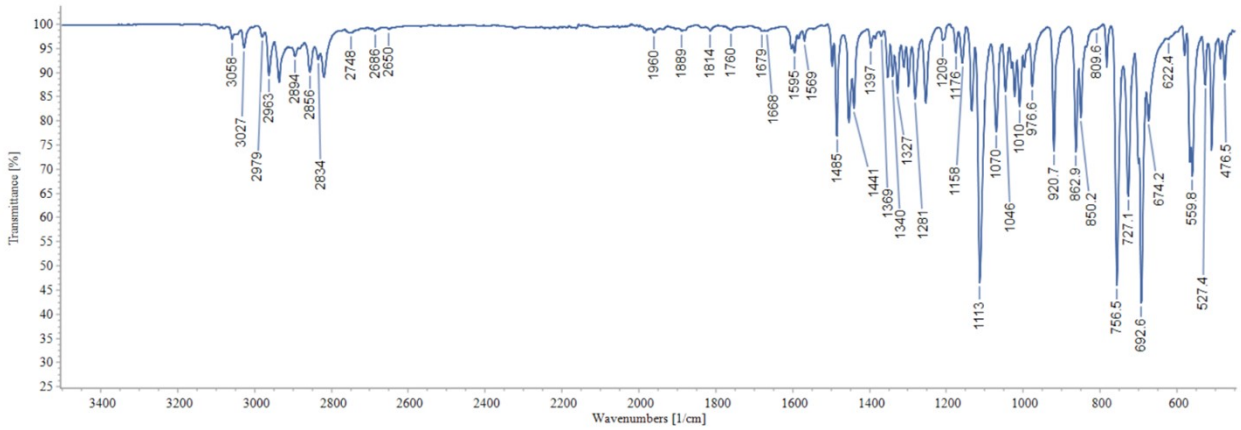

Figure S65. The ATR spectrum of trisubstituted propargylamine **12b**.

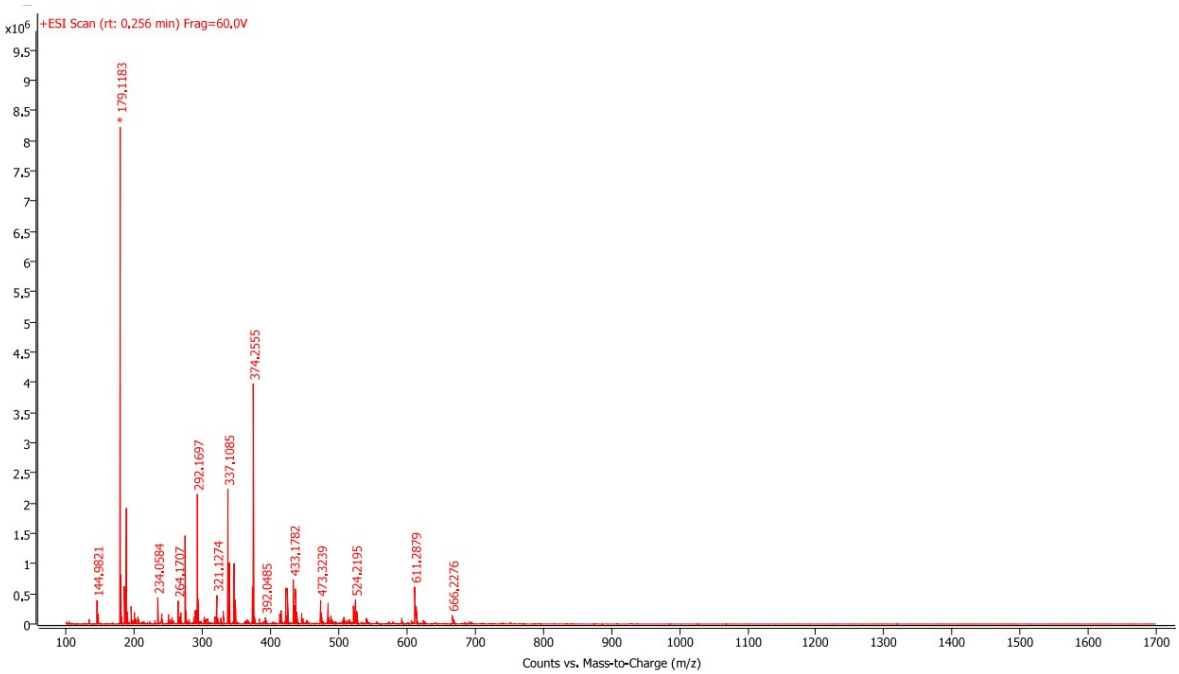

Figure S66. HRMS (ESI+) spectrum of trisubstituted propargylamine **12b**. $[M+H]^+$: Calc. 292.1696, found: 292.1697.

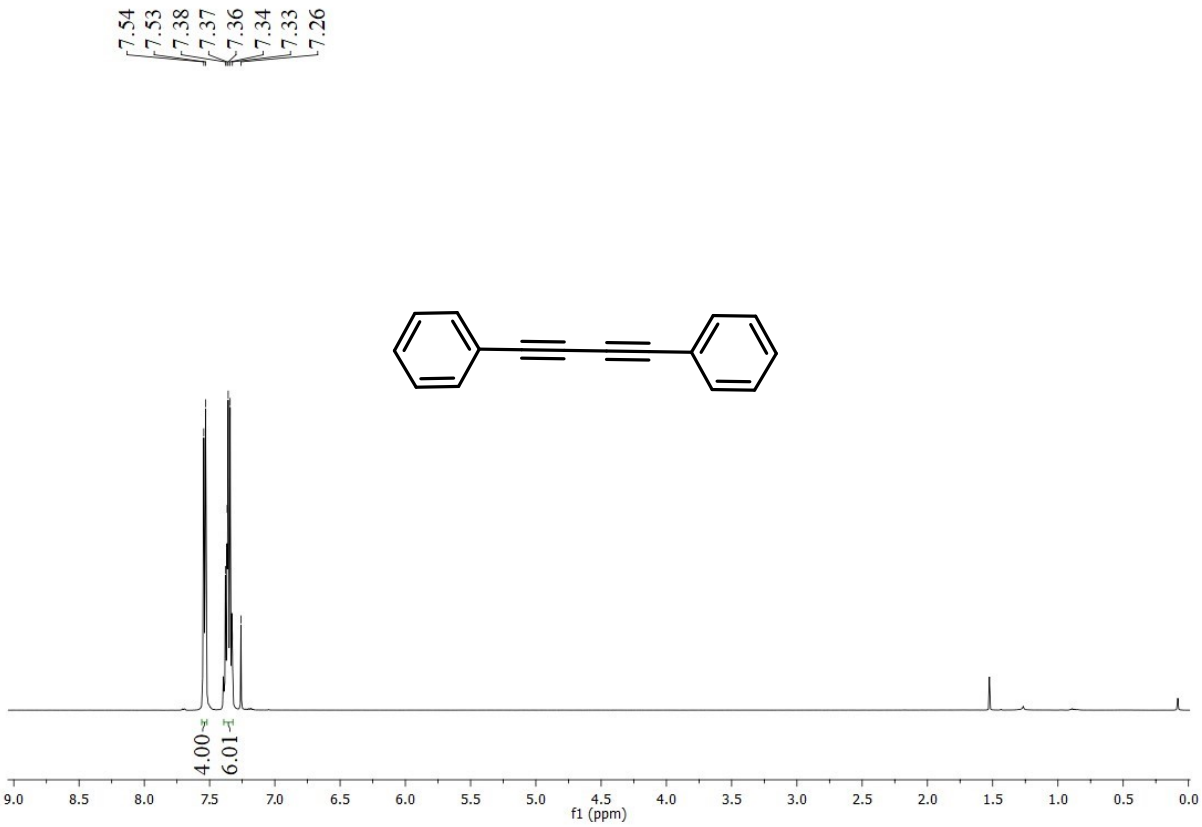

Figure S67. ^{1}H NMR (25 °C, 500 MHz) spectrum of phenylacetylene dimer **12c** in $CDCl_3$.

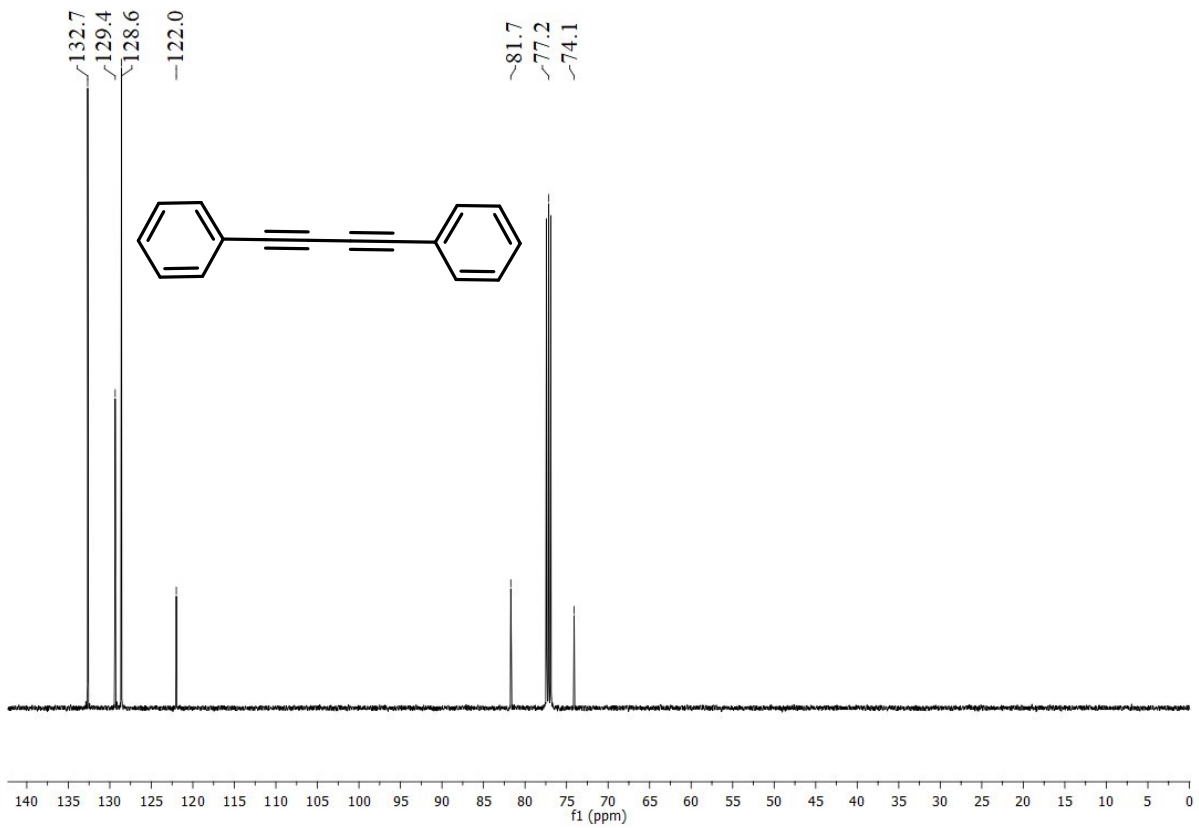

Figure S68. $^{13}C\{^{1}H\}$ NMR (25 °C, 125.7 MHz) spectrum of phenylacetylene dimer **12c** in $CDCl_3$.

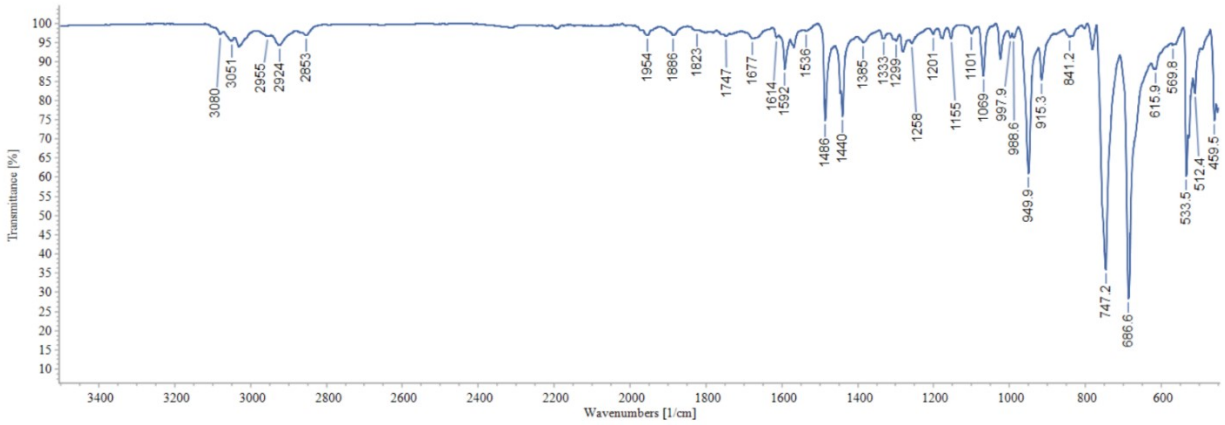

Figure S69. The ATR spectrum of phenylacetylene dimer **12c**.

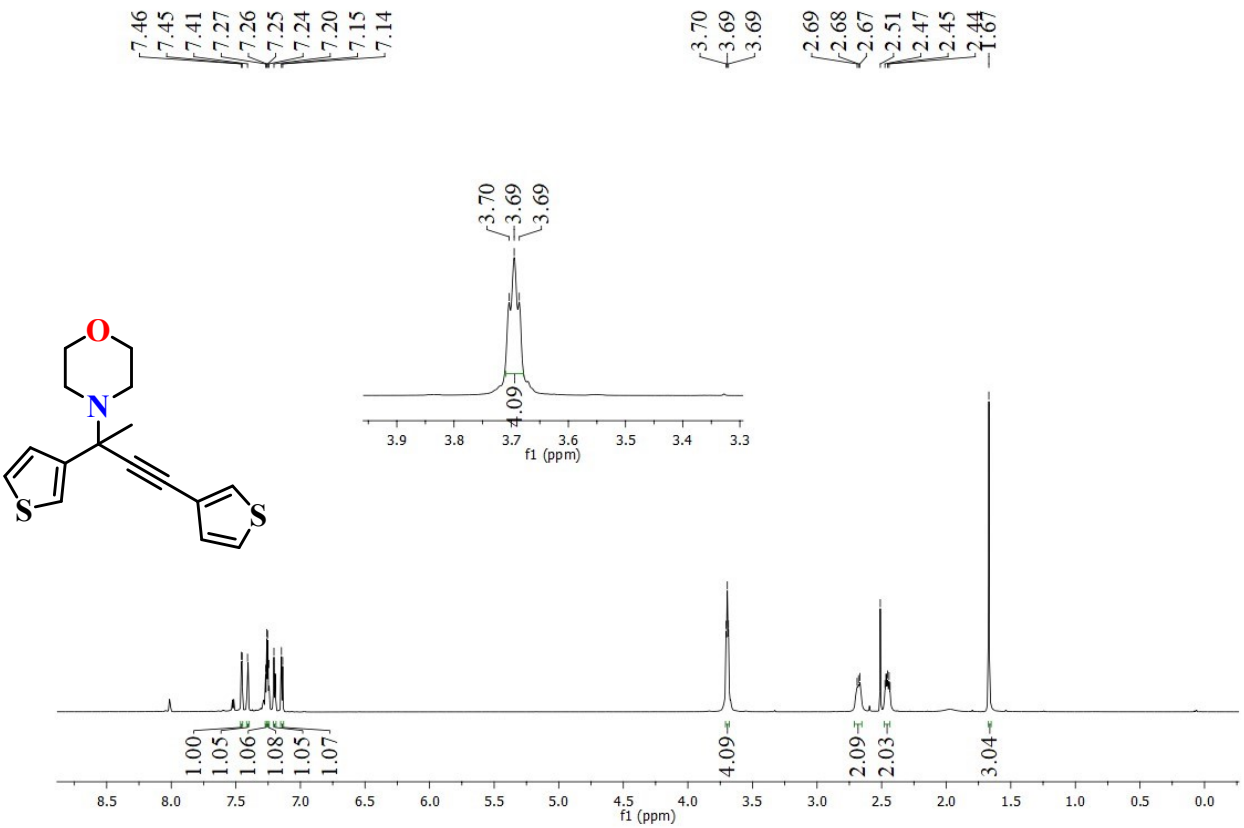

Figure S70. ^{1}H NMR (25 °C, 500 MHz) spectrum of the tetrasubstituted product **13a** from 3-ethynylthiophene in $CDCl_3$.

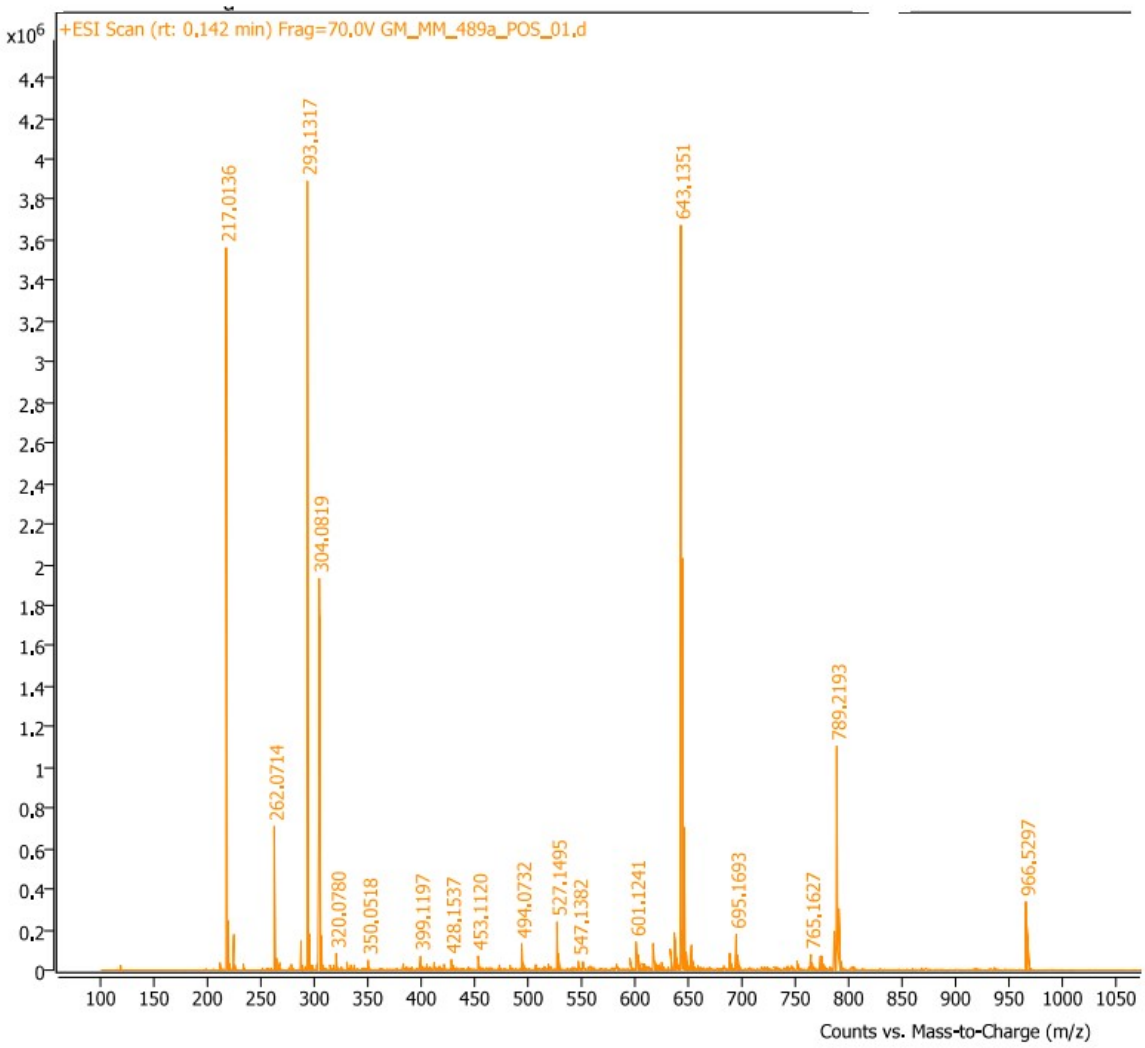

Figure S71. HRMS (+ESI) spectrum of the tetrasubstituted product from 3-ethynylthiophene **13a**. calcd *m/z* for $[M+H]^+$ $C_{16}H_{18}NOS_2^+$: 304.0825, found: 304.0819.

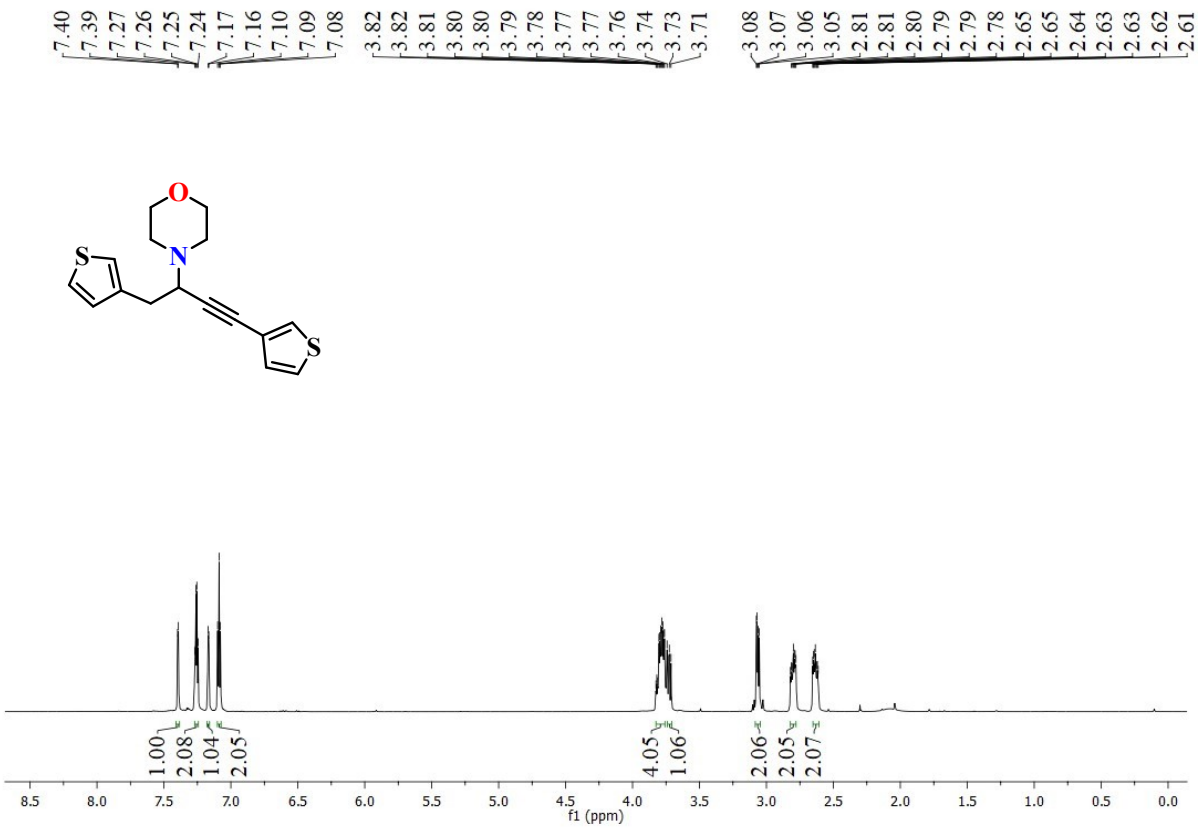

Figure S72. ^{1}H NMR (25 °C, 500 MHz) spectrum of the trisubstituted product **13b** from 3-ethynylthiophene in $CDCl_3$.

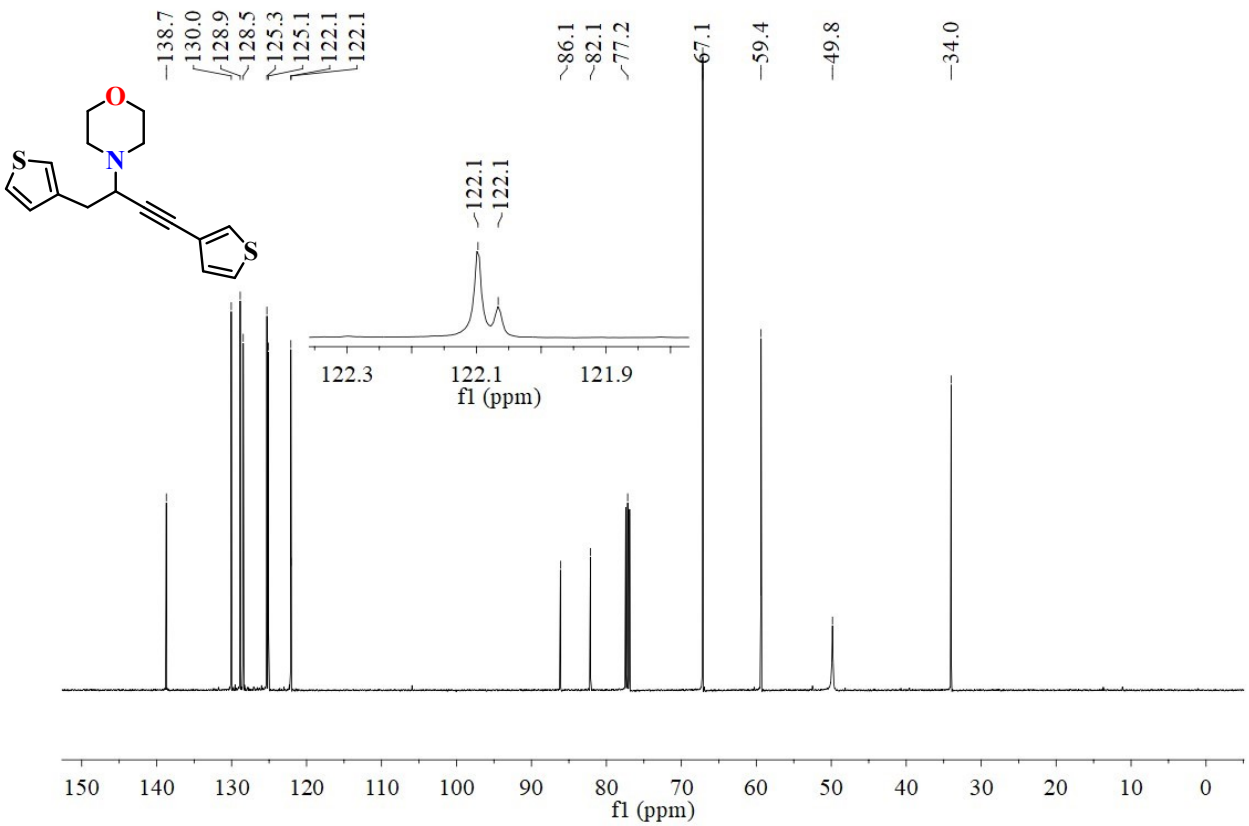

Figure S73. $^{13}C\{^{1}H\}$ NMR (25 °C, 125.7 MHz) spectrum of the trisubstituted product **13b** from 3-ethynylthiophene in $CDCl_3$.

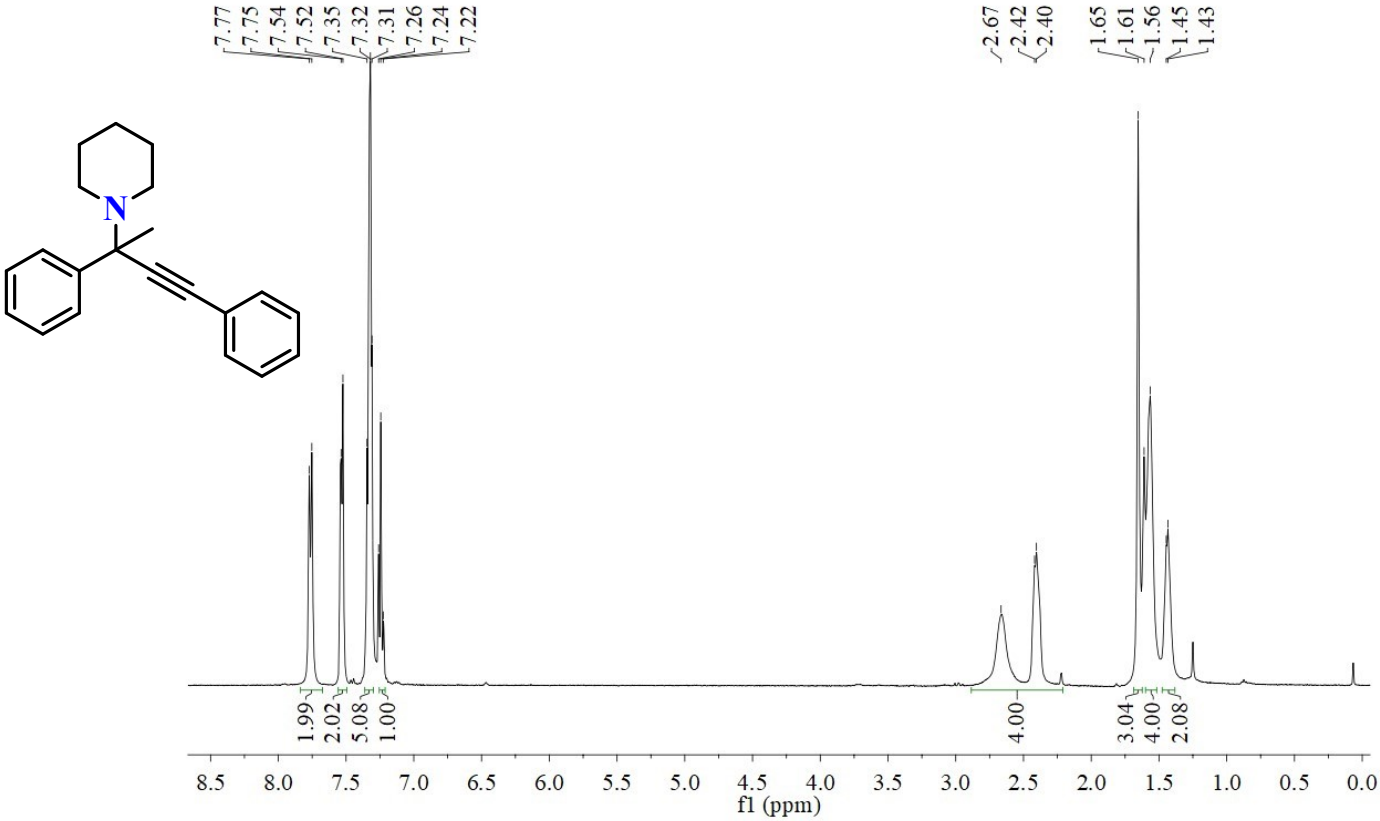

Figure S74. ^{1}H NMR (25 °C, 400 MHz) spectrum of the tetrasubstituted product **14a** from piperidine in $CDCl_3$.

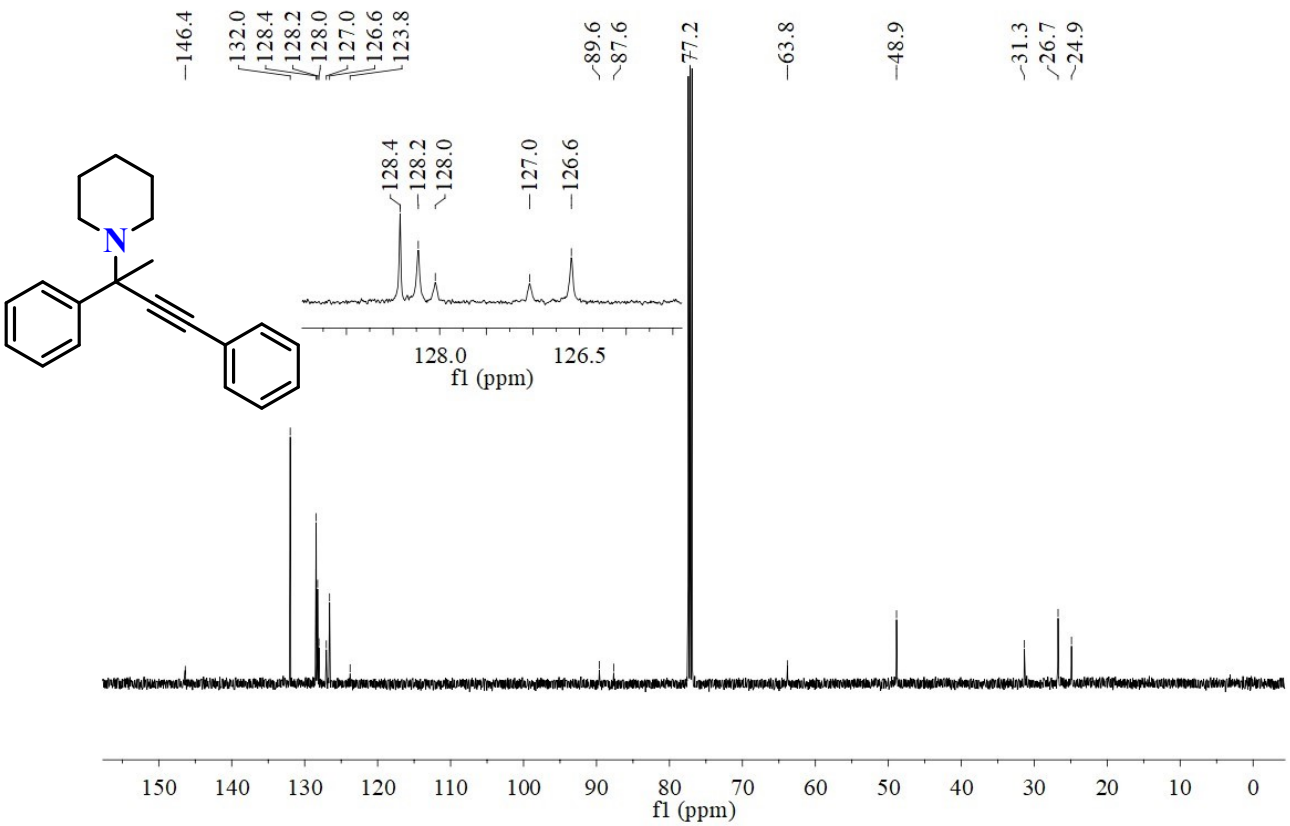

Figure S75. $^{13}C\{^{1}H\}$ NMR (25 °C, 125.7 MHz) spectrum of the tetrasubstituted product **14a** from piperidine in $CDCl_3$.

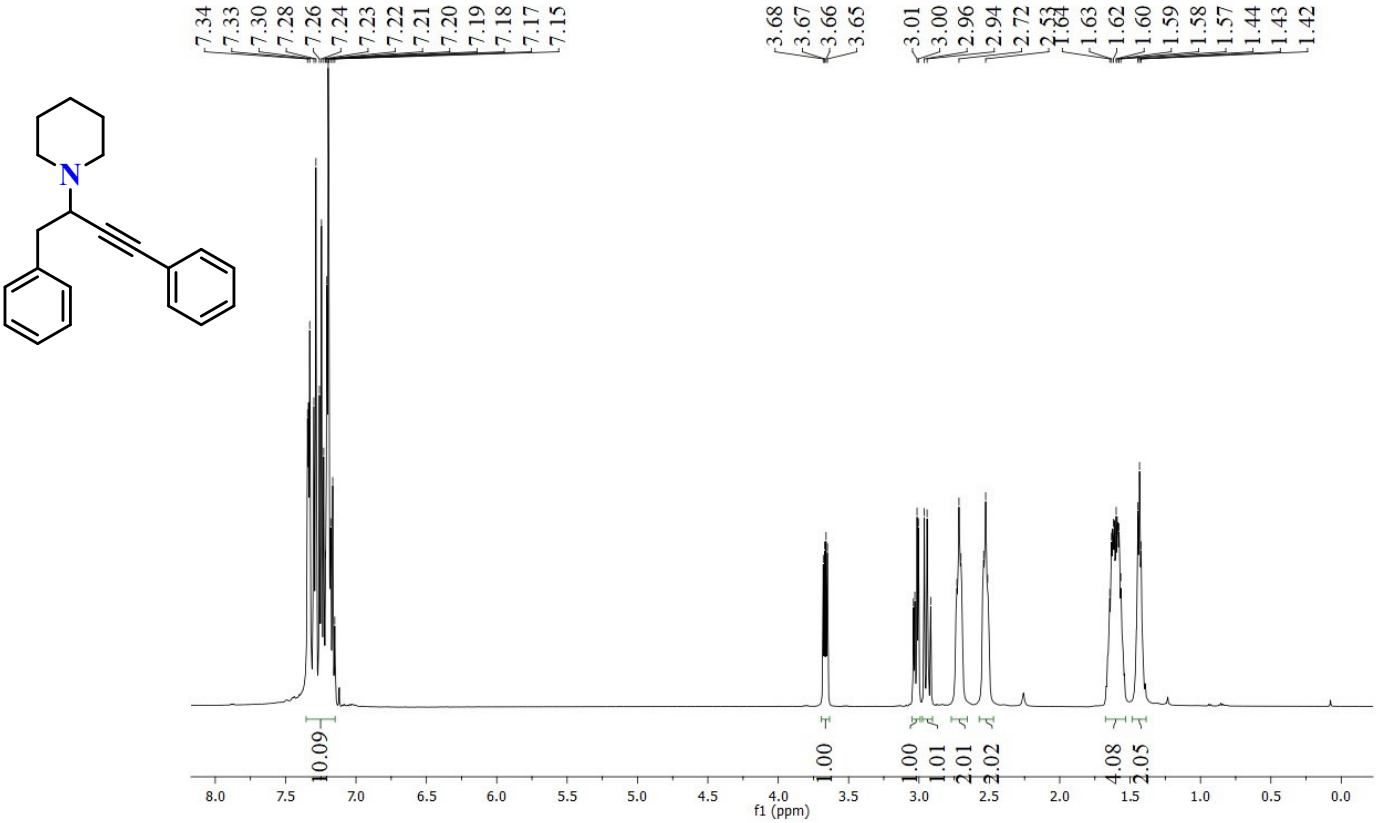

Figure S76. ^{1}H NMR (25 °C, 400 MHz) spectrum the trisubstituted product **14b** from piperidine $CDCl_3$.

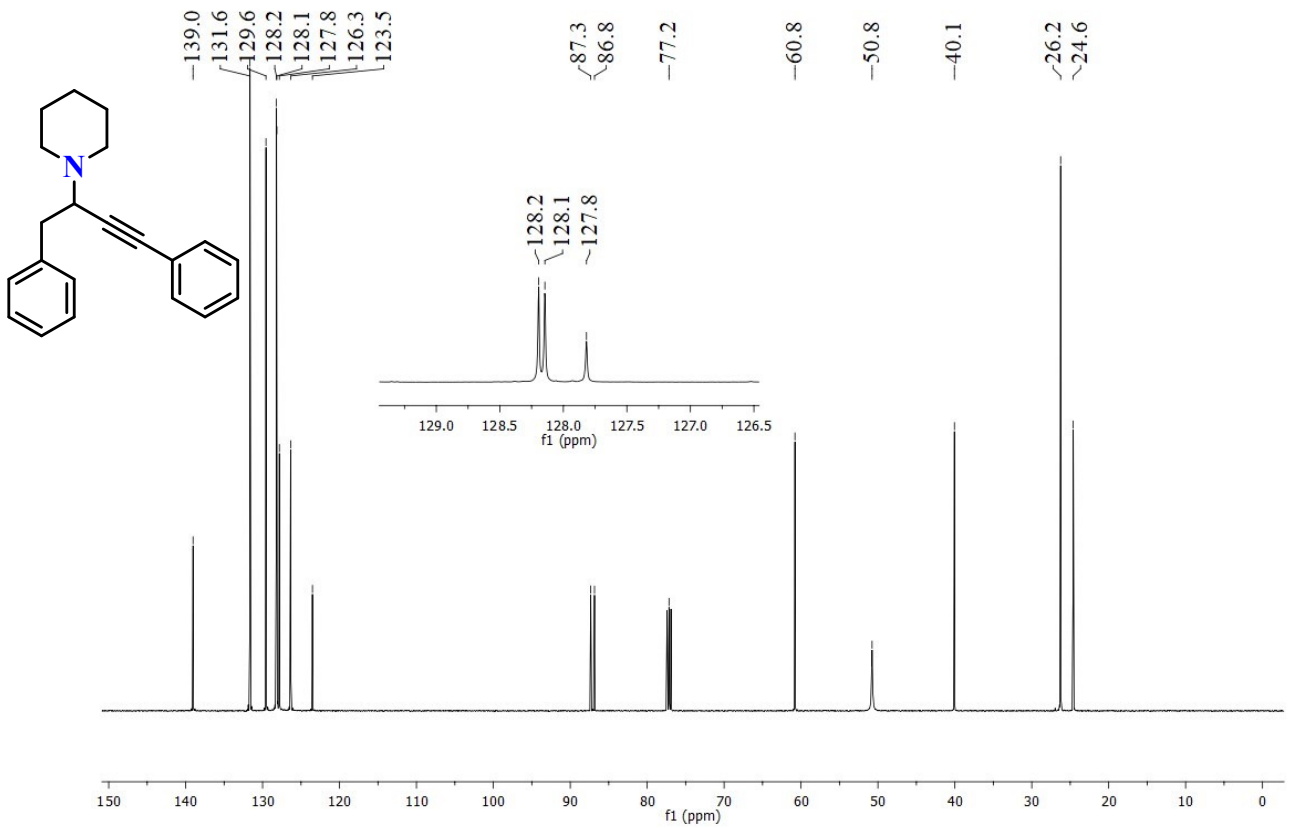

Figure S77. $^{13}C\{^{1}H\}$ NMR (25 °C, 125.7 MHz) spectrum of the trisubstituted product **14b** from piperidine $CDCl_3$.

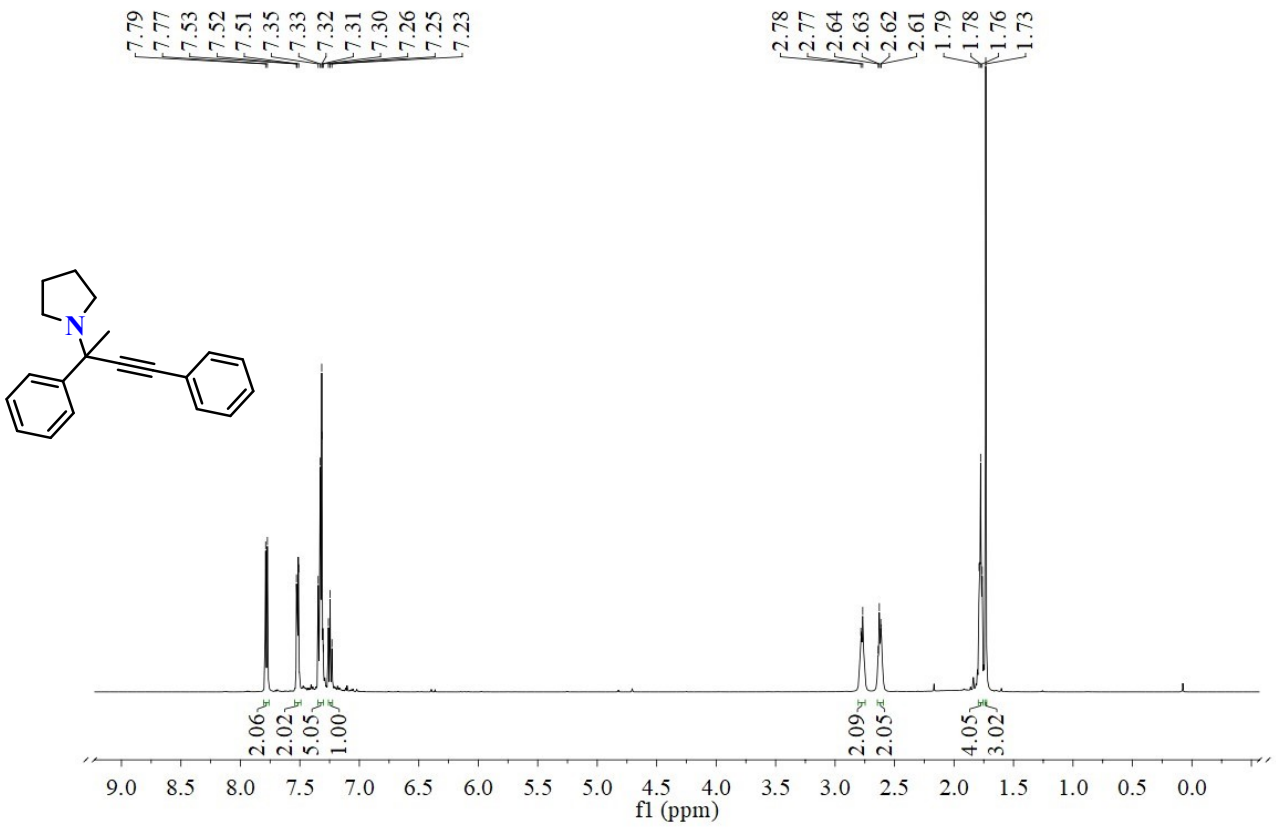

Figure S78. ^{1}H NMR (25 °C, 500 MHz) spectrum of the tetrasubstituted product **15a** from pyrrolidine in $CDCl_3$.

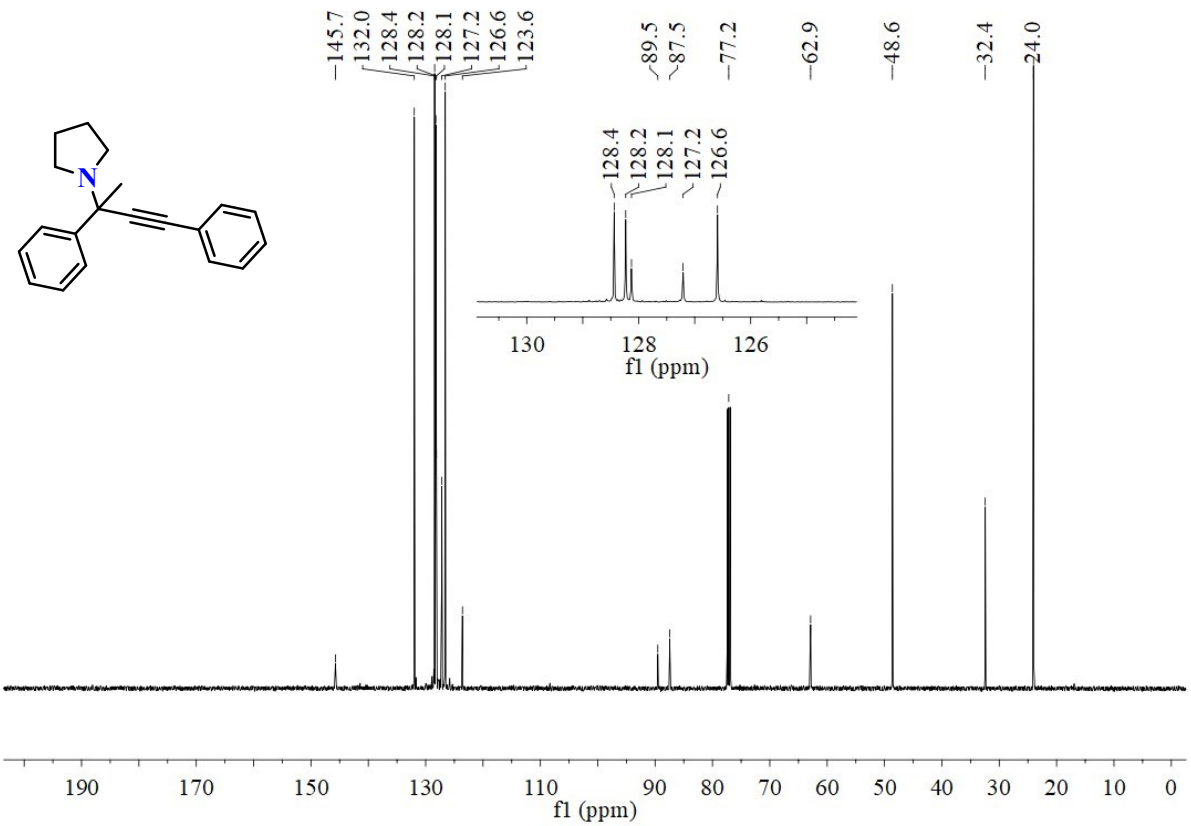

Figure S79. $^{13}C\{^{1}H\}$ NMR (25 °C, 125.7 MHz) spectrum of the tetrasubstituted product **15a** from pyrrolidine in $CDCl_3$.

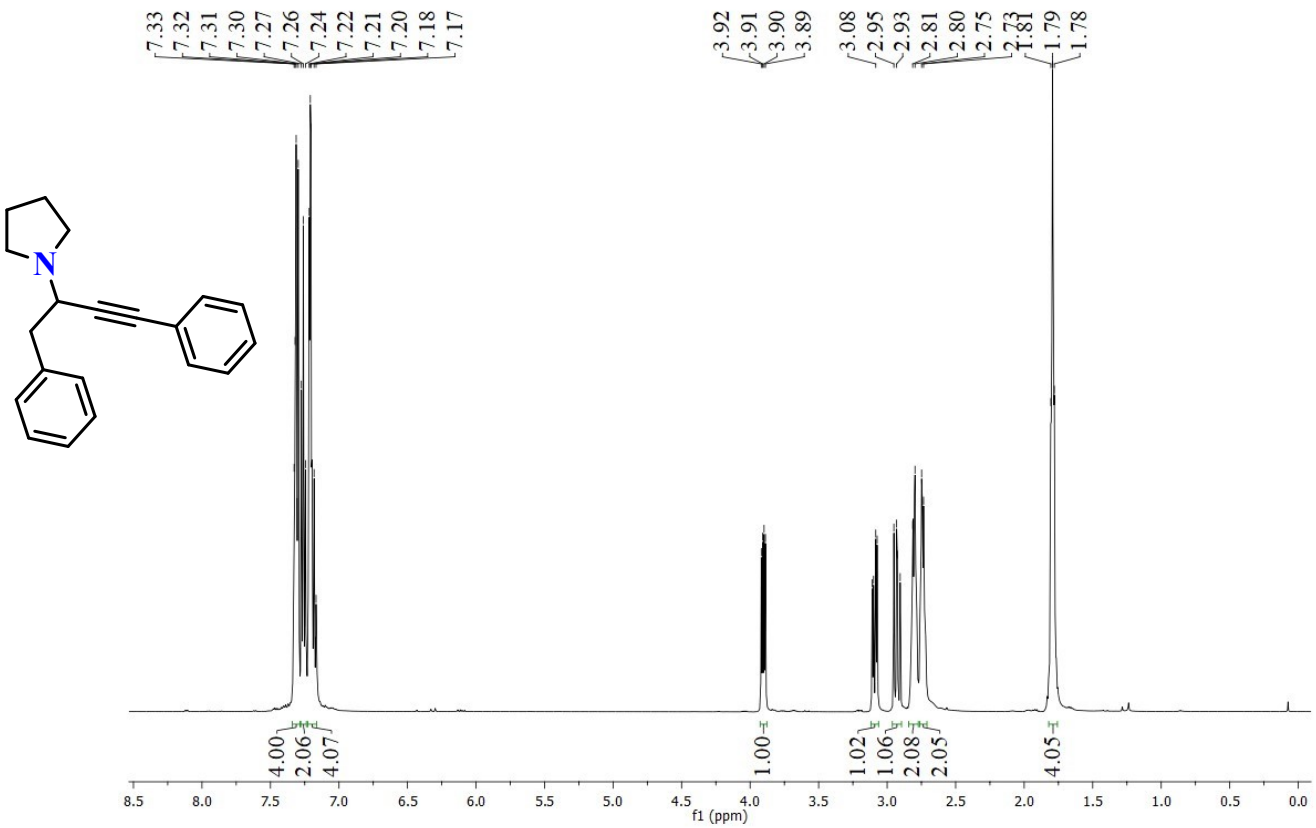

Figure S80. ^{1}H NMR (25 °C, 500 MHz) spectrum of the trisubstituted product **15b** from pyrrolidine in $CDCl_3$.

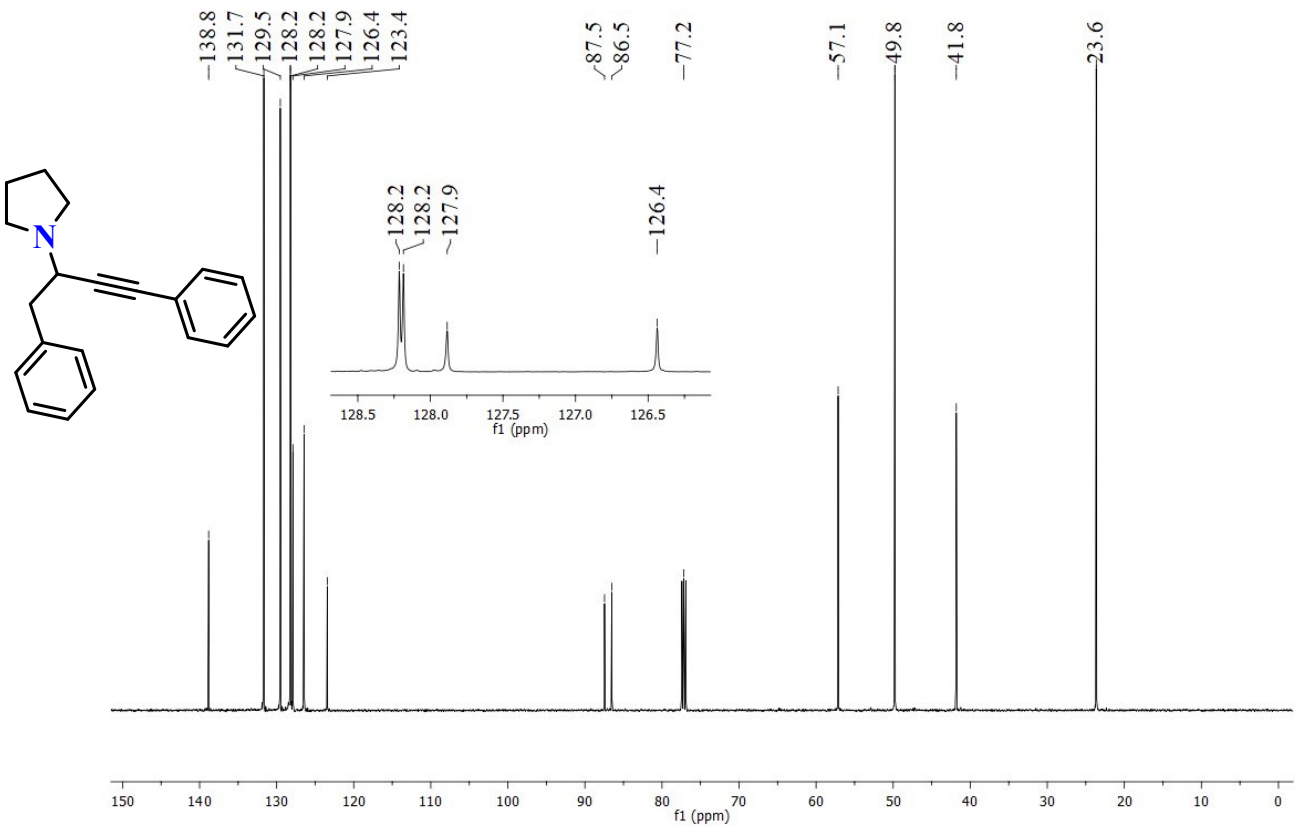

Figure S81. $^{13}C\{^{1}H\}$ NMR (25 °C, 125.7 MHz) spectrum of the trisubstituted product **15b** from pyrrolidine in $CDCl_3$.

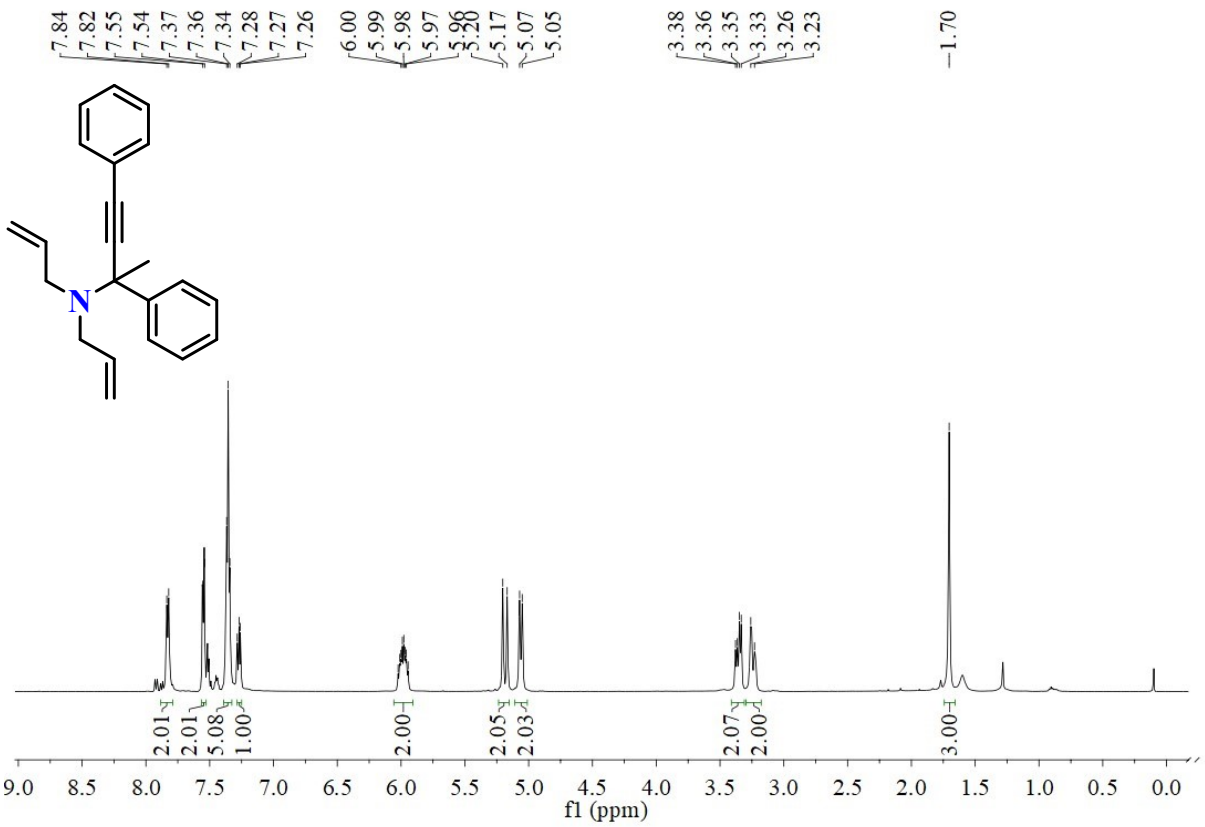

Figure S82. ^{1}H NMR (25 °C, 500 MHz) spectrum of the tetrasubstituted product **16a** from diallylamine in $CDCl_3$.

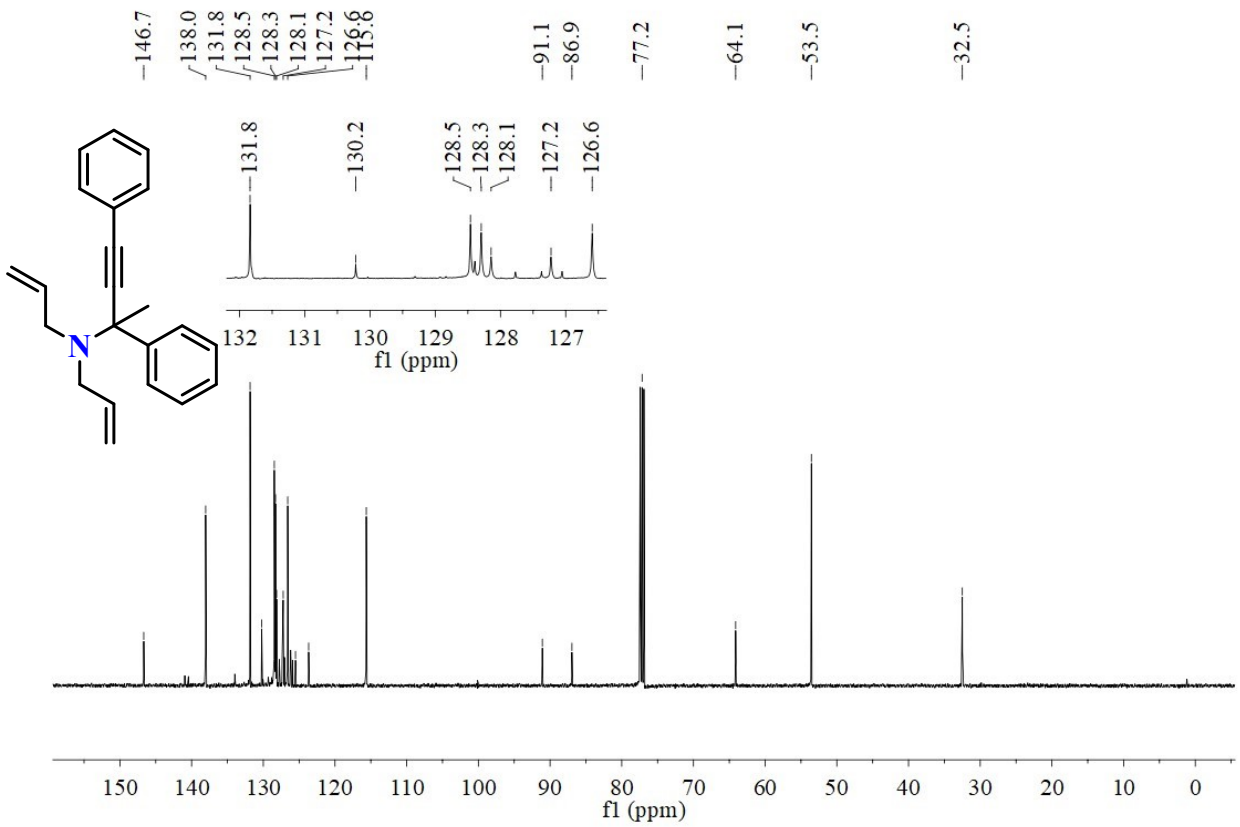

Figure S83. $^{13}C\{^{1}H\}$ NMR (25 °C, 125.7 MHz) spectrum of the tetrasubstituted product **16a** from diallylamine in $CDCl_3$.

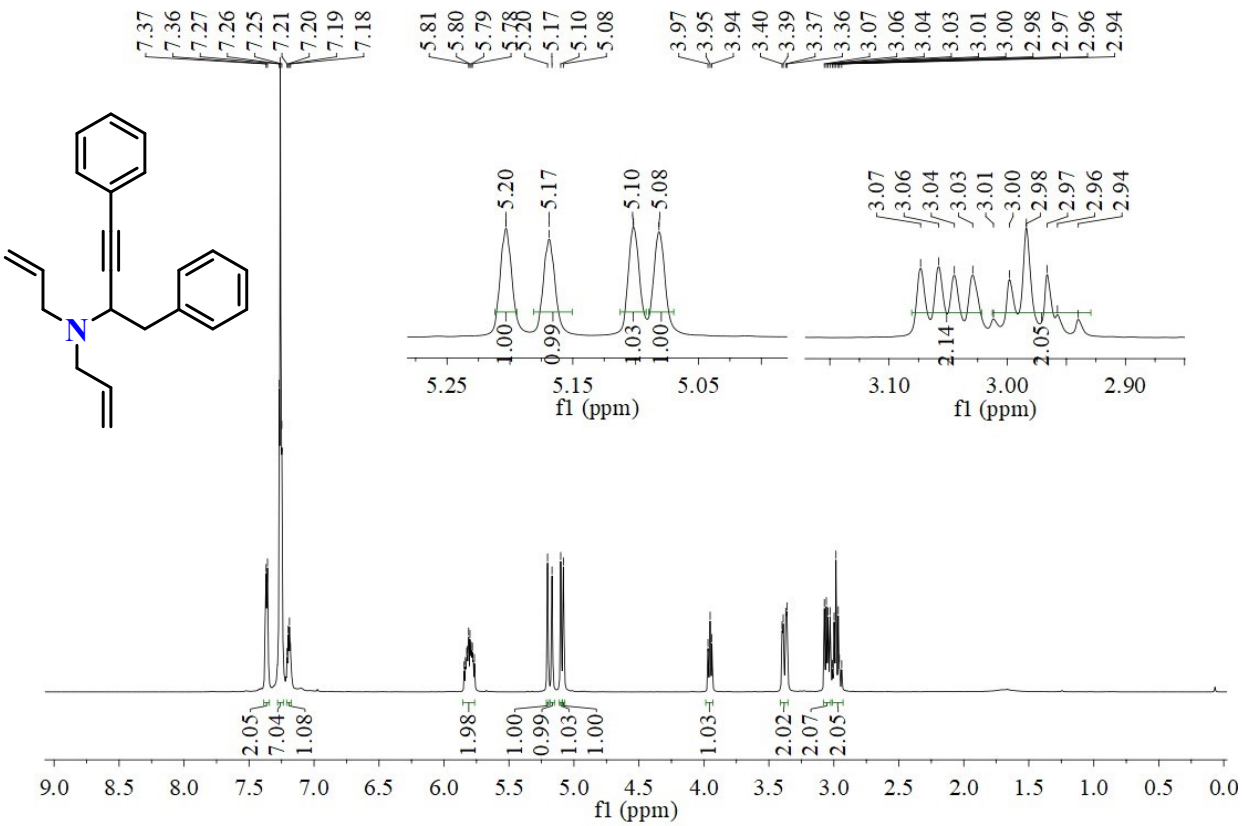

Figure S84. ^{1}H NMR (25 °C, 500 MHz) spectrum of the trisubstituted product **16b** from diallylamine in $CDCl_3$.

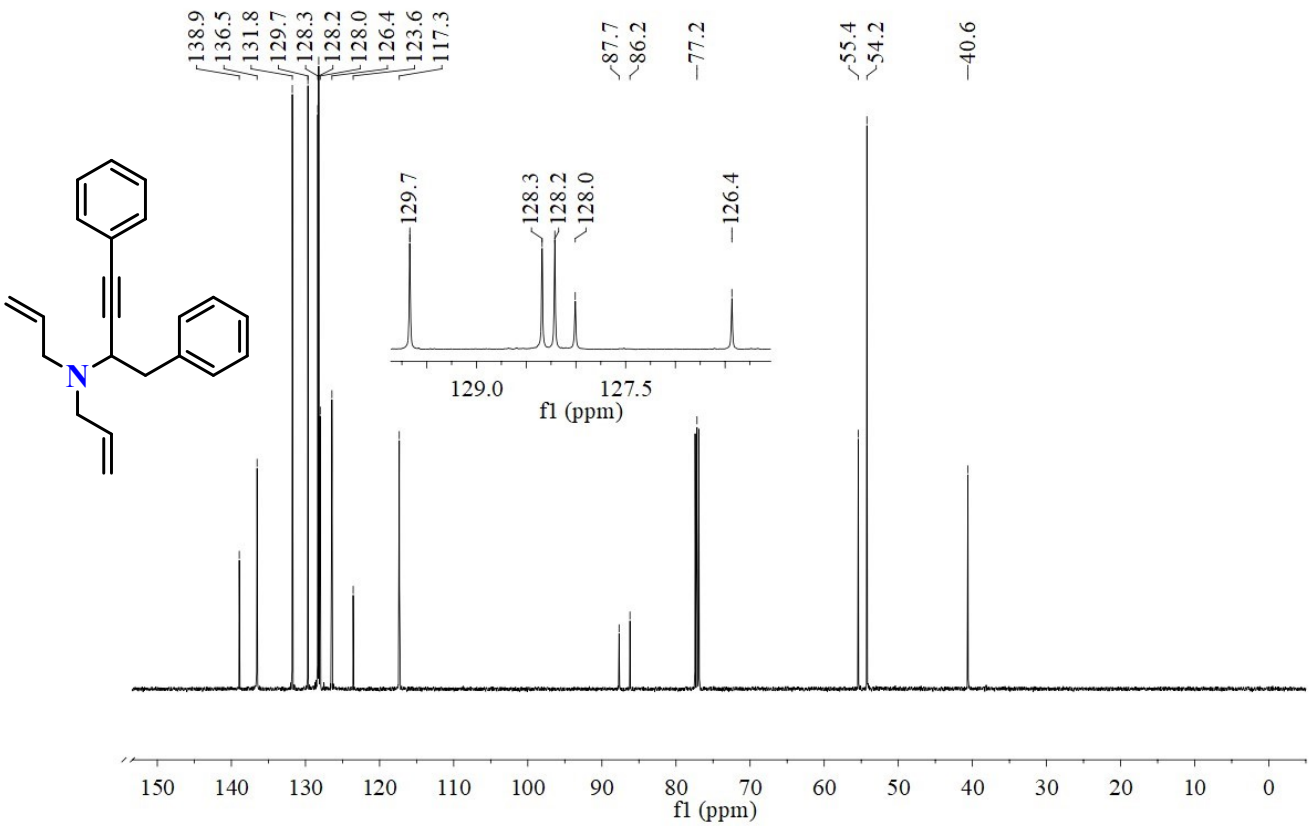

Figure S85. $^{13}C\{^{1}H\}$ NMR (25 °C, 125.7 MHz) spectrum of the trisubstituted product **16b** from diallylamine in $CDCl_3$.

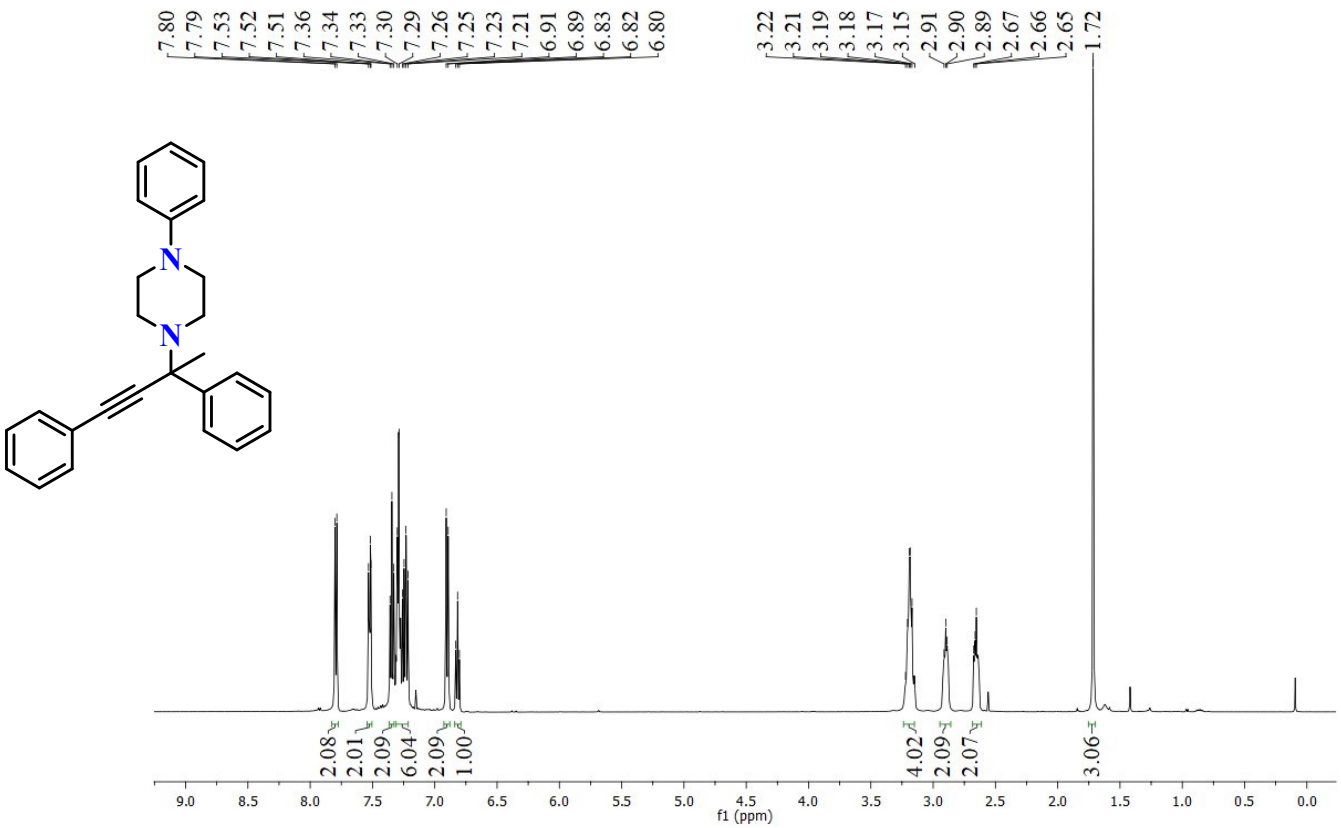

Figure S86. ^{1}H NMR (25 °C, 500 MHz) spectrum of the tetrasubstituted product **17a** from *N*-phenylpiperazine in $CDCl_3$.

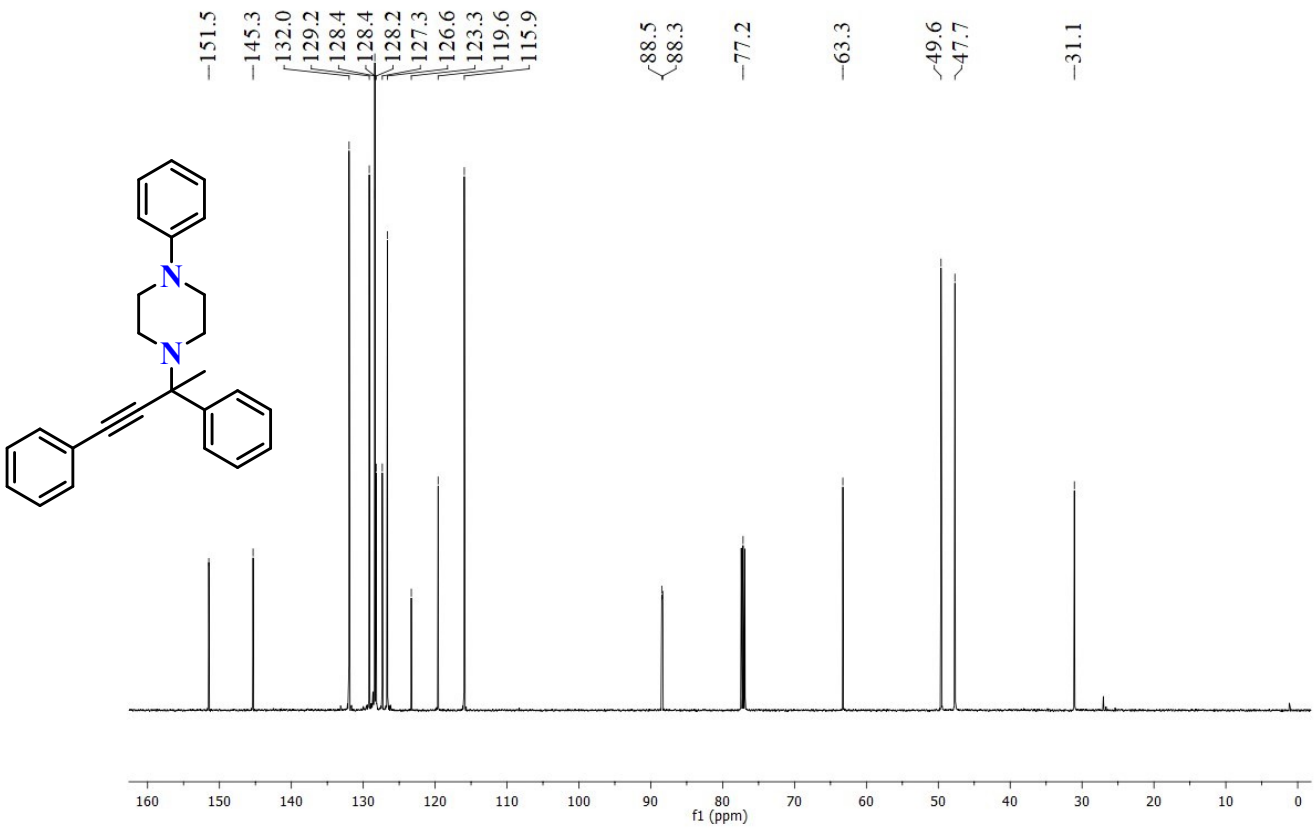

Figure S87. $^{13}C\{^{1}H\}$ NMR (25 °C, 125.7 MHz) spectrum of the tetrasubstituted product **17a** from *N*-phenylpiperazine in $CDCl_3$.

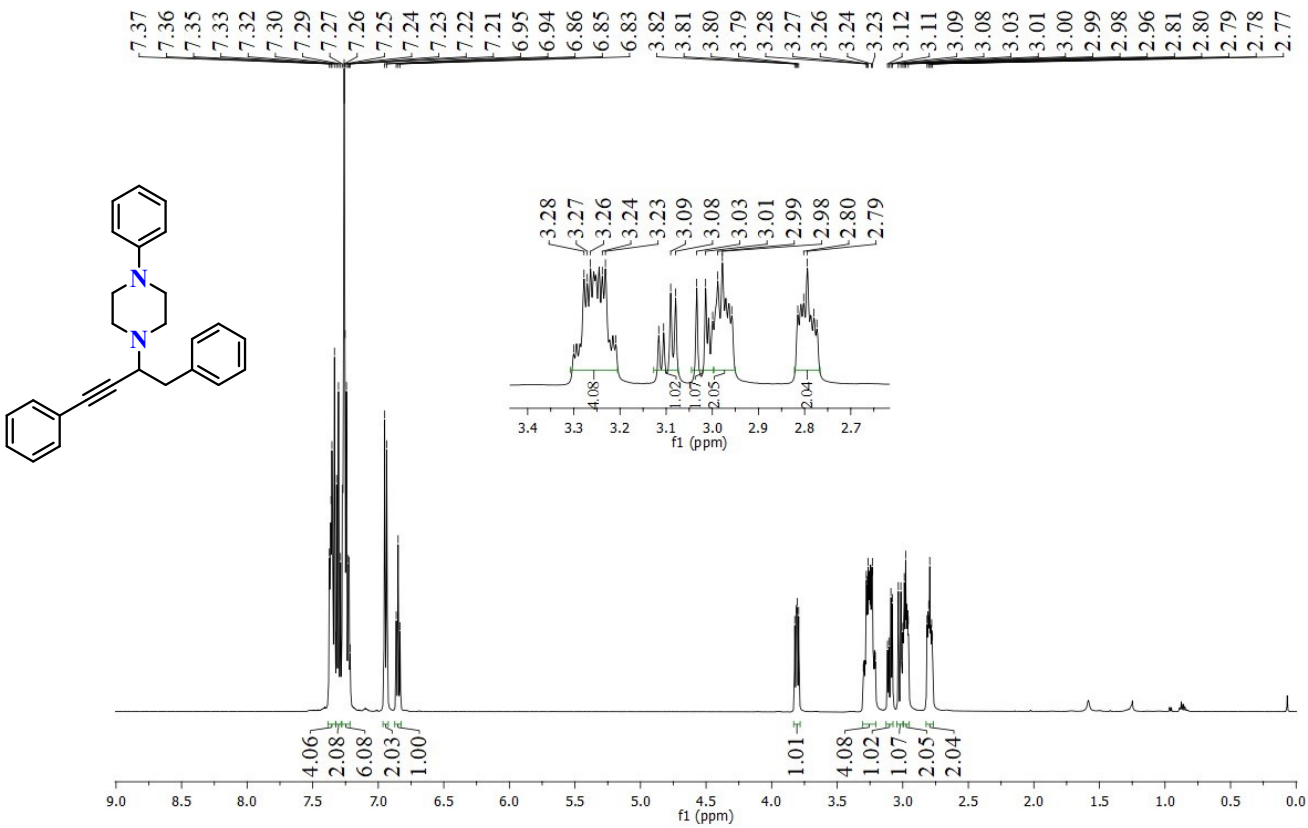

Figure S88. ^{1}H NMR (25 °C, 500 MHz) spectrum of the trisubstituted product **17b** from *N*-phenylpiperazine in $CDCl_3$.

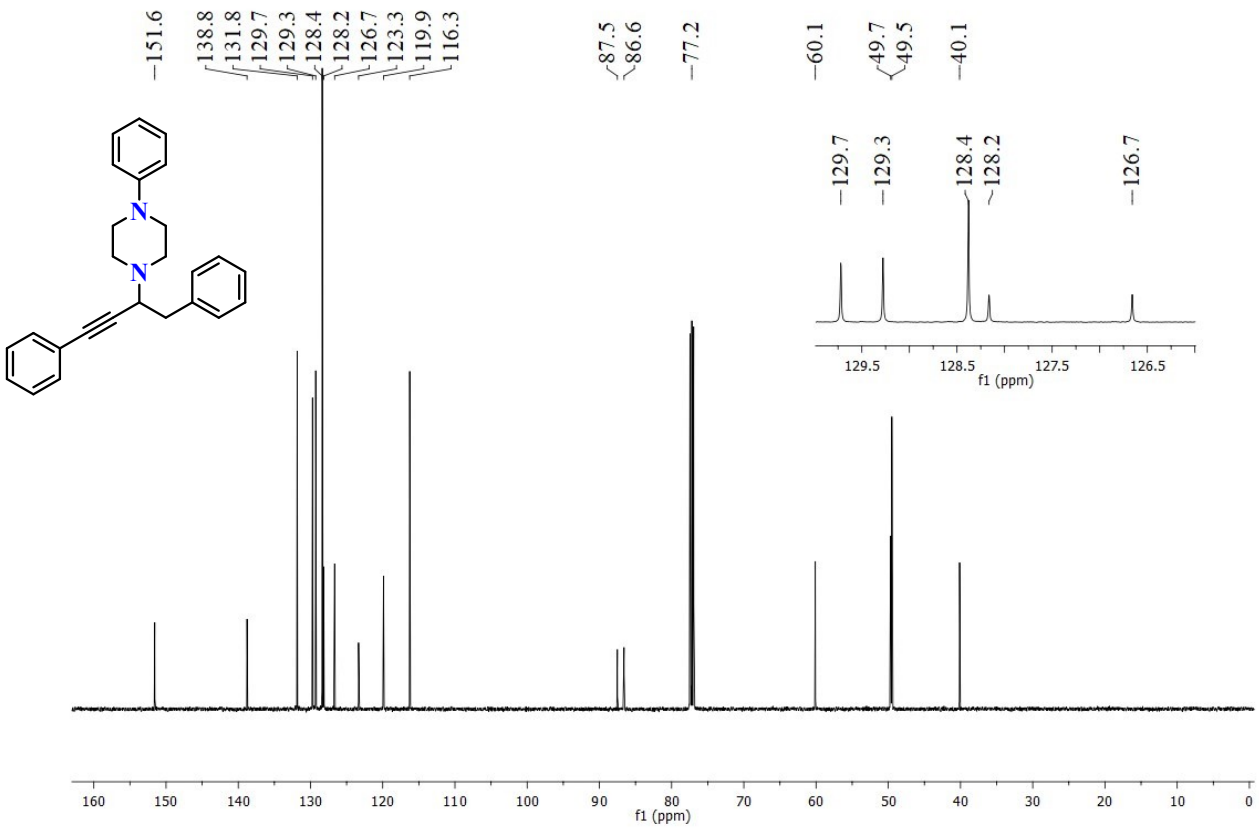

Figure S89. $^{13}C\{^{1}H\}$ NMR (25 °C, 125.7 MHz) spectrum of the trisubstituted product **17b** from *N*-phenylpiperazine in $CDCl_3$.

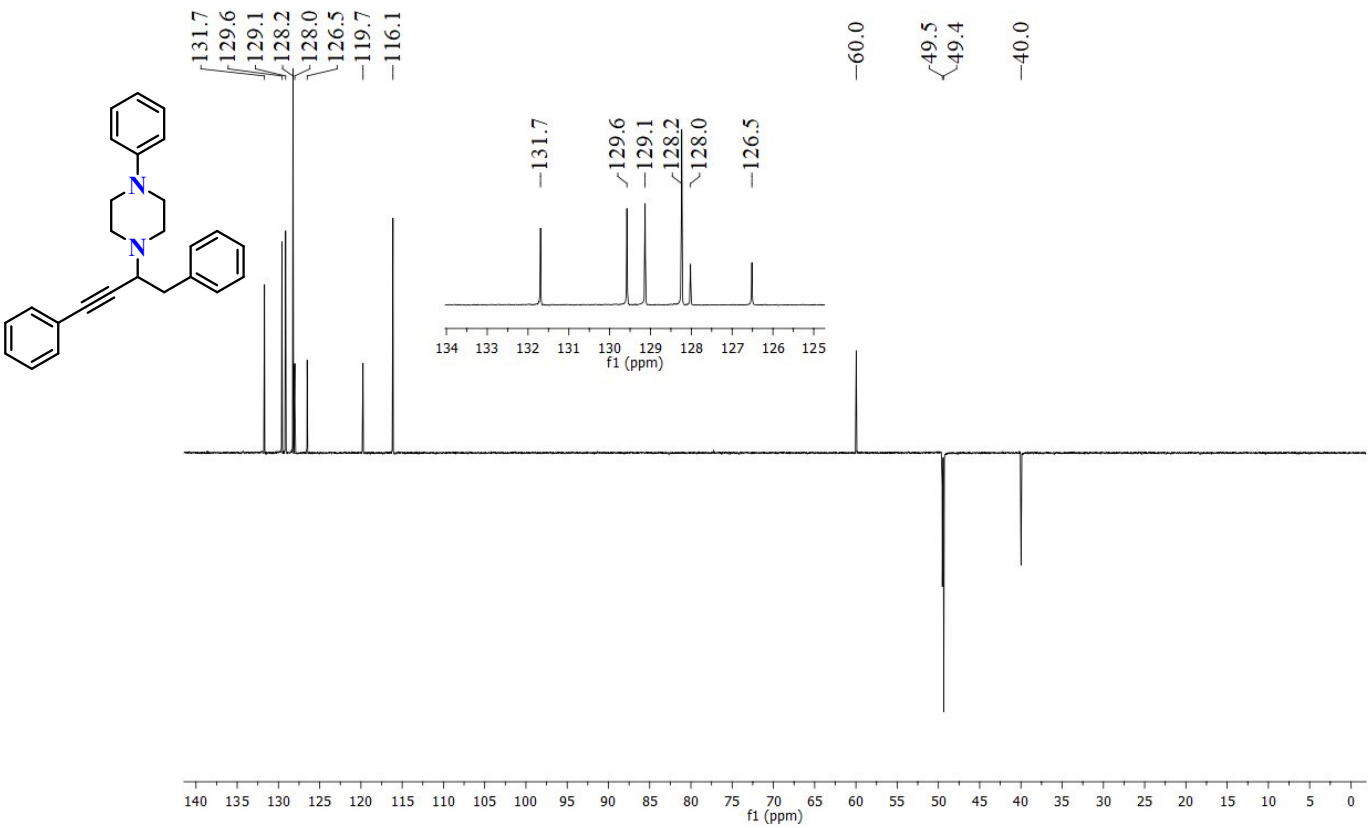

Figure S90. $^{13}C\{^{1}H\}$ DEPT NMR (25 °C, 125.7 MHz) spectrum of the trisubstituted product **17b** from *N*-phenylpiperazine in $CDCl_3$.

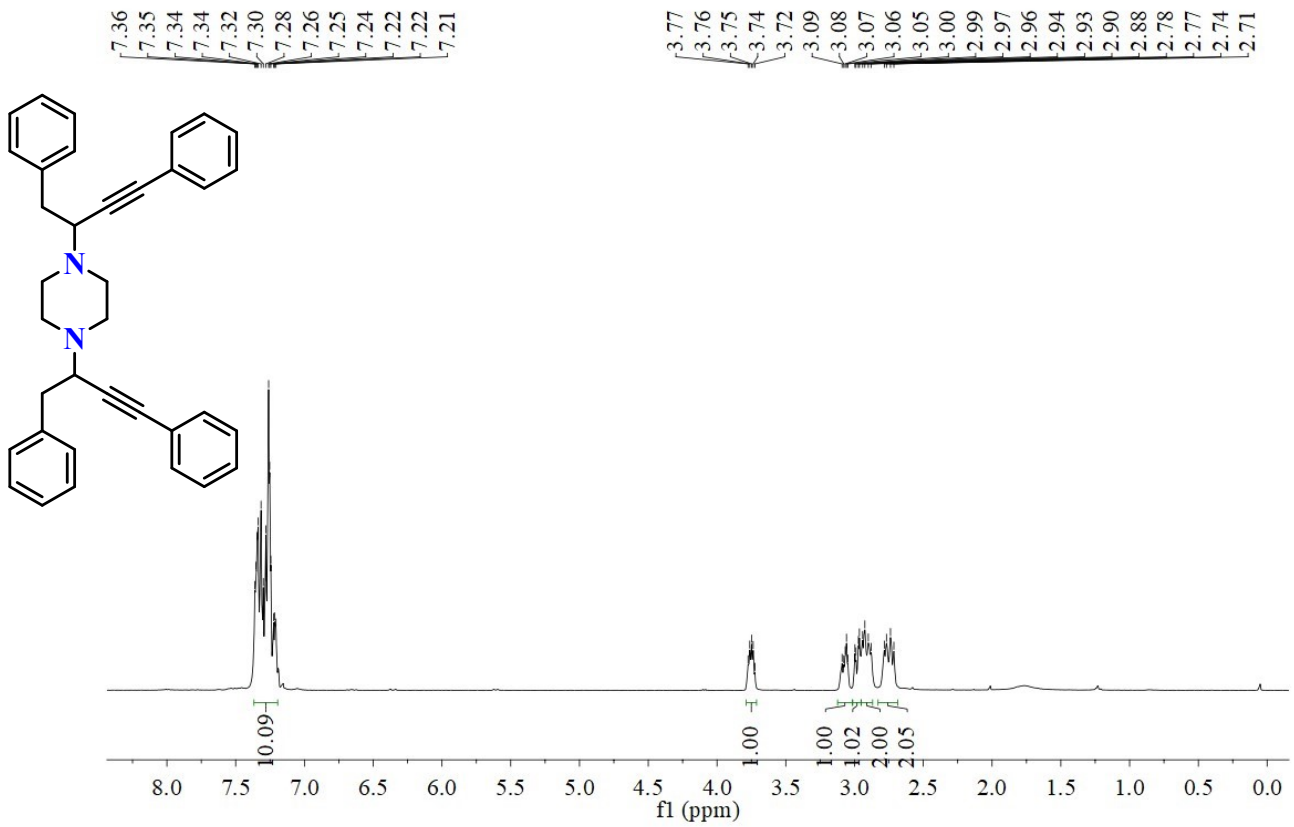

Figure S91. ^{1}H NMR (25 °C, 400 MHz) spectrum of the trisubstituted product **18** from piperazine in $CDCl_3$.

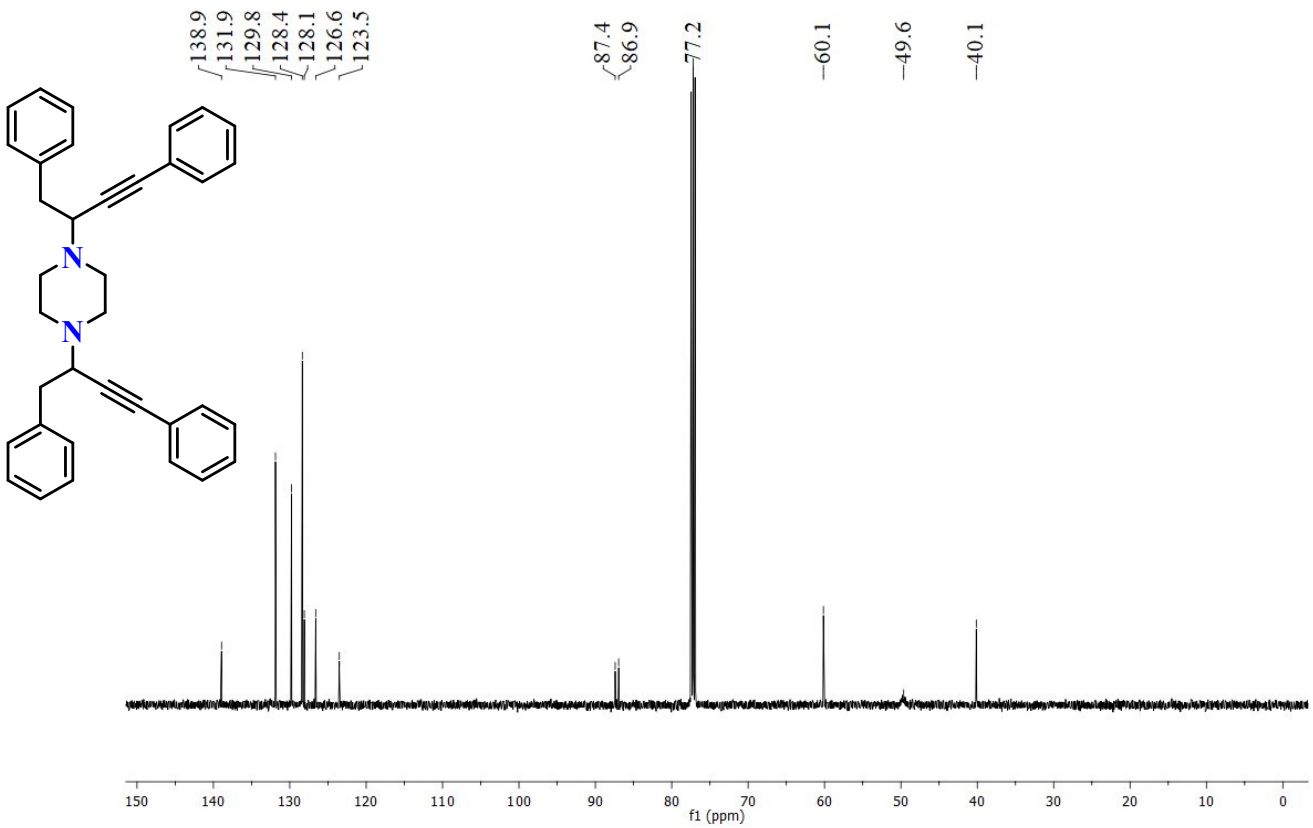

Figure S92. $^{13}C\{^{1}H\}$ NMR (25 °C, 125.7 MHz) spectrum of the trisubstituted product **18** from piperazine in $CDCl_3$.

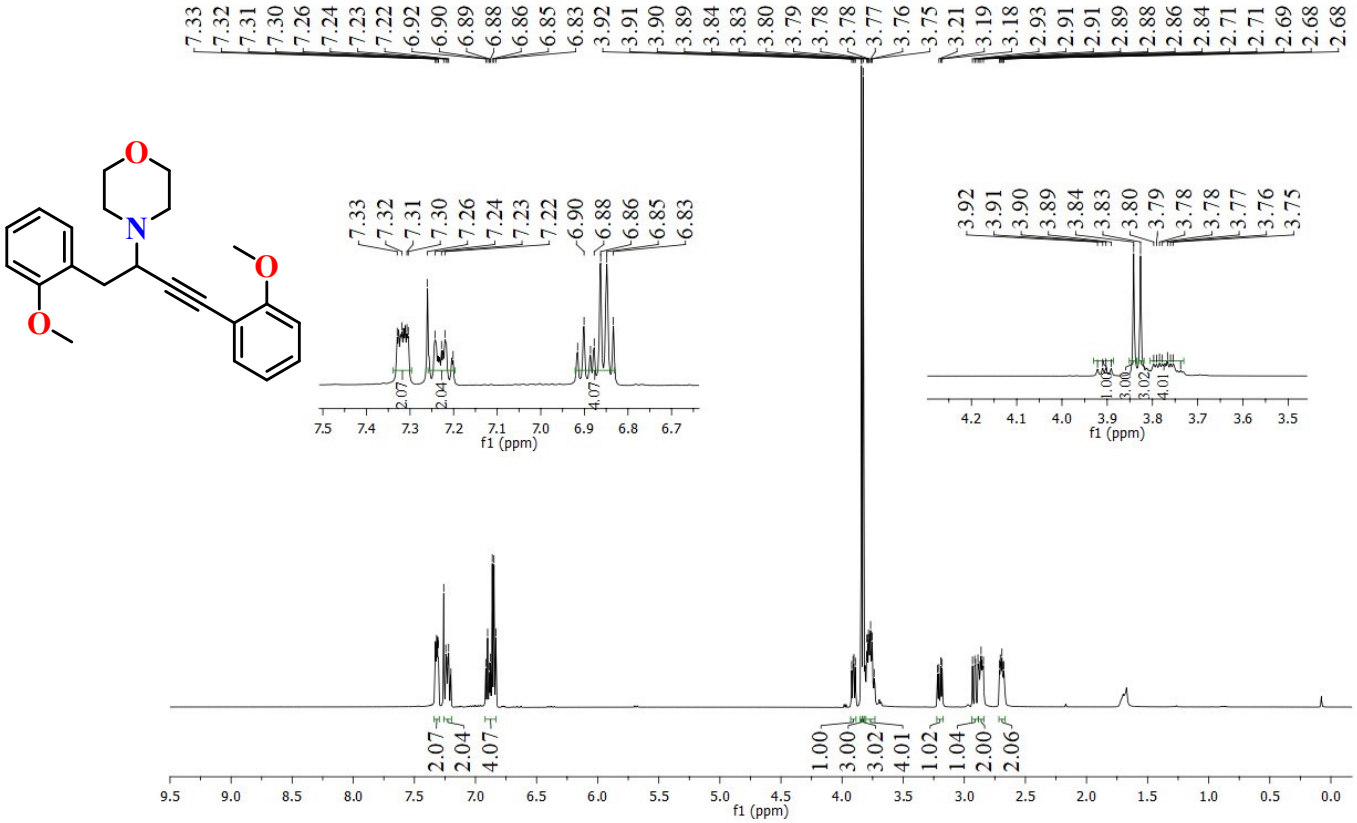

Figure S93. ^{1}H NMR (25 °C, 400 MHz) spectrum of the trisubstituted product **19** from 2-ethynylanisole in $CDCl_3$.

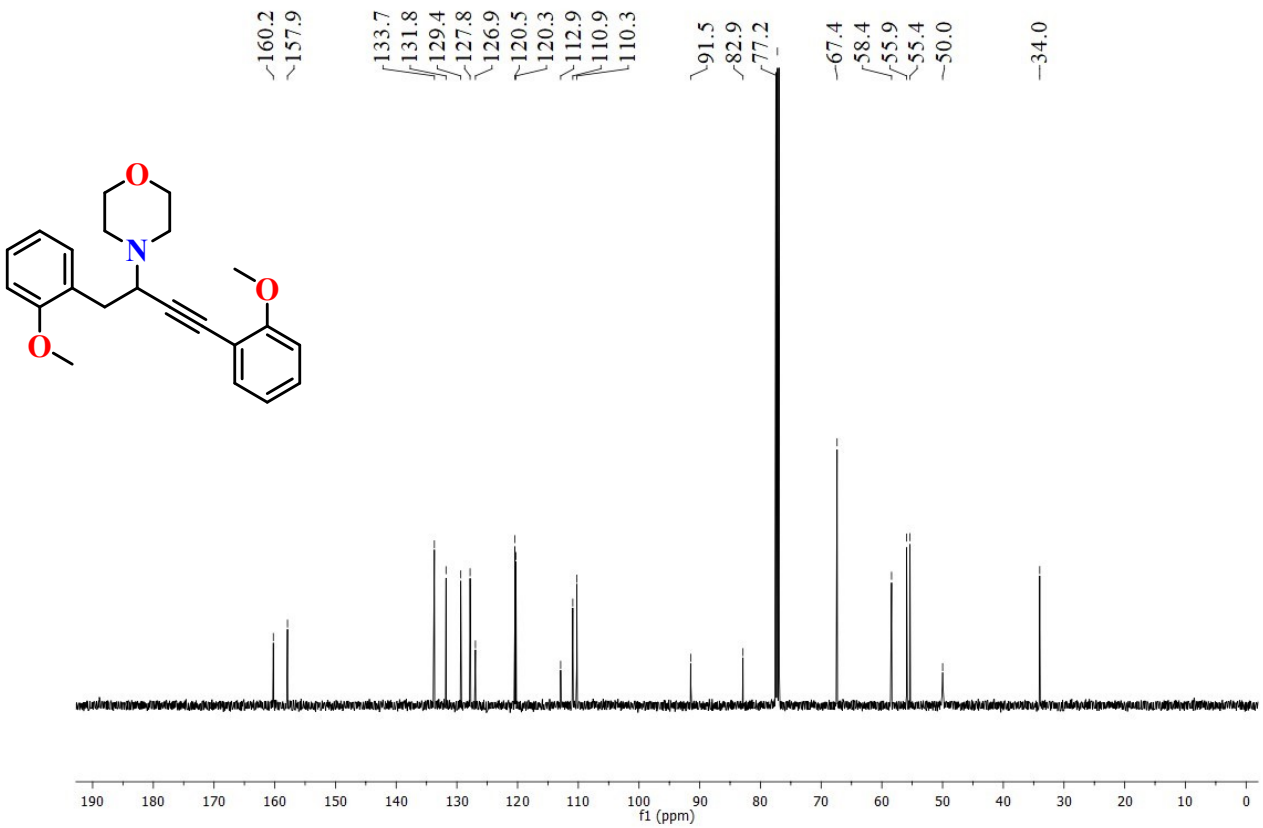

Figure S94. $^{13}C\{^{1}H\}$ NMR (25 °C, 125.7 MHz) spectrum of the trisubstituted product **19** from 2-ethynylanisole in $CDCl_3$.

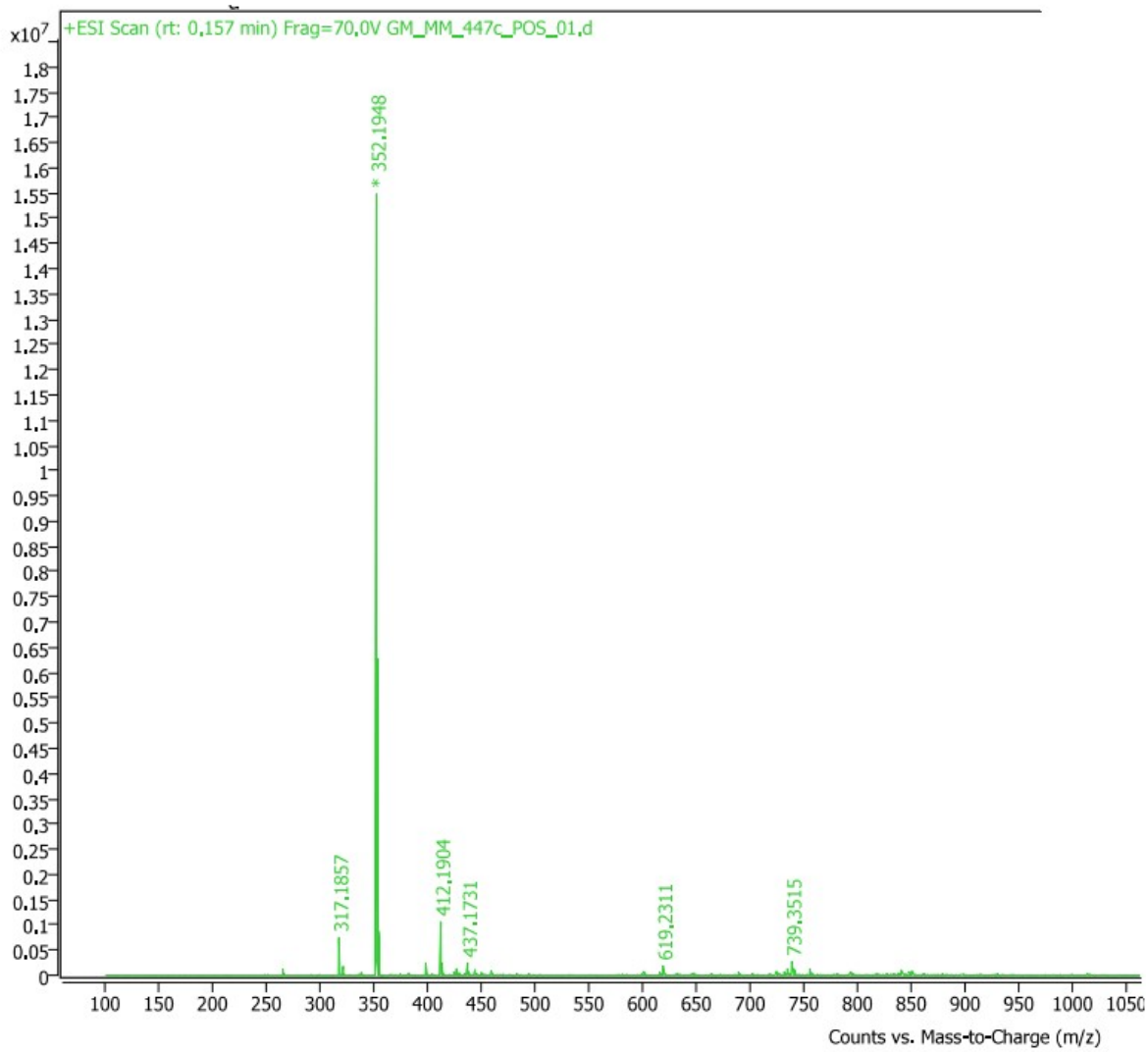

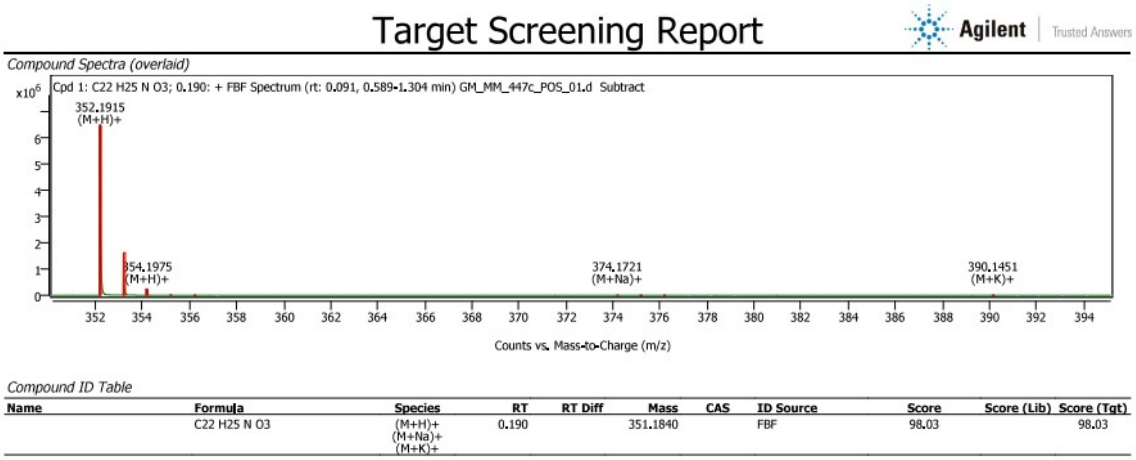

Name	Formula	Species	RT	RT Diff	Mass	CAS	ID Source	Score	Score (Lib)	Score (Tgt)
	C22 H25 N O3	(M+H)+ (M+Na)+ (M+K)+	0.190		351.1840		FBF	98.03		98.03

Figure S95. HRMS (+ESI) spectrum of the trisubstituted product from 2-ethynylanisole **19**. calcd *m/z* for $[M+H]^+$ $C_{22}H_{26}NO_3^+$: 352.1907, found: 352.1915.

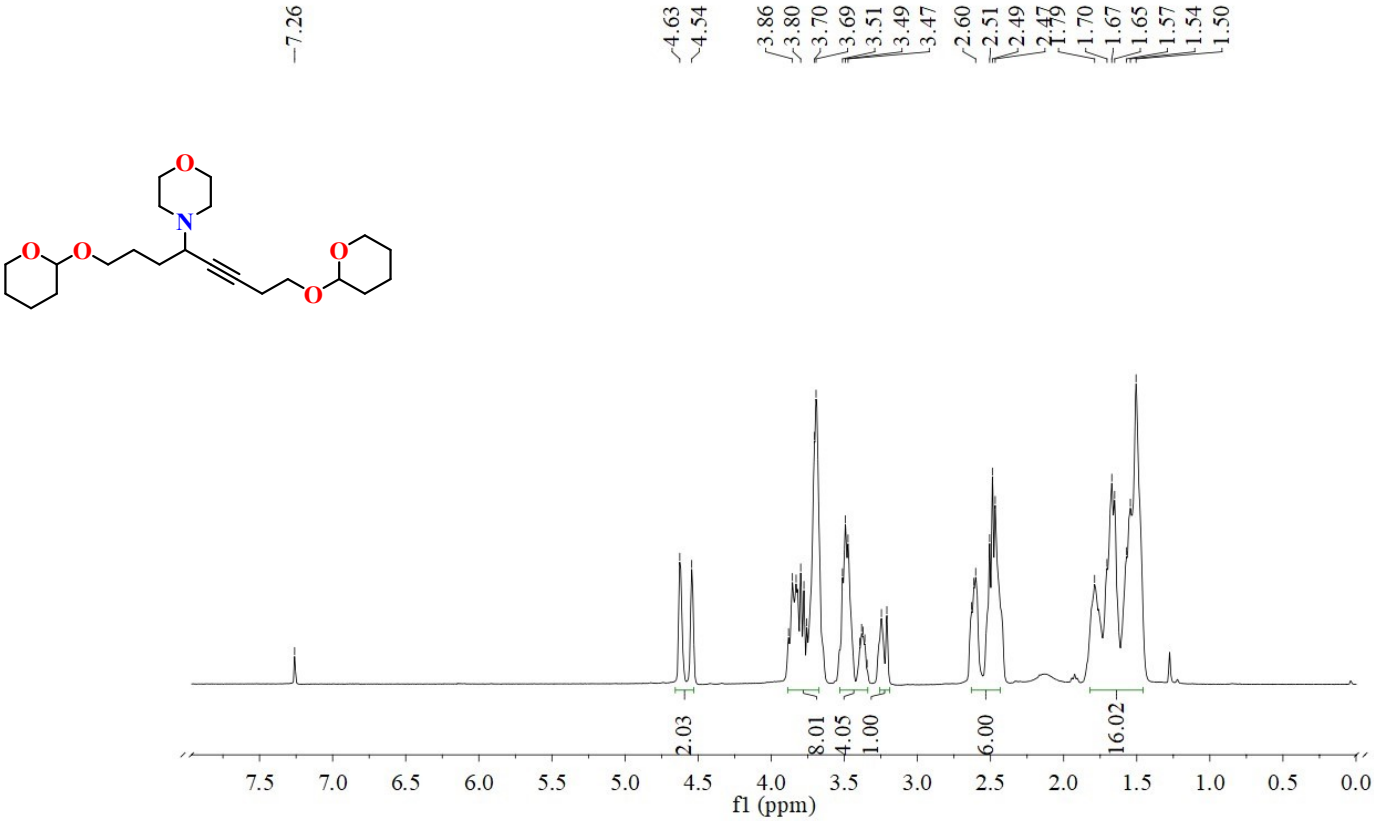

Figure S96. ^{1}H NMR (25 °C, 400 MHz) spectrum of the trisubstituted product **20** from (butynyloxy)tetrahydropyran in $CDCl_3$.

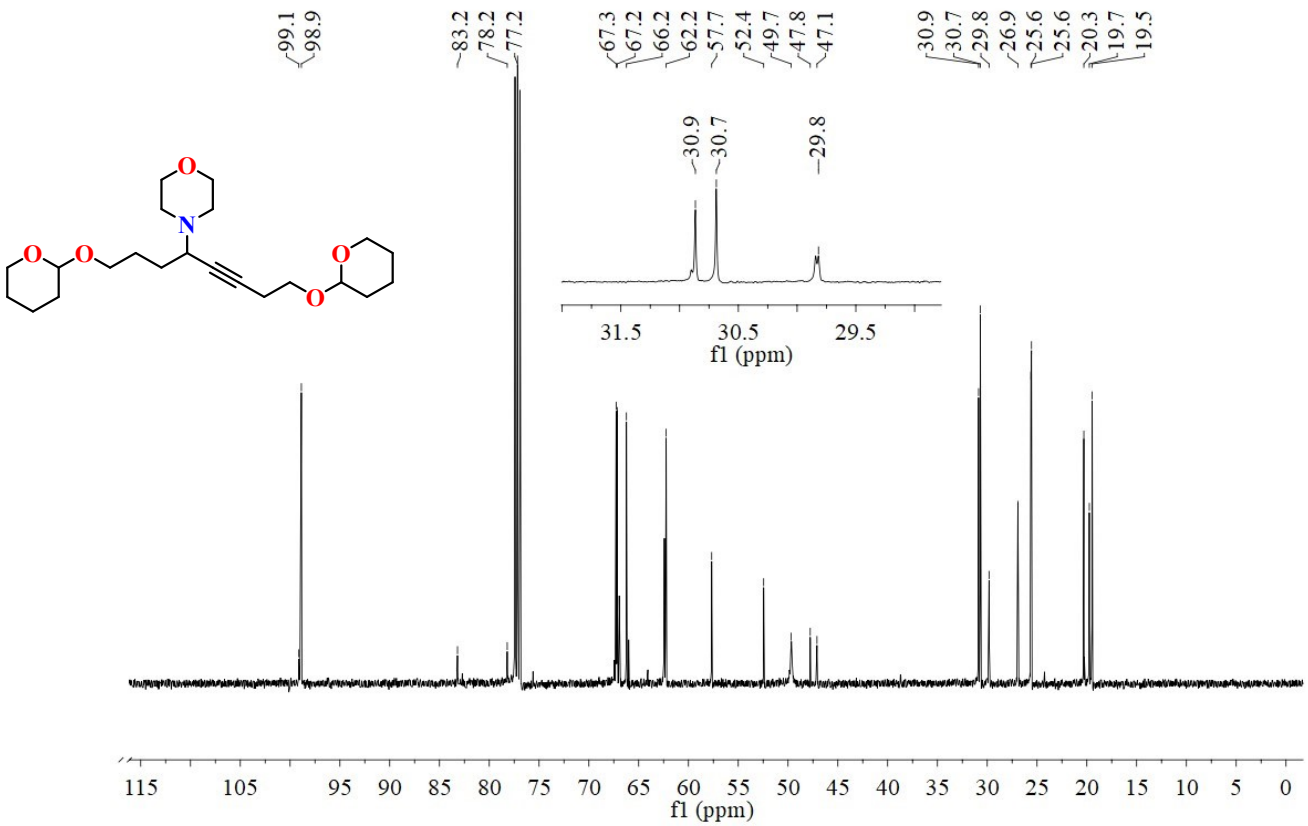

Figure S97. $^{13}C\{^{1}H\}$ NMR (25 °C, 125.7 MHz) spectrum of the trisubstituted product **20** from (butynyloxy)tetrahydropyran in $CDCl_3$.

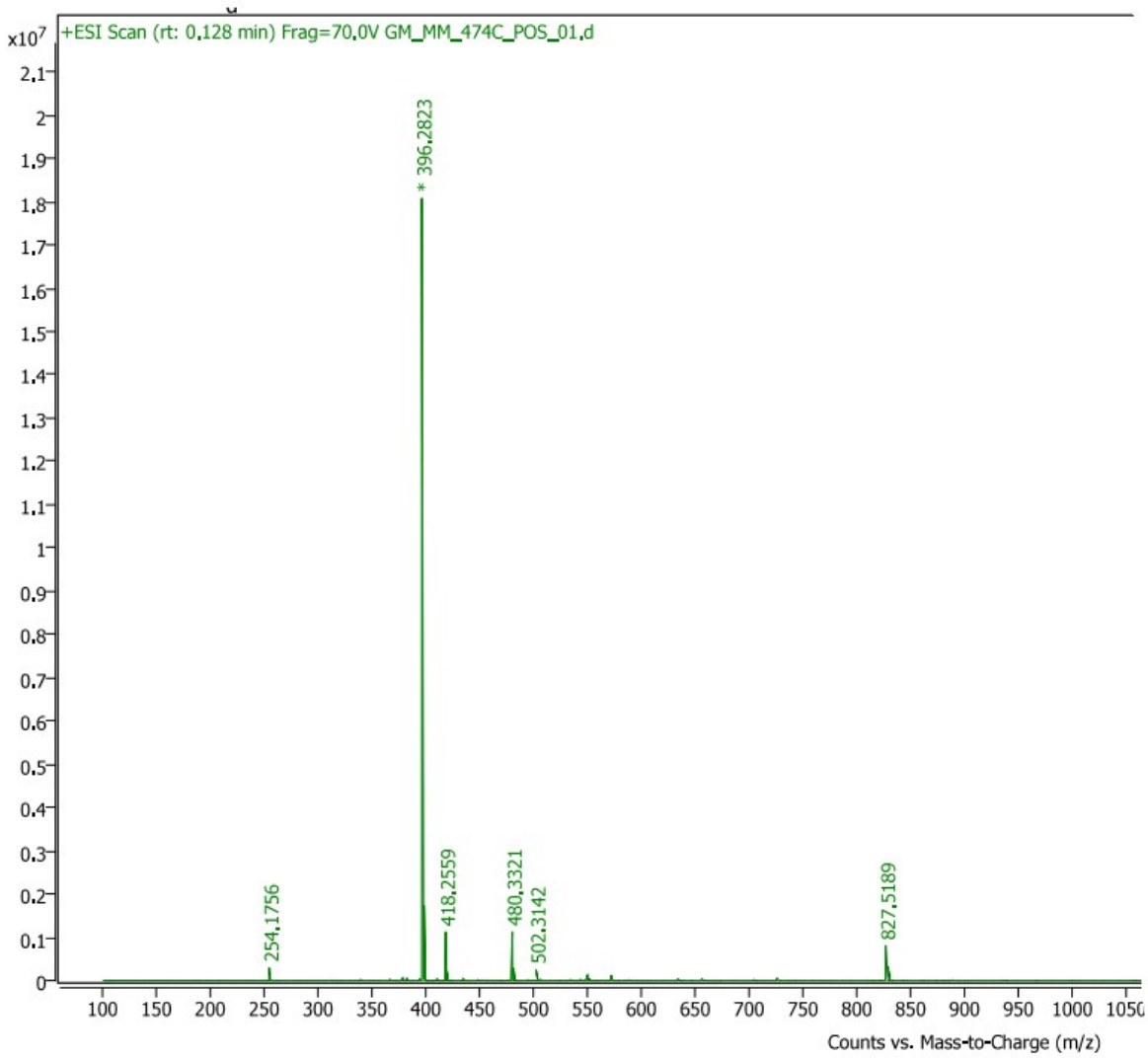

Figure S98. HRMS (+ESI) spectrum of the trisubstituted product **20** from (butynyloxy)tetrahydropyran. calcd *m/z* for $[M+Na]^+$ $C_{22}H_{37}NO_5Na^+$: 418.2564, found: 418.2559.

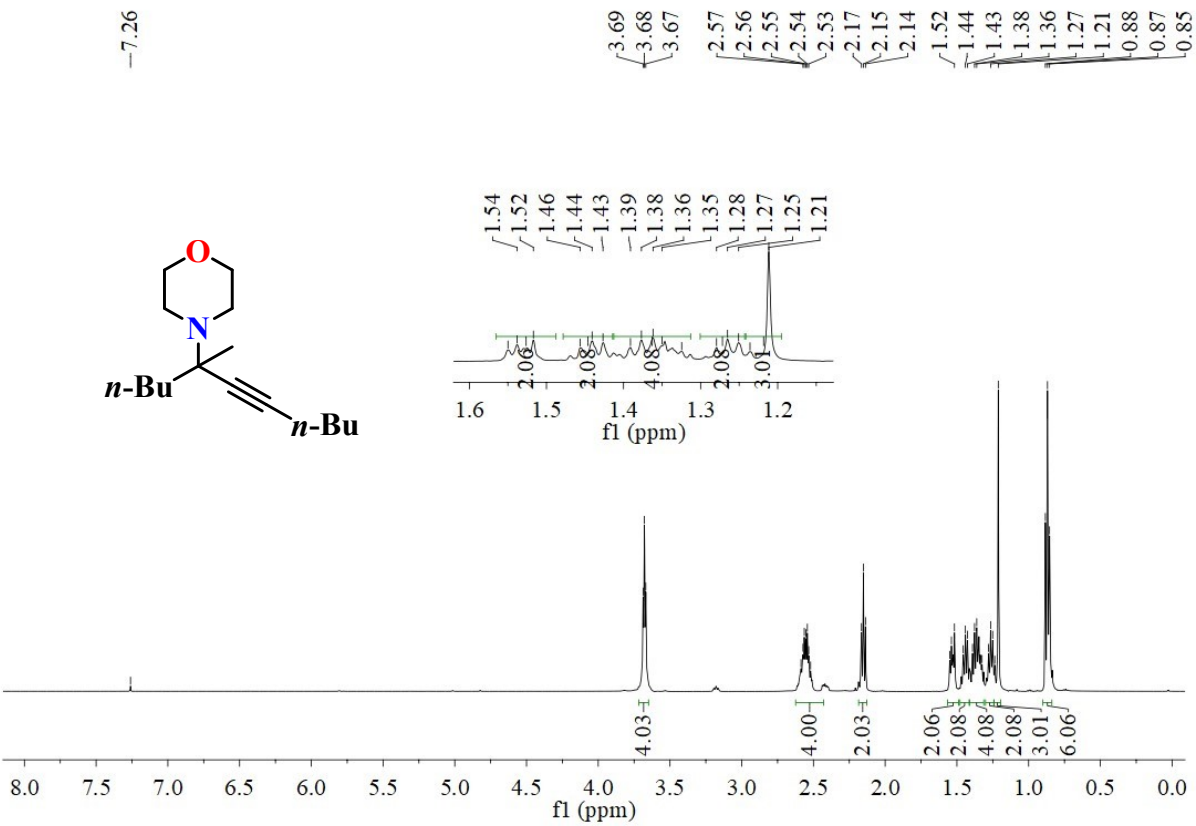

Figure S99. ^{1}H NMR (25 °C, 500 MHz) spectrum of the tetrasubstituted product **21** from 1-hexyne in $CDCl_3$.

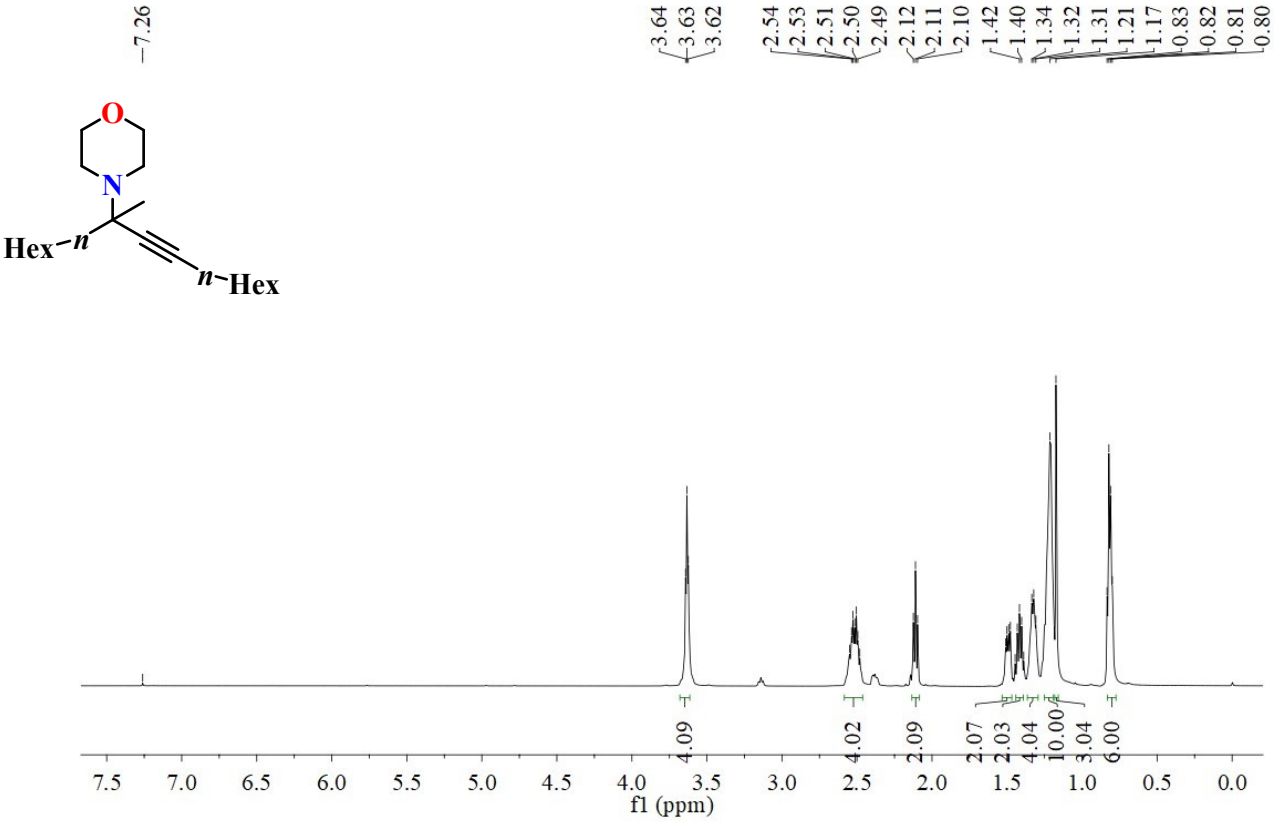

Figure S100. ^{1}H NMR (25 °C, 500 MHz) spectrum of the tetrasubstituted product **22** from 1-octyne in $CDCl_3$.

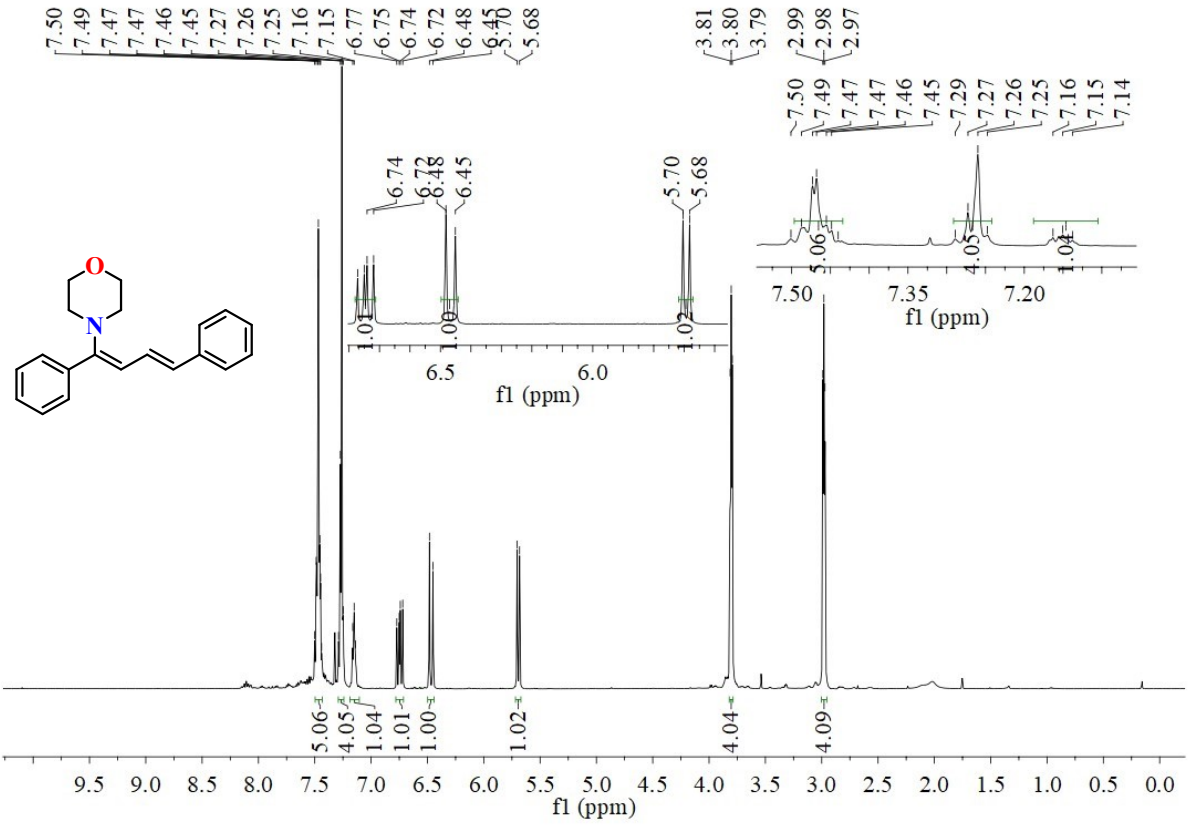

Figure S101. ^{1}H NMR (25 °C, 500 MHz) spectrum of 1-aminodiene **23** in $CDCl_3$.

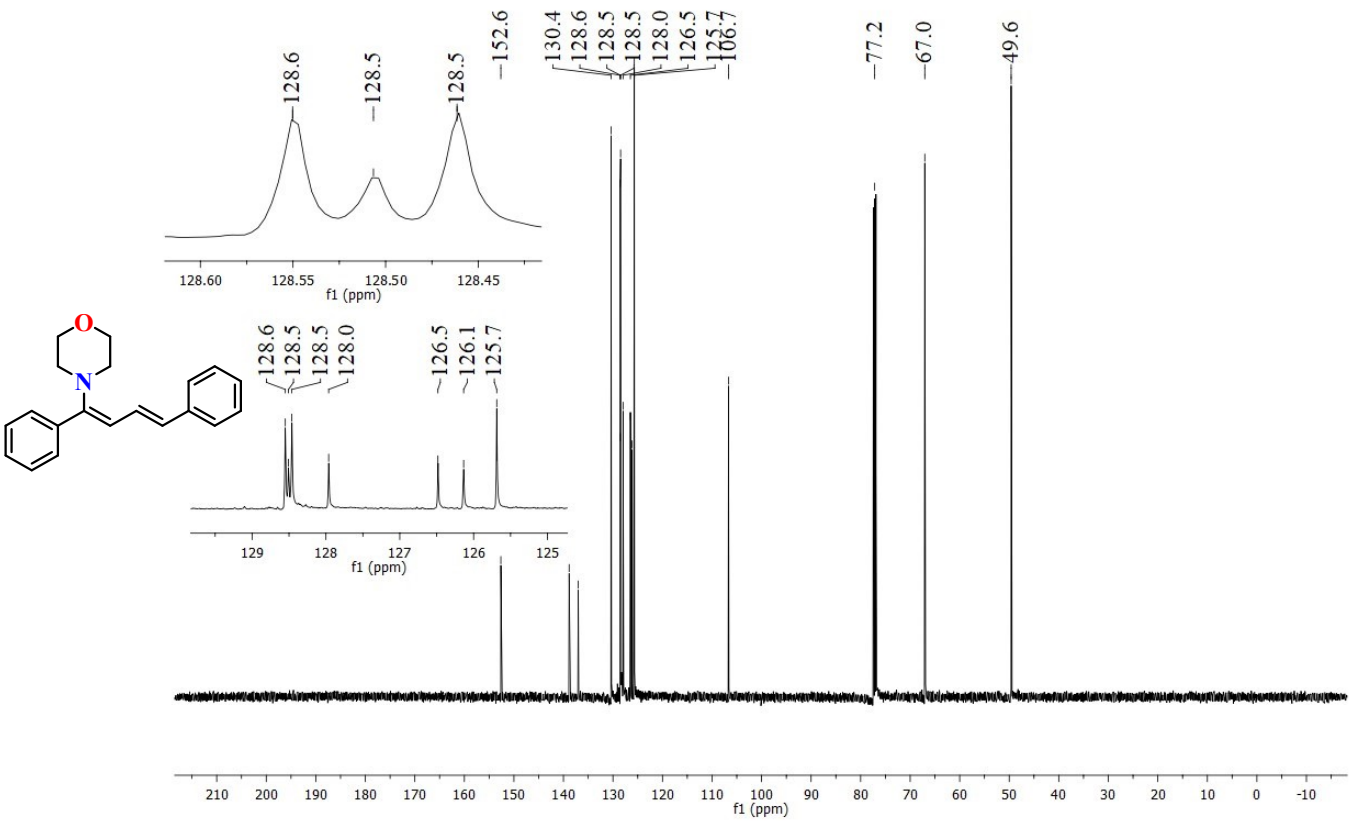

Figure S102. $^{13}C\{^{1}H\}$ NMR (25 °C, 125.7 MHz) spectrum of 1-aminodiene **23** in $CDCl_3$.

Mechanistic evidence

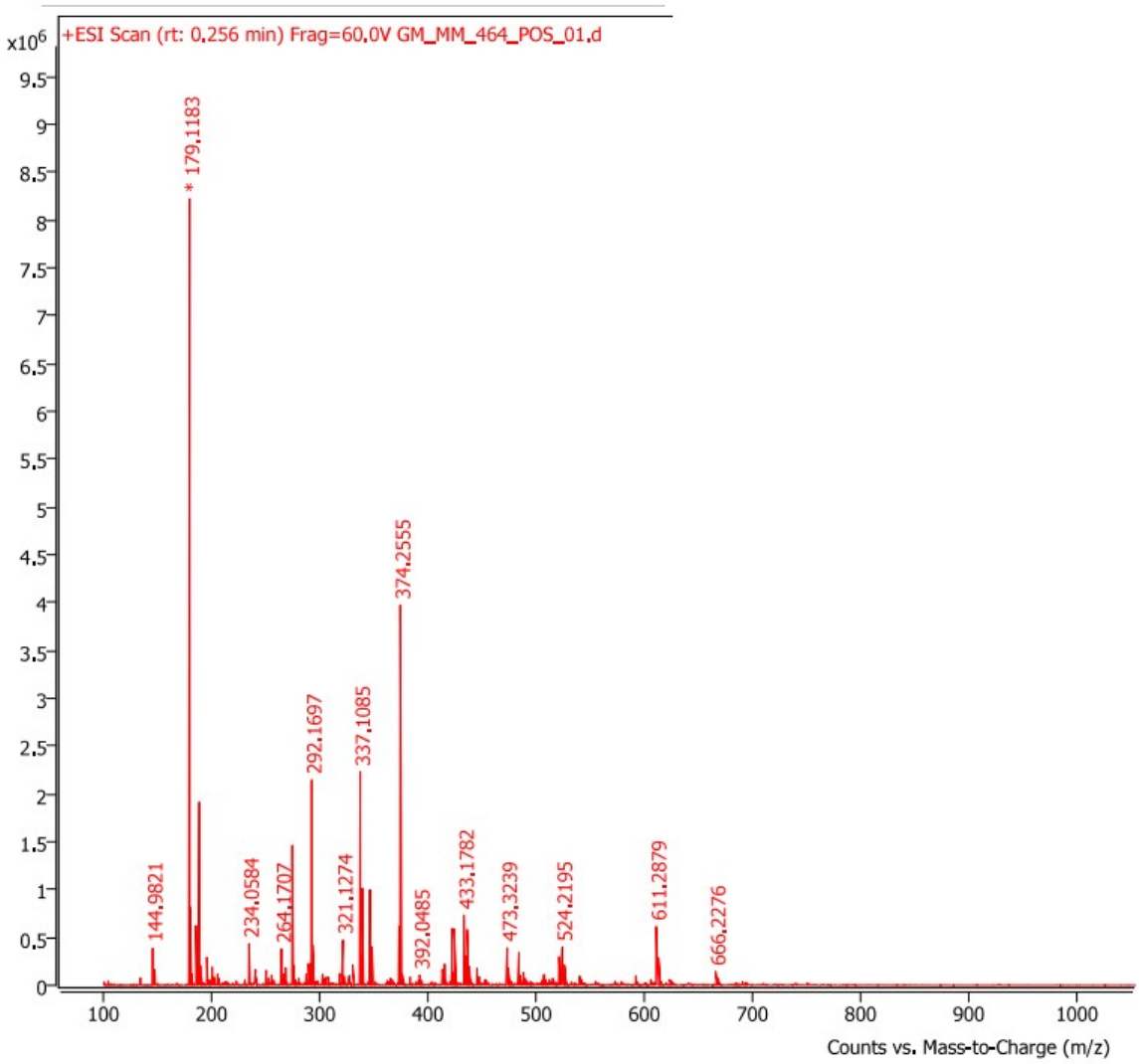

Figure S103. HRMS (ESI+) spectrum of the reaction mixture of copper(I) chloride complex **8**, morpholine and phenylacetylene (1:1:4 equiv.) in 1 mL toluene at 110 °C for 1h. The peak at *m/z* 392.0485 (calc. 392.0489) shows the formation of $[Cu\{C_4H_3N\text{-}2\text{-}(CH_2Me_2pz)\text{-}5\text{-}(CH_2SO_2Ph)\text{-}\kappa^1\text{-}N\}]^+$; it can be the active catalyst as proposed in the mechanism. The peak at *m/z* 292.1697 represents the product of the reaction.

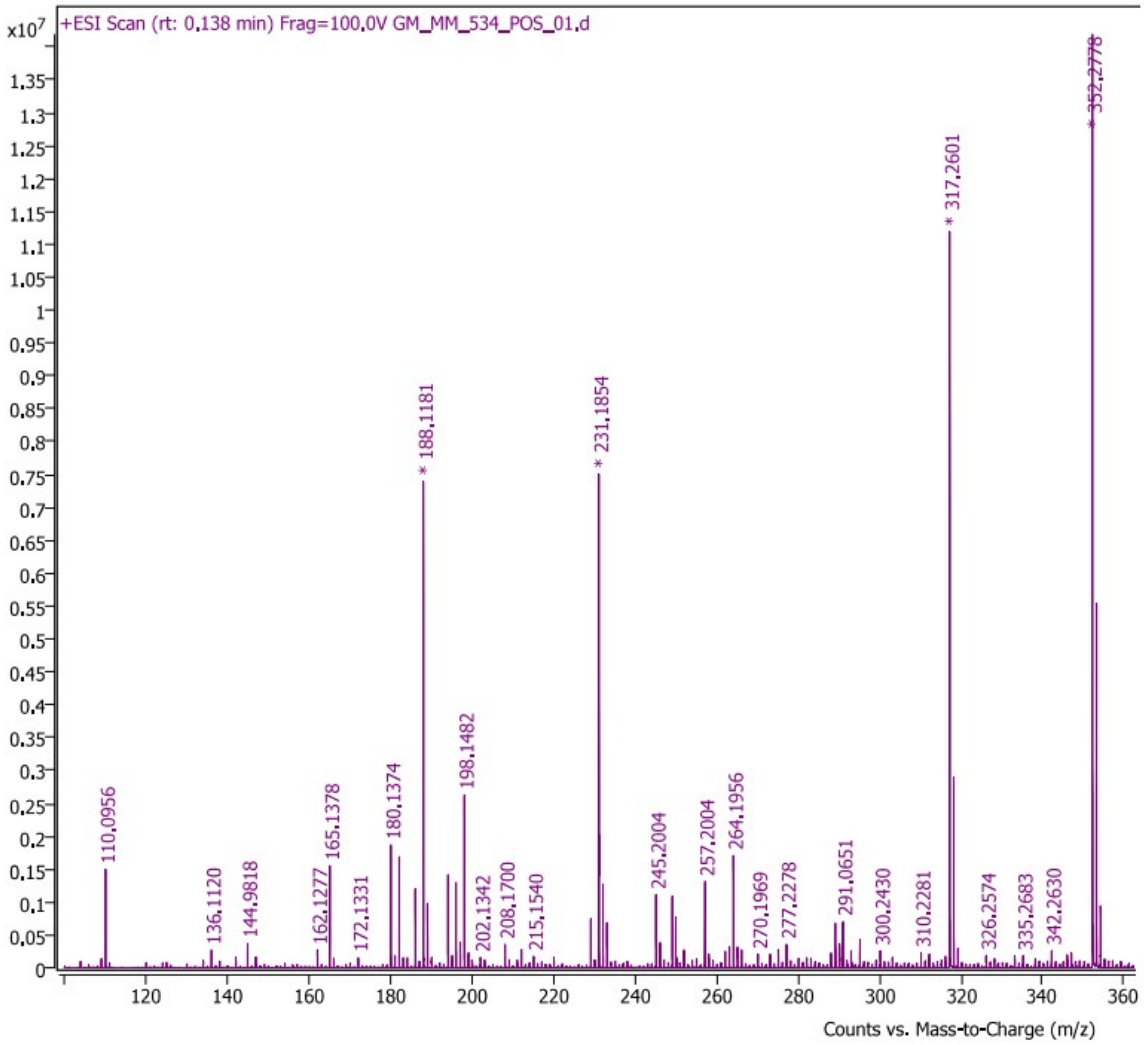

Figure S104. HRMS(ESI+) spectrum of the reaction mixture of bis(allyl)amine and pent-4-yn-1-ol (1:1) catalyzed by complex **5** (1 mol%) at 70 °C for 2 h under nitrogen atmosphere.

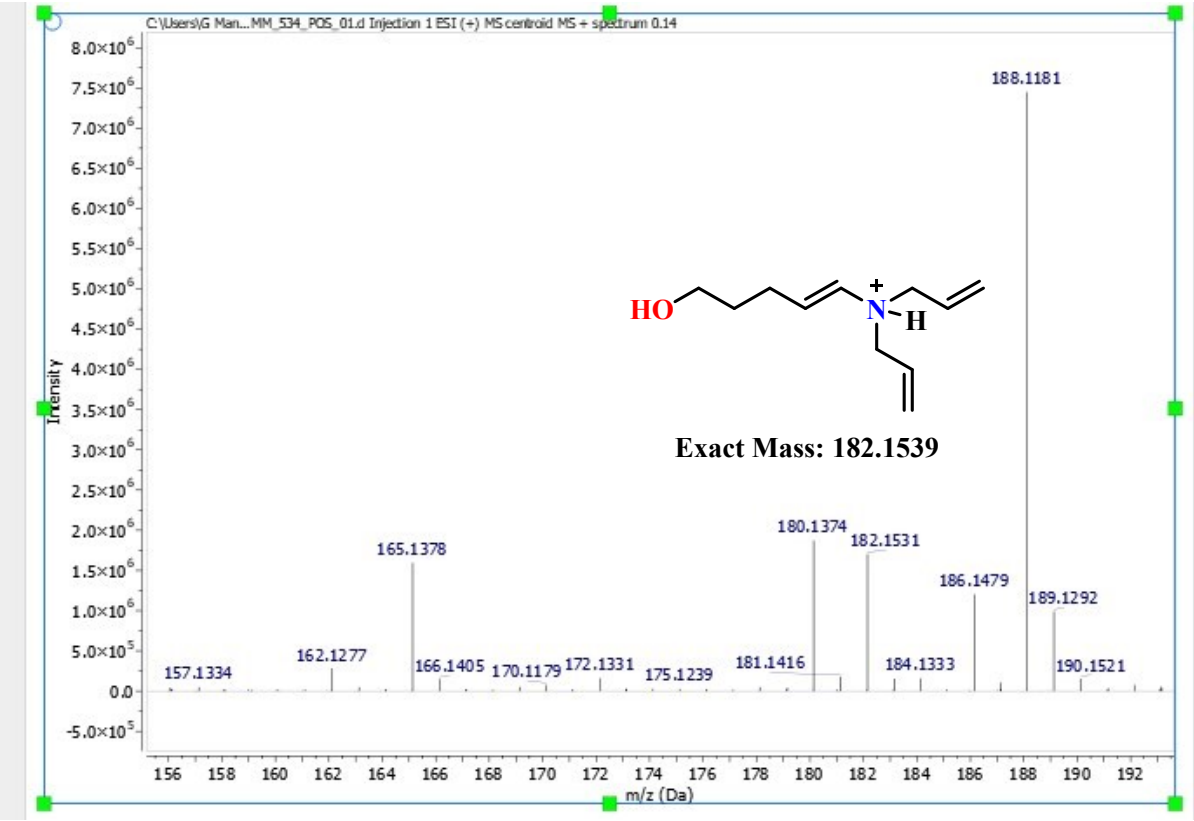

Figure S105. Partial HRMS(ESI+) spectrum of the reaction mixture of bis(allyl)amine and pent-4-yn-1-ol (1:1) catalyzed by complex **5** (1 mol%) at 70 °C for 2 h under nitrogen atmosphere.

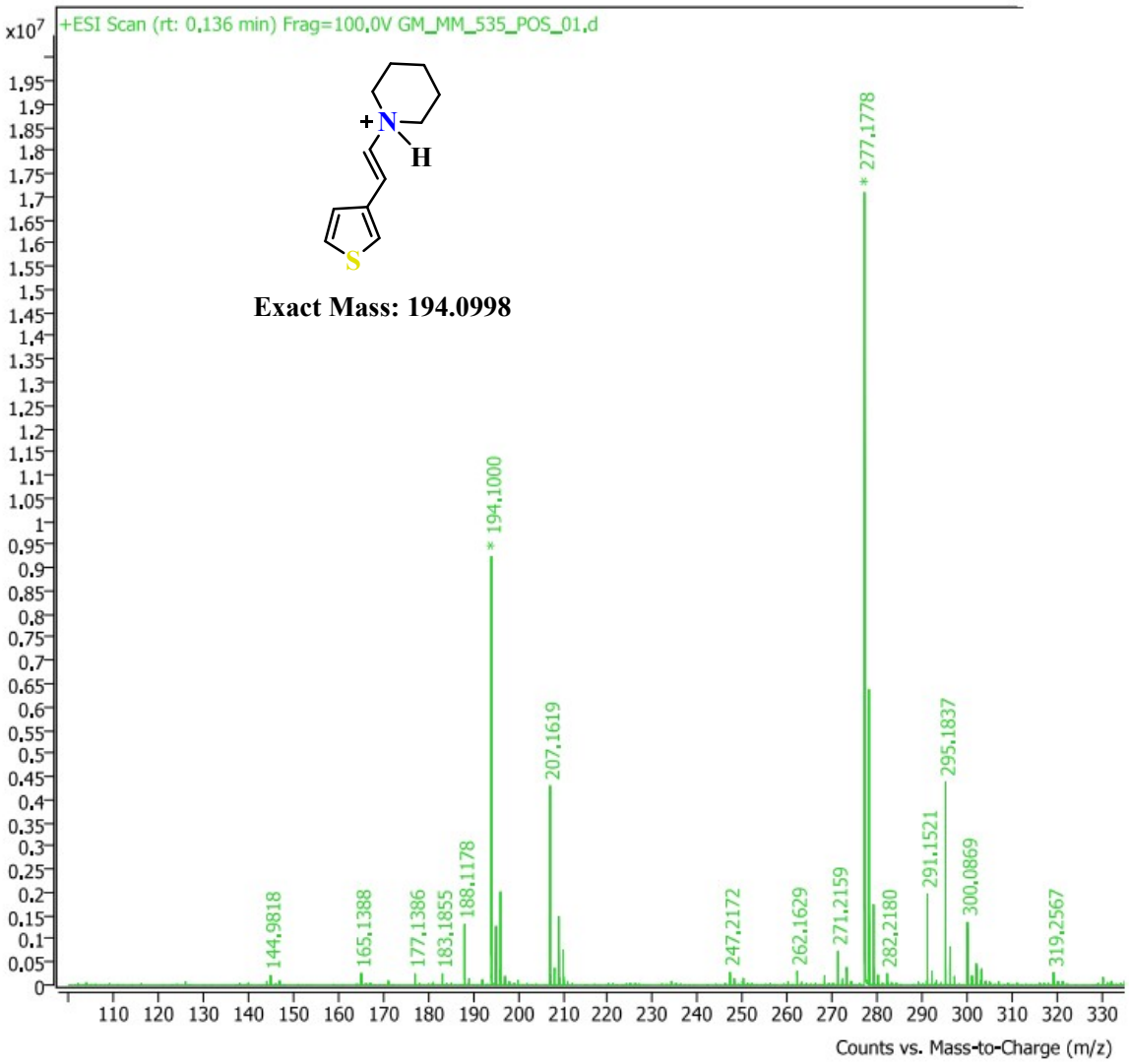

Figure S106. HRMS(ESI+) spectrum of the reaction mixture of bis(allyl)amine and 3-ethynylthiophene (1:1) catalyzed by complex **5** (1 mol%) at 70 °C for 2 h under nitrogen atmosphere.

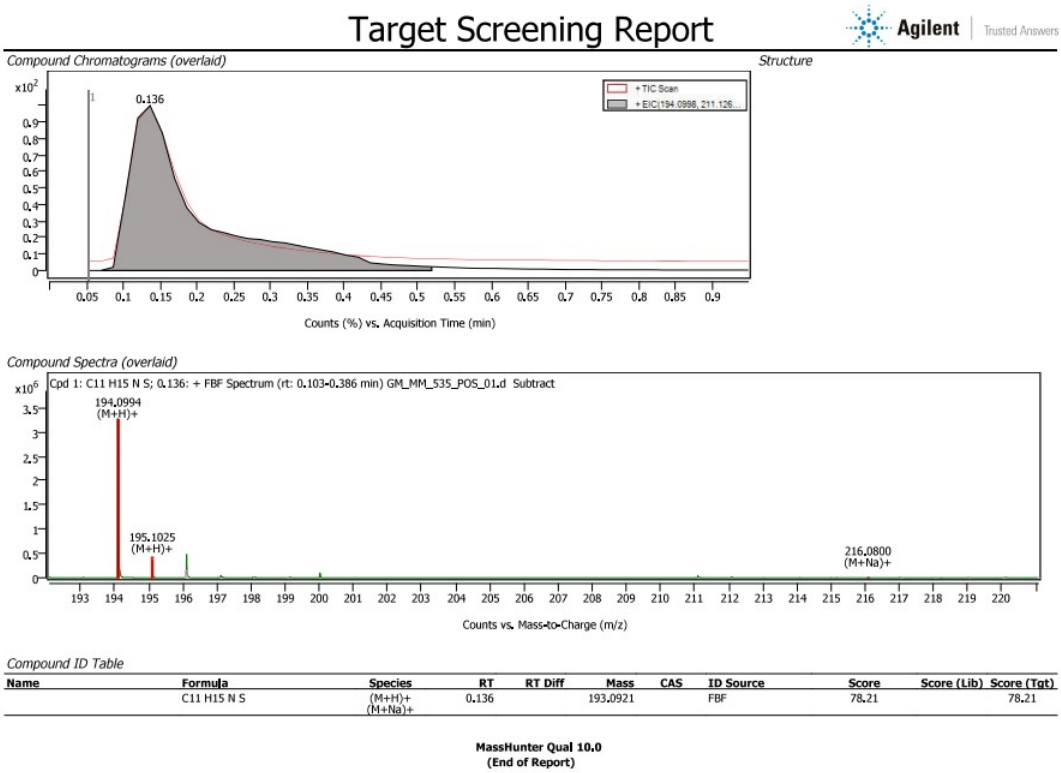

Figure S107. Target screening HRMS(ESI+) spectrum of the reaction mixture of bis(allyl)amine and 3-ethynylthiophene (1:1) catalyzed by complex **5** (1 mol%) at 70 °C for 2 h under nitrogen atmosphere.

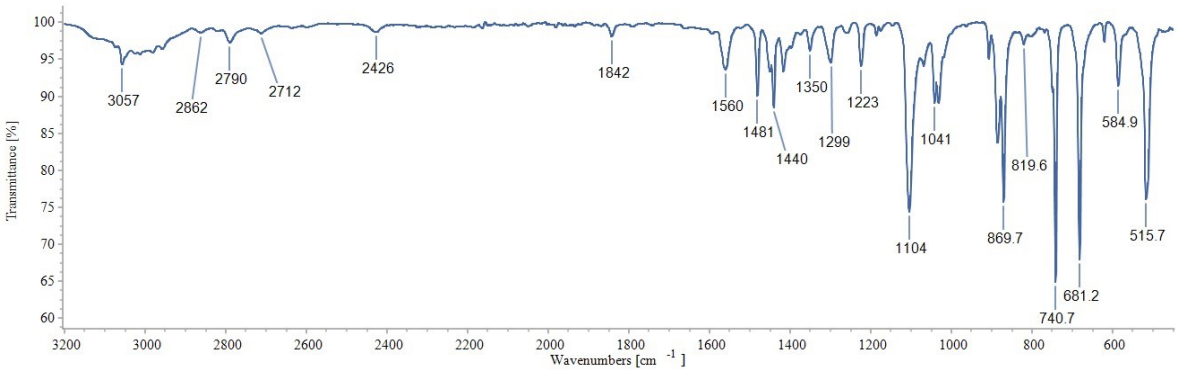

Figure S108. ATR spectrum of the morpholinium copper(I) salt $[C_4H_{10}NO]_4^+[Cu_2Cl_6]^{4-}$.

For NMR yields

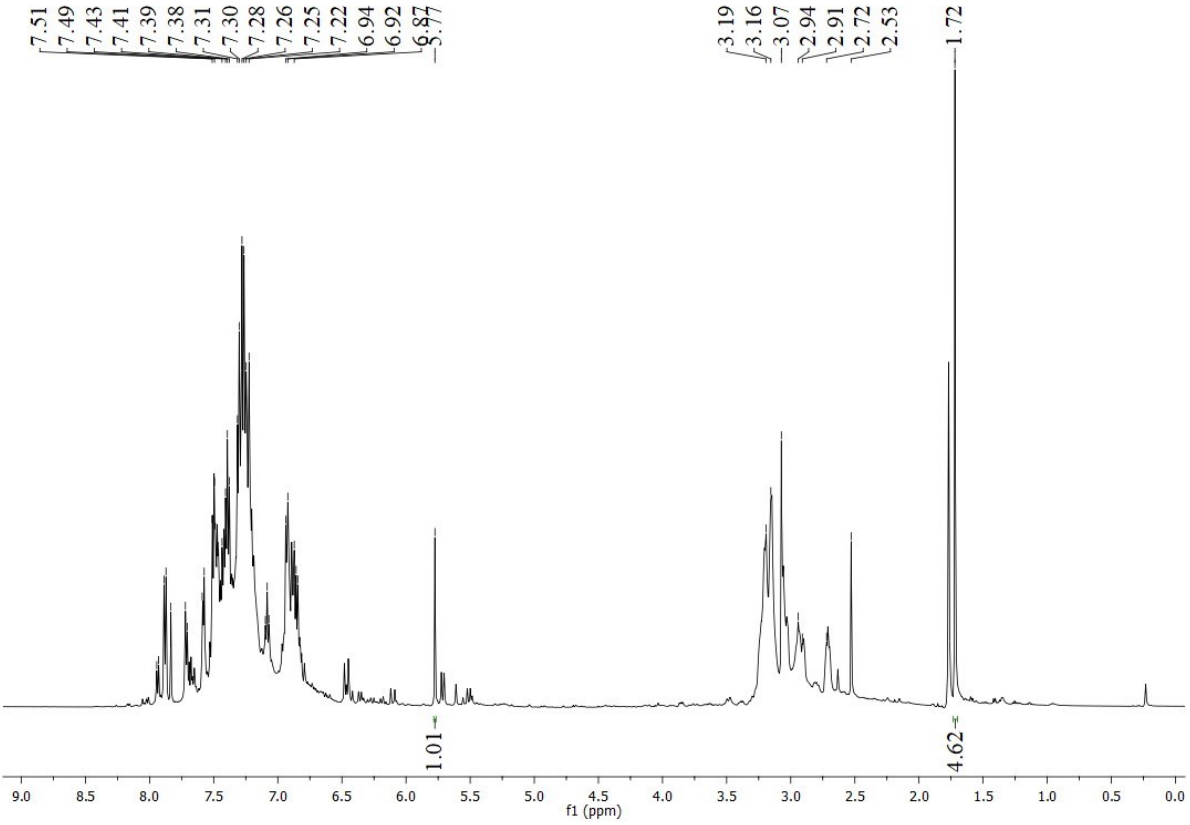

Figure S109. The ^{1}H NMR (25 °C, 500 MHz) spectrum of the catalytic reaction mixture obtained after the reaction between *N*-phenylpiperazine and PhCCH in the presence of $[Cu(CH_3CN)_4]BF_4$ (10 mo%) at 110 °C for 24 h. 1,1,2,2-Tetrachloroethane was used as an internal standard (δ 5.77 ppm). The yield of tetrasubstituted propargylamine **17a** is 92%.

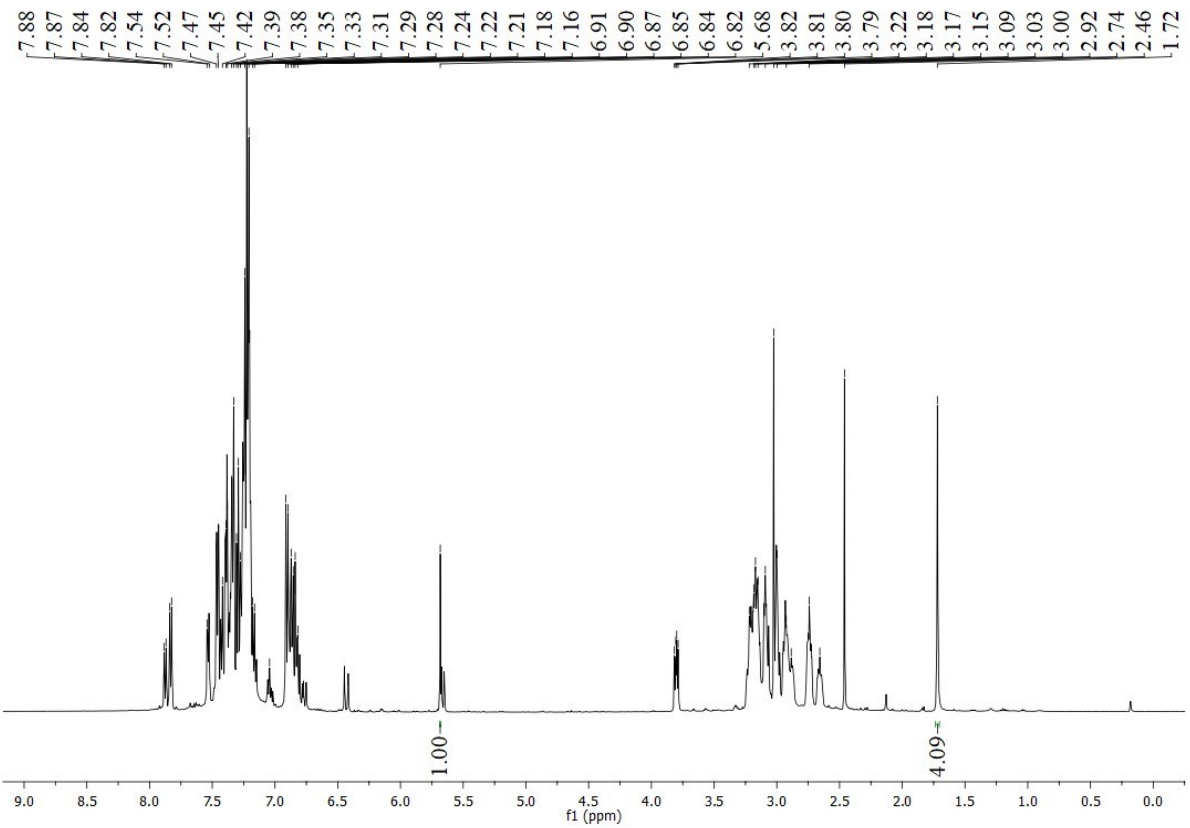

Figure S110. The ^{1}H NMR (25 °C, 500 MHz) spectrum of the catalytic reaction mixture obtained after the reaction between *N*-phenylpiperazine and PhCCH in the presence of complex **11b** (1 mo%) at 110 °C for 12 h. 1,1,2,2-Tetrachloroethane was used as an internal standard (δ 5.77 ppm). The yield of tetrasubstituted propargylamine **17a** is 82%.

5. References

1. Sheldrick, G. M. *Acta Cryst. Sect. A: Found. Crystallogr.*, **2015**, *71*, 3.
2. Sheldrick, G. M. *Acta Cryst. Sect. C: Struct. Chem.,* **2015**, *71*, 3.
3. van der Sluis, P.; Spek, A. L. BYPASS: an Effective Method for the Refinement of Crystal Structures Containing Disordered Solvent Regions. *Acta Cryst. A* **1990**, *46*, 194–201.
4. Pierce, C. J.; Yoo, H.; Larsen, C. H. A Unique Route to Tetrasubstituted Propargylic Amines by Catalytic Markovnikov Hydroamination–Alkynylation. *Adv. Synth. Catal*. **2013**, *355*, 3586–3590.
5. Zhou, L.; Bohle, D. S.; Jiang, H. F.; Li, C. J. Synthesis of Propargylamines by a Copper-Catalyzed Tandem Anti-Markovnikov Hydroamination and Alkyne Addition. *Synlett*. **2009**, *6*, 937-940.
6. Liu, Q.; Burton, D. J. A Facile Synthesis of Diynes. *Tetrahedron Lett.* **1997**, *38*, 4371-4374.
7. Aliaga, M. J.; Ramón, D. J.; Yus, M. Impregnated copper on magnetite: an efficient and green catalyst for the multicomponent preparation of propargylamines under solvent free conditions. *Org. Biomol. Chem.* **2010**, *8*, 43-46.
8. Cai, Y.; Tang, X.; Ma, S. Identifying a Highly Active Copper Catalyst for KA^2 Reaction of Aromatic Ketones. *Chem. Eur. J*. **2016**, *22*, 2266–2269.
9. Palchak, Z. L.; Lussier, D. J.; Pierce, C. J.; Yoo, H.; Larsen, C. H. Catalytic Tandem Markovnikov Hydroamination–Alkynylation and Markovnikov Hydroamination–Hydrovinylation. *Adv. Synth. Catal*. **2015**, *357*, 539-548.